The occurrence, pathology and morphological development of *Paranucleospora theridion* in salmon louse (*Lepeophtheirus salmonis*)

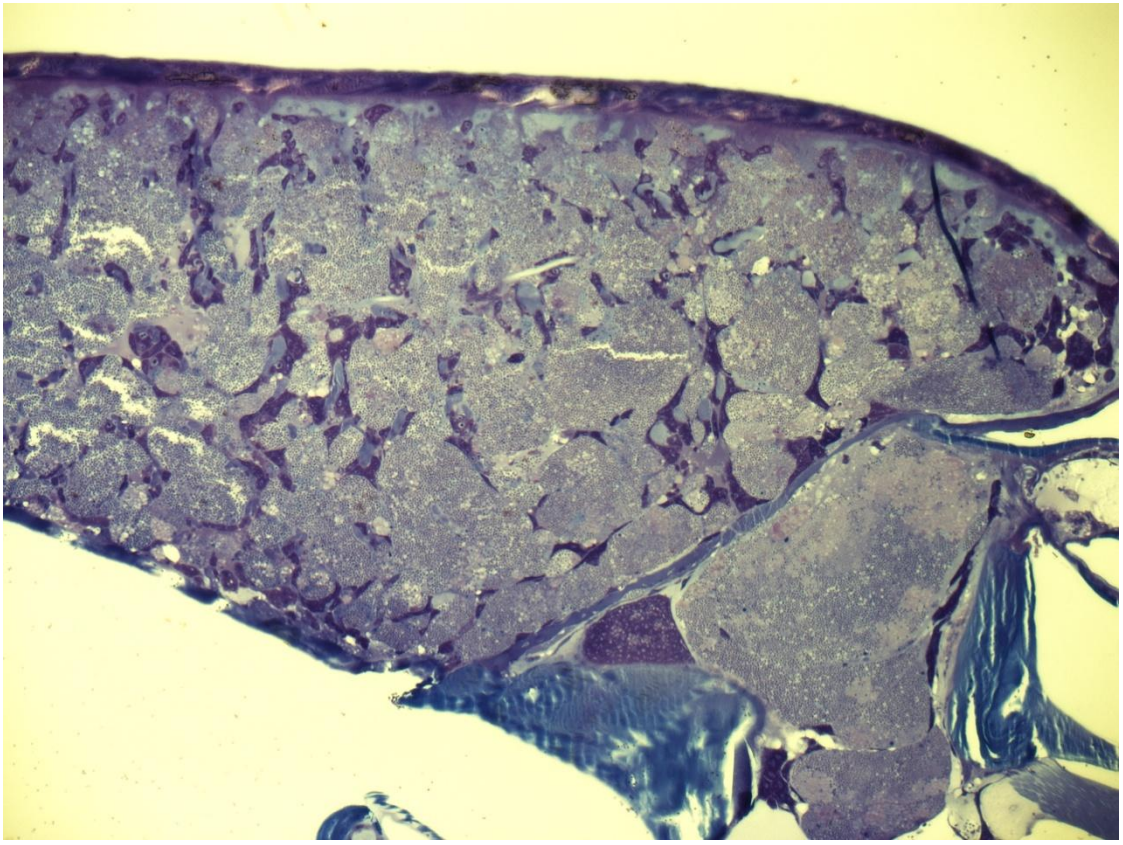

Arnfinn Lodden Økland

Thesis for the degree Master of Science in Aquamedicine
Department of Biology

UNIVERSITY OF BERGEN

June 2012

Acknowledgements

I would like to thank everyone who has provided me with material for this study.

I am sincerely grateful towards Are Nylund for guidance, help and support during the present study. I would also like to thank Kuninori Watanabe for all guidance and help with the microscopical part of this study. Heidrun Nylund also deserves thanks for guidance and help considering molecular techniques.

I would also like to thank all classmates for disturbance during the last year.

Last, but not least, I would like to thank my wife Hege and my daughter Ea for making me come home at 15:30 every day and changing my train of thoughts.

Bergen, June 2012 Arnfinn Lodden Økland

Table of Contents

Abstract

In 2003 a microsporidian parasite was discovered in salmon lice (*Lepeophtheirus salmonis*). The same parasite was later described from Atlantic salmon (*Salmo salar*) and salmon lice and was identified as *Paranucleospora theridion*. *P. theridion* is associated with disease in both salmon lice and Atlantic salmon. In the present study Real-time RT-PCR has been used to study the prevalence and intensity of *P. theridion* in the developmental stages of salmon lice. Light microscopy and electron microscopy has been used to study the pathology and morphological development of *P.theridion* in salmon lice.

The present study shows that the salmon lice are infected with *P. theridion* in the first chalimus stage and that a prevalence of 100% is reached before the free-moving first preadult stage. This indicates that the lice get infected while feeding on *P. theridion* infected epithelial cells of Atlantic salmon. The intensity of *P. theridion* in salmon lice development increases from chalimus stage 1 until the preadult stages are reached. This show that there is a proliferation of *P. theridion* during the salmon lice development. A drop in intensity in adult lice may be explained by the death of heavily infected lice. Registrations of prevalence of medium to heavy *P. theridion* infected salmon based on visual examination showed that the prevalence is highest in winter and that the development of *P. theridion* may be temperature dependent.

Morphological studies of *P. theridion* development in salmon lice indicates sexual reproduction based on the presence of synaptonemal complexes, loss of nuclear membrane and the alteration between diplokaryotic and monokaryotic nuclei. A hypothesis including cytoplasmic fusion of meronts, mitotic division of diplokarya and the fusion of monokarya resulting in diploid monokarya has been suggested.

Virus-like particles, a unicellular organism and bacteria associated with pathology in salmon lice were observed during microscopical examination of the development of *P. theridion*. In addition a potentially new species of *Udonella* were observed during examination of the presence of *P. theridion* in *Caligus centrodonti*.

1. Introduction

Microsporidia is a large group of obligate intracellular parasites of eukaryotes. They have previously been ranked as protists (Wittner, 1999) but are now ranked as fungi (Lee et al., 2008). Microsporidia consist of approximately 150 described genera and over 1200 described species (Keeling and Fast, 2002). Most species infect arthropods and fish, however all five classes of vertebrates and nearly all invertebrates including protists such as ciliates and gregarines have been reported to be infected by microsporidians (Wittner, 1999). More than 150 species of microsporidians from at least 14 genera are known to infect fish (Lom and Nilsen, 2003). Some of the most known microsporidians causing disease in fish are *Glugea anomala*, *Pleistophora* spp, *Nucleospora salmonis* and *Loma* sp. (Wittner, 1999). Most microsporidians infecting fish are thought to have a direct life cycle with horizontal and/or vertical transmission (Dunn and Smith, 2001) although there is lack of evidence of such transmission in the genus *Pleistophora* (Lom and Nilsen, 2003).

In 2003 Freeman et al. discovered and gave an incomplete description of a hyperparasitic microsporidian infecting the salmon louse (*Lepeophtheirus salmonis*) in Scotland. The same microsporidian was later detected in Atlantic salmon (*Salmo salar*), rainbow trout (*Oncorhynchus mykiss*), salmon louse and *Caligus elongatus* in Norwegian aquaculture (Nylund et al., 2009). Nylund et al gave a further description of the microsporidian including its development and pathology in salmon. Phylogenetic studies showed that the new microsporidian was a close relative of *Enterocytozoon bieneusi* and *N. salmonis*. The name *Paranucleospora theridion* was then suggested (Nylund et al., 2009, Nylund et al., 2010).

Proliferative gill inflammation (PGI) has caused severe losses in the Norwegian aquaculture. The etiology is not clear but there are several agents associated with the disease; *Ichthyobodo* spp (Poppe and Håstein, 1982), salmon gill poxvirus (Nylund et al., 2008), *Candidatus* Piscichlamydia salmonis (Draghi et al., 2004), *Candidatus* Clavochlamydia salmonicola (Karlsen et al., 2008), *Neoparamoeba perurans* (Steinum et al., 2008), Atlantic salmon paramyxovirus (Kvellestad et al., 2005) and *Paranucleospora theridion* (Nylund et al., 2010). All of the abovementioned agents are able to induce gill pathology but it is not clear if these are secondary invaders or primary pathogens. A recent study indicate that *P. theridion* may be a primary pathogen as fish with PGI are particularly heavily infected with *P. theridion* (Nylund et al., 2011).

Microsporidian morphology

Microsporidians are characterized by the formation of spores and the presence of unique organelles such as the extrusion apparatus (Fig 1.1). Unlike other eukaryotes they lack mitochondria, typical Golgi apparatus and microbodylike organelles (Vavra and Larsson, 1999). In addition their ribosomes have more resemblance with the ribosomes of prokaryotes than the ribosomes of eukaryotes (Ishihara and Hayashi, 1968). Spores may have a size from 1-40µm. The shape is mostly static within a genus and may vary from oval, spherical, rodlike, bellshaped, langeniform and shaped like a horseshoe, and the most common shape is oval. The spore wall consists of three layers; exospore, endospore and plasma membrane. The exospore is the outermost layer and is a uniform electron dense layer and may vary from 10nm to 200nm thick. The endospore lies beneath the exospore and is electron transparent and is usually 100nm or thinner. The plasma membrane lines the inner surface of the exospore and is a classical unit membrane (Vavra and Larsson, 1999). The nucleus is typical eukaryotic and is either an individual nucleus, monokaryon, or two closely arranged nuclei, diplokaryon. It is covered by a unit membrane and separated by a perinuclear space (Vavra and Larsson, 1999). Microsporidians may alternate between monokaryotic and diplokaryotic nuclear configuration during their life cycle (Cali and Takvorian, 1999). Characterizing organelles of the microsporidian spore are the sporoplasm and the three organelles that composes the extrusion apparatus; polar filament, polaroplast and posterior vacuole. The polar filament is hollow tube with a length from 50 to 500 µm, which is connected to the anchoring disc in the anterior part of the spore. It has a straight part (manubroid) through the polaroplast and coils around the remaining contents of the spore with its posterior part near the posterior vacuole, and the number of coils vary from 4 to over 30 (Keohane and Weiss, 1999). The polaroplast is located in the anterior part of the spore. It occupies one third to half of the spore's volume and consist of lamellar compartments. The anterior part of the polaroplast is called the lamellar polaroplast with densely packed lamellas. The vesicular polaroplast is the posterior part where the lamellas are loosely arranged (Vavra and Larsson, 1999). The posterior vacuole is a membrane lined vesicle with a clear to spongy content. In fish microsporidians it usually occupies half of the spore's volume (Vavra and Larsson, 1999). A dense sporoplasm abundant in ribosomes fills up the rest of the spores volume (Cali and Takvorian, 1999).

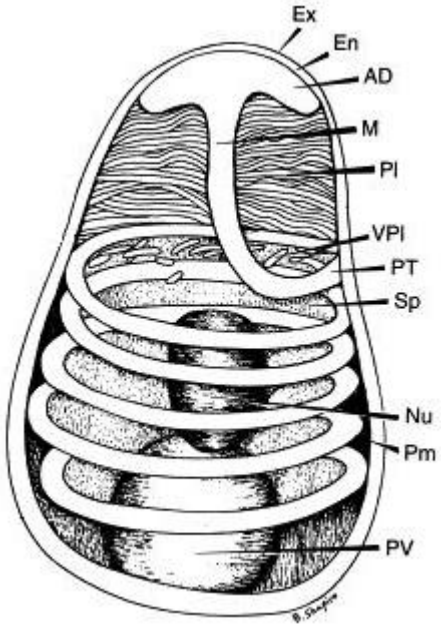

Figure 1.1 Diagram of a microsporidian spore. The spore wall: exospore (Ex),endospore (En) and plasmamembrane (Pm). The extrusion apparatus: polar tube (PT), manubroid (M), lamellar polaroplast (Pl), vesicular polaroplast (VPl) and posterior vacuole (PV). The nucleus (Nu) is located in the sporoplasm (Sp) and is in this diagram illustrated as a monokaryon. Figure modified from Keohane and Weiss (1999).

Microsporidian life cycle

Production of environmental spores and the use of an extrusion apparatus to infect a cell characterize the microsporidian life cycle. The life cycle can be divided into three phases; the infective phase, the proliferative phase and the sporogonic phase. The infective phase includes the release of the spores, their survival in the environment and the infection of the host (Wittner, 1999). Spores may be released into the environment via feces, urine, sputum, regurgitation or by the death of its host depending on the target cells and the virulence of the species (Cali and Takvorian, 1999). The spores are resistant to heat and freezing and may survive temperatures from -19°C to 60°C (Amigó et al., 1996). Microsporidian spores have been reported to survive for several years in the environment (Cali and Takvorian, 1999). To infect a new host the spore shoots its polar tube into a cell and expels its sporoplasm through the polar tube. This process requires a physical or chemical trigger which varies among the different species of Microsporida. The trigger probably reflects the microsporidians adaptation to its environment and its host. After triggering the pressure in the spore increases due to increase in osmotic pressure and swelling of the polaroplast and the polar tube is discharged (Keohane and Weiss, 1999). It has also been reported that spores may germinate immediately after their formation in their host cell and infect other nearby cells (Avery and Anthony, 1983). There are even reports that spores may enter a cell by phagocytosis and then escape the maturing lysosome by germinating into the cytoplasm (Franzen, 2005). The sporoplasm that is expelled is rich in ribosomes and contains the nucleus, a weakly developed

ER and some vesicles. It is covered by an external unit membrane which is obtained from the extrusion apparatus during its passage through the polar tube (Vavra and Larsson, 1999). The development of most microsporidians occur in the cytoplasm of its host cell, however the genus *Nucleospora* and *Paranucleospora* develops in the nucleoplasm (Docker et al., 1997, Nylund et al., 2010). During the proliferative phase the sporoplasm develops into a meront. Nuclear division occurs at this stage and the meront will keep its nuclear configuration. After the nuclear division the meronts may divide by binary fission or continue to grow and produce multinucleate cells. The multinucleate cells may divide by plasmotomy or by schizogony (Cali and Takvorian, 1999). The third phase in microsporidian development is the sporogonic phase. This phase include three different developmental stages: sporonts, sporoblasts and spores. The beginning of this phase is defined at the occurrence of meiosis in species that have meiosis or at the separation of diplokaryon in diplokaryotic genera. A visible marker to this transition is the deposition of a dense material on the plasmalemma (Cali and Takvorian, 1999). There are, however, examples where the deposition occurs early in the proliferative phase (Avery and Anthony, 1983) or in the late stages of the sporogonic phase (Cali and Owen, 1990, Nylund et al., 2010). The sporonts may divide in three different manners. They may divide by karyokinesis linked to cytokinesis were each sporont go through a nuclear division prior to the binary fission of the cell. They may also divide by cytokinesis not linked to karyokinesis were there is two nuclear division processes followed by cytokinesis which results in four sporoblasts (schizogony). If the nuclear division is repeated several times the cell will become a sporogonial plasmodium which may contain from eight to over a hundred nuclei. These plasmodia may divide by schizogony or plasmotomy. The sporoblasts are not dividing and undergo morphogenesis into spores. During their morphogenesis the extrusion apparatus is formed and their cytoplasmic density increases as a result of a large production of ribosomes and fast development of ER and Golgi complex (Cali and Takvorian, 1999). The electron dense material on the plasmalemma thickens and will eventually form the exospore. As the cell polarizes the transition from sporoblast to spore is defined as complete (Larsson, 1986).

Life cycle of *P.theridion*

P. theridion has three described developmental cycles in two different hosts (Freeman et al., 2003, Freeman and Sommerville, 2009, Nylund et al., 2010). Salmonids are hosts for the first two developmental cycles. The two developmental cycles have been described from Atlantic salmon (*Salmo salar*) (Nylund et al., 2010) and *P.theridion* has been detected in rainbow trout (*Oncorhynchus mykiss*) and sea trout (*Salmo trutta*) (Nylund et al., 2009). It is thought that the spores produced from the first developmental cycle are autoinfective and will spread and infect other cells when the host cells degenerate. The spores produced from the second developmental cycle develops in the nucleus of epithelial cells in the skin and gills, and are thought to infect salmon lice while it feeds on the epidermal cells (Nylund et al., 2010). The last developmental stage has been described from salmon louse (*L.salmonis*) (Freeman et al., 2003, Freeman and Sommerville, 2009, Nylund et al., 2010). *P.theridion* is diplokaryotic during all developmental stages in salmon and the development is therefore probably haplophasic. In salmon lice the developmental stages alternate between diplokaryotic and monokaryotic. It is therefore likely that the sexual processes (meisosis and karyogamy) take place in the salmon louse. Based on this information salmonids have been defined as intermediate hosts and salmon louse has been defined as the definitive host (Nylund et al., 2010).

Developmental cycle I has been observed in the cytoplasm of polymorphonuclear leukocytes, macrophage-like cells, blood vessel endothelial cells in most organs and in epithelial cells in skin and gills of Atlantic salmon. Diplokaryotic meronts surrounded by a unit membrane in the cell cytoplasm are the earliest observed developmental stages. The meronts have a diameter of 0.8-1.8µm and their cytoplasm is abundant in ribosomes and most often contain a single ER lamellum. They undergo merogony which result in a merogonial plasmodium that contains two to more than 12 diplokarya. As a result of plasmotomy several plasmodia may be observed in a single host cell. Merogonial plasmodia are surrounded by host cell mitochondria and during the transition from meront to sporont there is no deposition of dense material on the plasmalemma. The sporonts have a diameter of 1.7-5.5µm and are distinguished from the meronts by dense discs which are thought to be precursors of the polar filament. In addition the sporont diplokarya are more rounded than the coffee bean shaped diplokarya of the meronts. Development and composition of the sporoblast organelles start in the sporogonial plasmodia. The last sporogonial division is a schizogonal division which results in diplokaryotic sporoblasts. Sporoblasts are covered by a 20nm thick amorphous

material and develops into sphaerical spores with a diameter of 0.9-1.2µm. These spores contain a short polar tube (1.1µm), a polaroplast consisting of loosely arranged lamella and a posterior vacuole with a dense granular content (Nylund et al., 2010).

Developmental cycle II has only been observed in the nucleus of epidermal cells in the skin and gills of Atlantic salmon. The meronts contain one to two diplokarya and are surrounded by a unit membrane in direct contact with the host cell nucleoplasm. Like the meronts in developmental cycle I their cytoplasm have an abundant amount of ribosomes and one ER lamella, and there is no deposition of dense material on the plasmalemma during the transition from meront to sporont. The sporonts are distinguished from the meronts by barrel shaped elements with a diameter of 80nm in the sporoplasm. Before a sporont is divided into two sporoblasts there is developed an extrusion apparatus for each sporoblast. The sporoblasts develops into ellipsoidal, diplokaryotic spores with a length of 2.4-2.7µm and a width of 2.0-2.1µm. Their polar tube have four to five coils with a diameter of 150nm and one or no coil with a diameter of 82-110nm. The spore wall consist of a thin endospore (28nm) and a thick exospore (100-130nm) (Nylund et al., 2010).

Developmental stages of *P.theridion* have been found in connective tissue cells (Freeman and Sommerville, 2009) , epithelial cells, gonadal cells, satellite cells and in haemocytes of salmon lice (Nylund et al., 2010). Infected cells are often hypertrophic and may form xenomas or xenoma-like cells. The first observed developmental stage is meronts which contain a rounded diplokaryotic nucleus, some few ER-profiles and a moderate amount of free ribosomes (Nylund et al., 2010, Freeman and Sommerville, 2009). Their morphology can vary from spherical with one or two diplokarya to multilobed plasmodia with more than eight diplokarya. The meronts are only observed in the host cell cytoplasma and are often observed close to other developmental stages such as sporonts, sporoblasts and mature spores. They reproduce either by binary fission or shizogony. By binary fission a single meront will divide its diplokaryon and form two diplokarya. The meront will then split to form two daughter cells. By schizogony a single meront will give rise to several daughter cells. The meront will form a merogonial plasmodium by dividing its diplokaryotic nucleus to form several diplokarya. For each diplokaryon there will be formed a lobe and a daughter cell will derive from each lobe (Freeman and Sommerville, 2009, Nylund et al., 2010). Sporonts are often monokaryotic and it is unknown if this is due to fusion or dissociation of diplokarya. There are two stages of sporonts. Stage I sporonts differ from meronts by having a 20 nm amorph substance on the plasmalemma and by having rough-ER. Stage II sporonts (2.0-2.7µm) are

smaller than Stage I sporonts (2.7-5.7µm). Their ER is more developed and early elements of the extrusion apparatus are present. The sporonts divide either by shizogony (Stage I) or binary fission (Stage I, Stage II) (Nylund et al., 2010). Sporoblasts have a more developed polartube with more coils than Stage II sporonts. Polar cap and anchoring disc occur in the periphery of the cell opposing an early stage of manubrium and a vesicular polaroplast. The sporoblasts are 2.3-2.6 µm and are not dividing although one can occasionally observe sporoblast-like cells with two sets of polar filaments (Nylund et al., 2010, Freeman and Sommerville, 2009). Spores develops from the sporoblasts, and they are spherical to weakly subspherical and have a diameter of 2.4 µm. The spore wall consists of a 28 nm thick exospore and a translucent endospore of 42-56 nm. The anisofilar polar filament consists of four to six coils. Macrospores with a diameter of 5 µm containing several unorganized extrusion apparatus have also been observed. They are, however, thought to be non-functional (Nylund et al., 2010).

Pathology of *P. theridion*

Clinical signs of a *P. theridion* infection in Atlantic salmon may be slightly pale gills with increased mucus production, skin hemorrhages and loss of scales. Histopathologically hypertrophy and hyperplasia of the gill epithelium is observed. Invasion of leucocytes is observed in the gills, kidney, heart, spleen, gut and exocrine pancreas (Nylund et al., 2010, Nylund et al., 2011). In the salmon louse the infection leads to xenoma-like cells near the cuticle due to the proliferation of the microsporidian. Such an infection may fill the entire haemocoelic cavity (Freeman et al., 2003, Nylund et al., 2010). The infection may influence the reproduction and survival of the salmon louse (Nylund et al., 2009).

Salmon louse biology

The salmon louse (*L.salmonis*) is a parasitic copepod belonging to the family *Caligidae.* Its host range is limited to salmonids and has been reported to infect 12 different species in the genera *Salmo, Salvelinus* and *Oncorhynchus*. The salmon louse is ectoparasitic and feed on the skin epidermal cells, mucus and blood (Costello, 2006). The life cycle of the salmon louse consists of ten life stages; two nauplius stages, one copepodid stage, four chalimus stages, two pre-adult stages and one adult stage (Johnson and Albright, 1991b). Its life cycle is direct and female lice from pre-adult I to adult are fertilized by adult males (Ritchie et al., 1996). An adult female lice may produce a new pair of egg strings each 10^{th} day and the egg strings may contain from approximately 50 to 700 eggs each (Heuch et al., 2000). The generation time is 99 days at 7°C, 55 days at 10°C and approximately 30 days at 12°C (Johnson and Albright,

1991a, Heuch et al., 2000). The nauplii are planktonic and non-feeding stages, and they are responsible for the dispersal of the salmon lice. They moult into a copepodid which is also free-living and infective (Costello, 2006). Copepodids may respond to light (shadows and flashes from the host), vibrations and chemicals which are probably factors involved in the triggering of infection (Costello, 2006, Heuch and Karlsen, 1997). The copepodid attaches to the host by a frontal filament (Bron et al., 1991). An attached copepodid may use 52 to 59 days to develop into an adult female at approximately 8.5°C (Tucker et al., 2002). After infection the copepodid moults into a chalimus. There are four chalimus stages and they are all sessile due to the attachment by the frontal filament (Costello, 2006). They feed on the skin and mucus near their attachment (Jones et al., 1990). The two pre-adult and the adult stages move freely on the hosts skin and feed (Costello, 2006).

Aims of the study

The aim of this study was to examine the development and pathology of *Paranucleospora theridion* in the salmon louse (*Lepeophtheirus salmonis*). Real time RT-PCR has been used to detect the occurrence and relative amount of *P. theridion* during salmon louse development. Light microscopy and transmission electron microscopy was used to examine the pathology and the morphologic development of *P. theridion* with emphasis on the merogonial and sporogonial stages.

2. Material and methods

Material

During this study 735 *L.salmonis* from the Norwegian county Sogn og Fjordane were collected and examined (Fig 2.1). 328 of these were collected the 02.09.11 and 377 were sampled the 10.11.11 (Table 2.1). They were all obtained from cultured Atlantic salmon. The temperature at the collection site were 15°C the 02.09.11 and 10.2°C the 10.11.11. Lice collected the 02.09.11 were roughly sorted on site and kept on ethanol or modified Karnovsky's fixative while the lice collected the 10.11.11 were stored live in seawater at 4°C until sorting the next day. They were then put on ethanol or modified Karnovsky's fixative. The samples kept on ethanol were first kept on 70% ethanol the first day and then transferred to 99.8% ethanol. All samples were kept at 4°C until processing. Egg strings from the lice were incubated at 10°C for sampling of the hatched nauplii which were stored at -50°C until processing. In addition 30 salmon lice from aquacultured rainbow trout in Sogn og Fjordane and 20 *Caligus centrodonti* from a *Labrus berggylta* broodstock facility in Hordaland were examined. They were collected and kept alive in seawater and sorted at the lab within 24 hours.

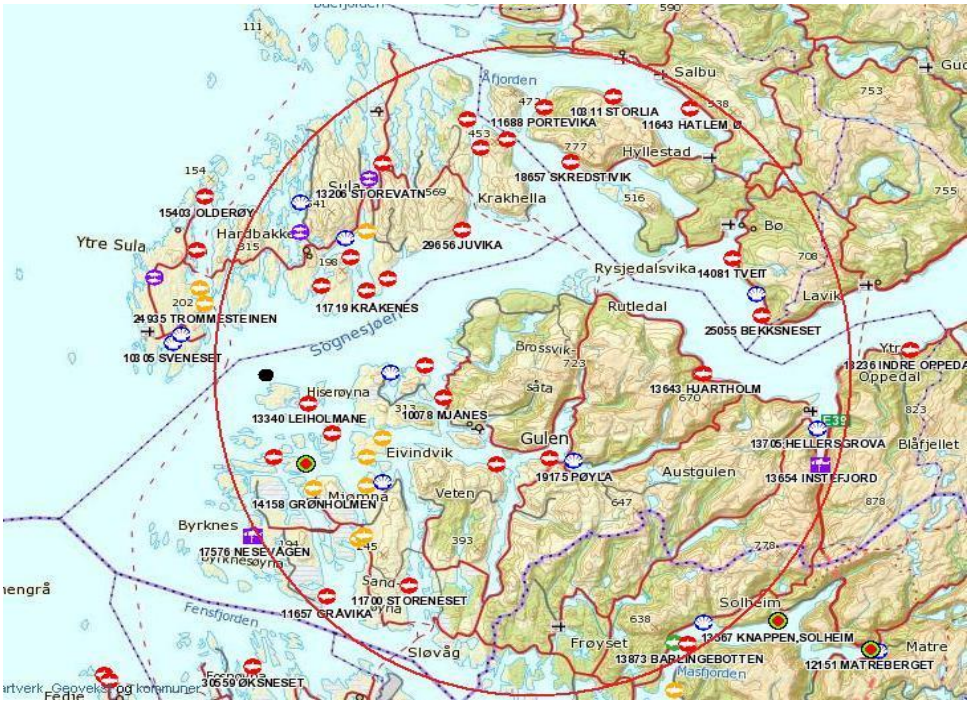

Figure 2.1 A map of the area were the lice were collected. The lice were collected at production sites within the red circle. The black dot represents Norwegian Institute of marine research hydrographic station where temperature data was obtained.

Table 2.1 An overview showing the number of lice that were collected for each developmental stage and the date they were obtained

Life stage	**02.09.11**	**10.11.11**	**Total**
Chalimus 1	0	9	9
Chalimus 2	2	8	10
Chalimus 3	4	56	60
Chalimus 4	4	22	26
1. Preadult male	13	28	41
1. Preadult female	19	58	77
2. Preadult male	28	44	72
2. Preadult female	39	24	63
Adult male	150	51	201
Adult female	69	73	142
Total	**328**	**373**	**701**

Methods

RNA and DNA extraction

RNA was extracted from all stages of *L. salmonis* and from adult *C. centrodonti*. The method described by Devold et al. (2000) was used with modifications. Isol-RNA lysis reagent (5-prime) was used during homogenization of the samples. 5 µl VHS-virus was added as an exogenous control. An additional washing step using 96% ethanol was added to increase the quality of the RNA extraction. The samples were eluted in 50 µl RNase-free water preheated to 70°C. To test for possible contamination negative controls were added at each RNA extraction.

DNA was also extracted from *Udonella sp* from *L. salmonis, Udonella sp* from *C. centrodonti* and from *L. salmonis* by using QIAGEN DNeasy® Blood and tissue kit according to the manufacturer's instructions.

The purity and concentration of RNA and DNA was tested using NanoDrop ND-1000TM spectrophotometer.

Real-time RT-PCR

Real-time RT-PCR is a fast and efficient technique to detect and quantify nucleic acids in a sample. The technique is based on a fluorescent signal which occurs when specific primers and probes detect the target template. This signal will increase exponentionally as more template is synthesized during each cycle until the components are deplenished. Ct-value refers to the amount of cycles required to reach a threshold value and is therefore opposite proportional to the amount of target template present in the sample (Kubista et al., 2006).

In this study AgPath-ID™ One-Step RT-PCR Kit (Applied Biosystems) were used for the real-time RT-PCR analysis. The following assays were used: NUC (*P. theridion*) (Nylund et al., 2010), VHSV (*Viral hemorrhagic syndrome virus*) (Duesund et al., 2010), ELF-LS (Elongation factor *L. salmonis*) (Frost and Nilsen, 2003) (Table 2.2). The real-time RT-PCR reaction was run in a 12.5 µl reaction containing 6.25 µl 2X RT-PCR, 1.0 µl 10mM forward primer, 1.0 µl 10mM reverse primer, 0.22 µl 10mM probe, 0.25 µl 25X RT-PCR enzyme mix, 1.75 µl RNase-free H_2O and 2.0 µl template. The real-time RT-PCR analysis was run by using an Applied Biosystems 7500 Fast Real-Time PCR System (Applied Biosystems) with following conditions: reverse transcriptase at 45°C for 10 min, polymerase activation at 95°C for 10 min, and 45 cycles of DNA dissociation at 95°C for 15 seconds and annealing/elongation at 60°C for 45 sec. The amplification curves were analyzed by using 7500 Software v2.0.6 (Applied Biosystems) and given a fixed threshold line at 0.1. To reduce the probability of contamination and false positives the negative controls from RNA extraction and negative template controls (NTCs) were analyzed. The NTCs were used to ensure that the kits and water were free of contaminants.

PCR and sequencing

PCR and sequencing was performed to verify the presence of *P.theridion* in samples that tested positive in real-time RT-PCR and to compare sequences of *Udonella* from *L.salmonis* and *Udonella* from *C.centrodonti.* cDNA was synthesized by running RT-PCR with GeneAmp™ PCR system 2700 (Applied Biosystems). The first step in the RT-PCR reaction was run in a 10.0 µl reaction containing 4.0 µl RNA, 1.0 µl 10mM primer (Table 2.2) and 5.0 µl RNase-free H_2O. 16.0 µl RT-mix containing 5.0 µl 5x buffer, 2.5 µl 10 mM dNTP, 0.15 µl 10mM MMLV and 8.35 µl RNase-free H_2O was then added. The RT-PCR reaction was run under following conditions: incubation 70°C, 5min, incubation 37°C, 60min. Veriti® 96-Well Thermal Cycler (Applied Biosystems) was used to run the PCR reaction in a 50.0 µl reaction

containing 2.0 µl cDNA, 5.0 µl 10x buffer, 5.0 µl 10 mM dNTP, 2.0 µl 10mM of both forward and reverse primer, 34.0 µl RNase-free H_2O and 0.3 µl TAQ DNA polymerase (1.5 units) under following conditions: initial denaturation (2 min, 94°C) followed by 35 cycles of denaturation (30 sek, 94°C), annealing (1 min, 50°C), and elongation (1 min 30 sek, 72°C), additional extension (72°C, 10 min).

1% agarose gel (Appendix) with 2.5 µl GelRed™ was made and immersed in 1x TAE buffer (Appendix). 5µl of the PCR-product was then mixed with 1µl loading buffer (6x) (Appendix) and transferred to the gel. 2.5 µl Smart Ladder (Eurogenetics), a molecular weight marker, was added to the gel as a size comparison. The gel was then connected to 80V for approximately 30 minutes. The result was visualized using GelLogic 212 Pro (Carestream) and Carestream Molecular Imaging Software, Standard Edition, Version 5.0.2.30

The PCR-product was purified using ExoSAP-It (USB®) according to the manufacturers protocol. The sequencing laboratory at the University of Bergen sequenced the samples by using BigDye ™ v3.1 terminator cycle sequencing reaction kit (Applied Biosystems). VectorNTI software (Invitrogen) was used to analyse, process and assemble the data.

Table 2.2 Primers and probes used for real-time PCR analysis and PCR and sequencing of *P.theridion*[a] and *Udonella* sp.[b]. The name of the primer and probes and their sequence, product length, position and reference are presented.

Primer / probe	Sequence	Product length	Position	Reference/ GenBank accession number
Real-time RT-PCR				
Nuc-fwd	5'-CGGACAGGGAGCATGGTATAG-3'		522-542	(Nylund et al., 2010)
Nuc-rev	5'-GGTCCAGGTTGGGTCTTGAG-3'	59	580-561	/FJ 594990
Nuc-probe	5'-6-FAM-TTGGCGAAGAATGAAA-MGB-3'		544-559	
VHSV-fwd	5'-TGTCCGTKCTTCTCTCCTATGTACT-3'		312-336	(Duesund et al., 2010)
VHSV-rev	5'-GCCCTRCTGMCTGTGTCA-3'	109	420-402	/EU 481506
VHSV-probe	5'-6-FAM-CTCACAGACATGGG-MGB-3'		380-393	
ELF-LS-fwd	5'-CATCGCCTGCAAGTTTAACCAAATT-3'		1152-1176	(Frost and Nilsen, 2003)
ELF-LS-rev	5'-CCGGCATCACCAGACTTGA-3'	99	1250-1232	/EF 490880
ELF-LS-probe	5'-6-FAM-ACGTACTGGTAAATCCAC-MGB-3'		1194-1211	
PCR				
Sin F1[b]	5'-GTCTCAAAGATTAAGCCATGC-3'	1282	13-33	Present study
Sin R2[b]	5'-TTAAGCCGCAGGCTCCAC-3'		1294-1277	Present study /FJ 946831
Sin F1[b]	5'-GTCTCAAAGATTAAGCCATGC-3'	1796	13-33	Present study
18g[b]	5'-GGTAGTAGCGACGGGCGGTGTG-3'		1808-1787	Present study /FJ 946831
V1F[a]	5'-CACCAGGTTGATTCTGCC-3'	1753	1-18	(Nilsen, 2000)
Mic R1[a]	5'-GGAAGTTACTACCTCCCGTTCC-3'		1753-1732	Present study /FJ 594990
Mic F1[a]	5'-GGCGAACGGCTCAGTAATGTTGC-3'	1675	79-101	Present study
Mic R1[a]	5'-GGAAGTTACTACCTCCCGTTCC-3'		1753-1732	Present study /FJ 594990

Assay efficacy test and normalization

To test the ELF-LS assay's efficacy to detect the target template an efficacy test was performed. This was carried out by using a tenfold dilution series of the template. The dilutions were run in a real-time RT-PCR experiment as triplicates. Microsoft Excel 2010 was used to create a standard curve by plotting the Ct-values against the dilution. The regression number and slope was calculated. To calculate the assay efficacy (E) the formula by Pfaffl (2004) (Formula 1) was used.

Formula 1: $E = (10^{-1/\text{-slope}})$

Normalization was performed for relative quantification. Normalization will also take account for errors from sampling, extraction of RNA and real-time RT-PCR. Normalized expression was calculated on the basis of the efficacy (E) and Ct-values of the different assays by using the formula by (Muller et al., 2002) (Formula 2)

Formula 2: $$NE = \frac{(E_{target})^{Ct\ target}}{(E_{ref})^{Ct\ ref}}$$

The NUC assay was normalized against ELF-LS and VHSV. The efficacy of NUC, 1,9697, and VHSV, 1,9839, were obtained from Repstad (2011) and Duesund et al. (2010)

Histology

Fixation

Salmon lice was fixed in a modified Karnovsky's fixative, where 4% (w/v) sucrose had been added and the distilled water has been replaced by Ringers solution (Nylund et al., 1995). The samples were stored at 4°C.

Embedding

To wash out Karnovsky's fixative the samples were rinsed 4 times with Ringers solution (Appendix). The samples were then post-fixated in 2% (w/v) OsO_4 for 60 minutes. OsO_4 was rinsed out with double distilled water two times for 15 minutes. Acetone (C_3H_6O) and propylene oxide (CH_3CHCH_2O) was used to dehydrate the samples (Appendix). To infiltrate the samples the samples were dehydrated through a series of acetone and EMBED 812 (Electron Microscopy Sciences) solutions (Appendix). The samples were then put to polymerize at 60°C for 24 hours.

Reichert-Jung Ultracut E (Leica) where used to cut semithin (0,5 µm) and ultrathin sections (30-40 nm). Semithin sections were stained with toluidine blue. Ultrathin sections were stained with 5% (w/v) aqueous uranyl acetate solution for 1,5 hours and then stained with lead citrate.

One heavily infected lice were embedded in Technovit 7100® (Heraeus Kulzer GmbH) according to the manufacturer's instructions. Thin sections (1,5 µm) were cut using Reichert Jung 2050 Supercut (Leica) and stained with toluidine blue.

3. Results

Efficacy test

The standard curve obtained from the efficacy test of ELF-LS is presented in **figure 3.1.**

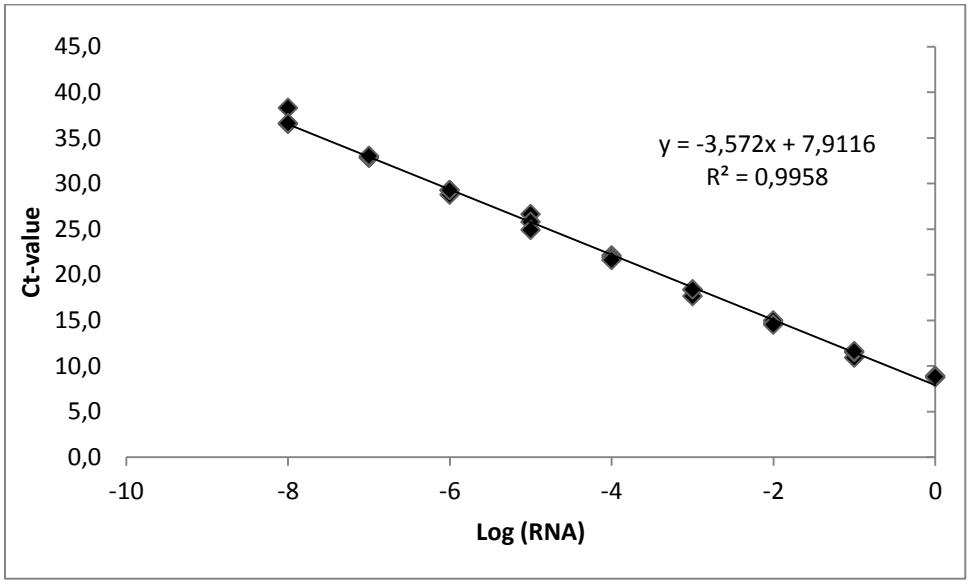

Figure 3.1 Standard curve for ELF-LS

The standard curve has a slope of -3.572. According to the formula E = ($10^{-1/\text{-slope}}$) the efficacy of the ELF-LS assay is 1.9053.

Presence of *P.theridion* in *L.salmonis*

30 lice from each developmental stage except chalimus 1 (9), 2 (10) and 4 (26) were examined for the presence of *P. theridion*. The prevalence of *P. theridion* increases from 66.7% in chalimus 1 to 100% in chalimus 3. From chalimus 3 to adult the prevalence varies from 100% to 96,7% (**Fig 3.2**). The intensity of *P. theridion* also increased from chalimus 1 to chalimus 4. From chalimus 4 to adult the intensity is slightly variable with a dip at preadult 1 female and a peak at preadult 2 female. The intensity of adult female is slightly lower than the intensity of chalimus 4 (**Fig 3.2**).

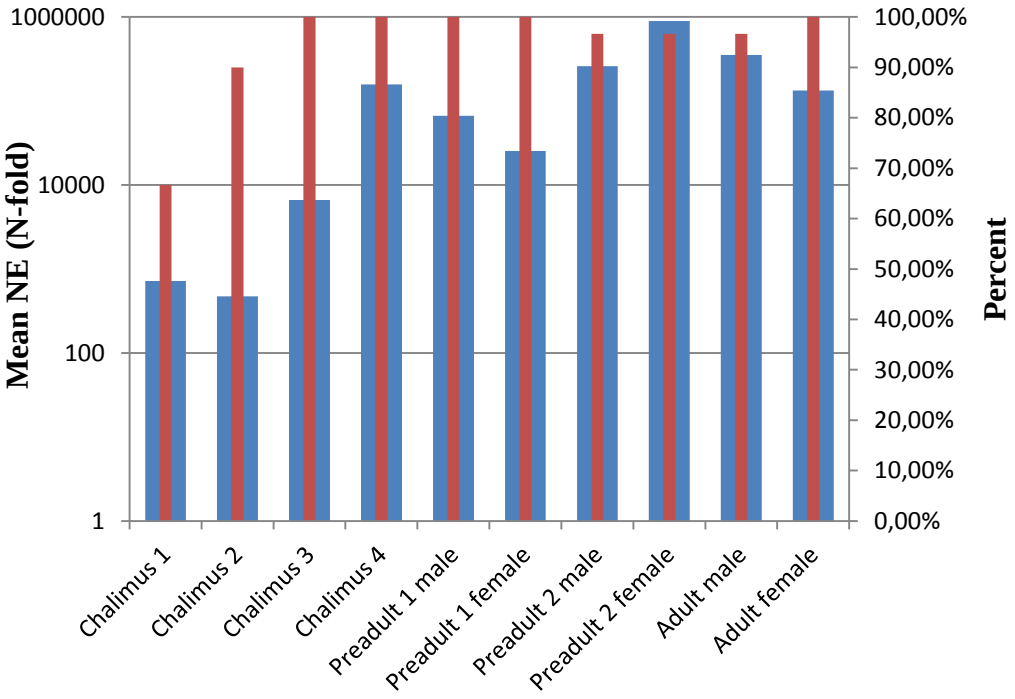

Figure 3.2 The development of prevalence and intensity of *P. theridion* during the salmon lice development. Prevalence is presented in percent and represents the red bars. Intensity is presented as mean normalized expression (N-fold) and represents the blue bars.

From December 2009 to February 2012 batches of adult salmon lice have been visually examined for the presence of *P. theridion*. The results are presented in figure 3.3 and show a trend of higher prevalence in the winter months December to February. Temperature data was obtained from 10 meters below the surface in Sognesjøen and was measured by the Norwegian Institute of marine research hydrographic station (Anonymous, 2012). The data show correlation between sea temperature and prevalence of *P. theridion* in salmon lice. The temperature in December and January is approximately 2 °C higher in 2011 than in 2010 and 2009. The temperature was also higher during the autumn months in 2011. This is reflected in the prevalence in January and February as it was 2.5 and 12.2 % in 2012, 0.7 % in January 2011, 0 % in January 2010 and 1.7 % in February 2010.

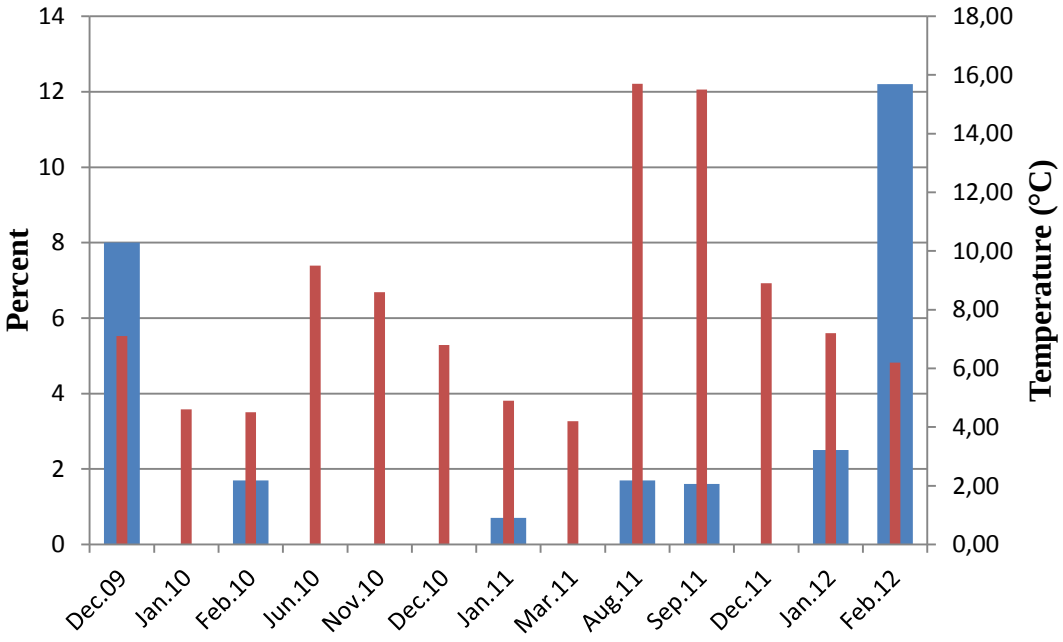

Figure 3.3 The visually recorded prevalence of *P. theridion* in salmon lice and temperatures in the period from December 2009 to February 2012. Red bars represent the temperature (°C). Blue bars represent the prevalence (%).

14 *P. theridion* infected adult lice were visually examined, photographed and later examined for the presence of *P. theridion* by using real time RT-PCR. This was performed to check the correlation between the observed infection and the real time RT-PCR Ct-values. There was a significant correlation between the observed infection and the Ct-values. Figure 3.4 shows two different levels of infection. Louse A has a less pronounced infection and has a Ct-value of 19.7, while louse B has more pronounced infection with a Ct-value of 5.5. Infections with a Ct-value as high as 21.2 were possible to detect visually.

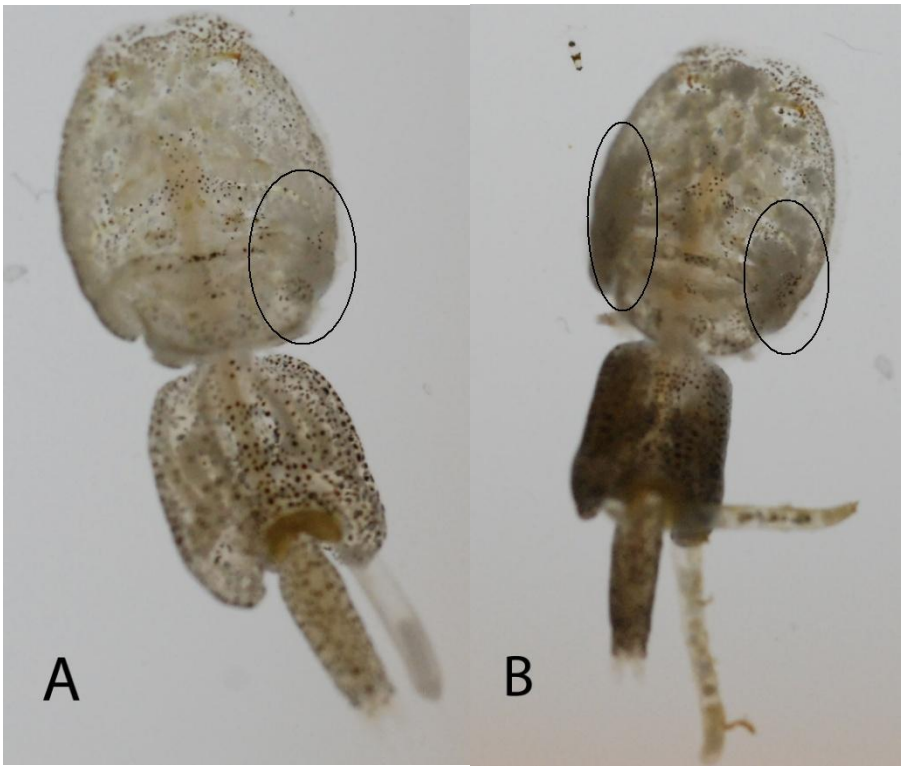

Figure 3.4 *P. theridion* infected lice. Louse A is weakly infected (NUC Ct = 19.7 and ELF-LS Ct = 10.7) and louse B is heavily infected (NUC Ct = 5.5 and ELF-LS Ct = 10.2).

Pathology of *P. theridion* in *L. salmonis*

P.theridion infected cells are present in the cephalothorax, gonadal segment, mouth tubule and other extremities (Fig. 3.5, 3.6, 3.7 and 3.8). The infections are most pronounced in the posterior lateral part of the cephalothorax (Fig 3.4 B and 3.5). The cephalothorax seems to be most affected, however large infections in close vicinity of the gut are more common in the gonadal segment (Fig 3.9 and 3.10). Few non-infected target cells are visible in heavily infected areas (Fig 3.11). Due to the proliferation of *P.theridion* the infected cells may become extremely hypertrophic and may contain hundreds of spores. Several host cell nuclei are observed in infected cells (Fig 3.12, 3.13 and 3.19). Other nuclear changes are condensation of nucleolus and lobed nucleus (Fig 3.13 and 3.14). The cells affected are haemocytes (Fig 3.15), fibroblasts/fibrocytes (Fig 3.16), epithelial cells (Fig 3.17) and tegmental gland cells (Fig 3.18)

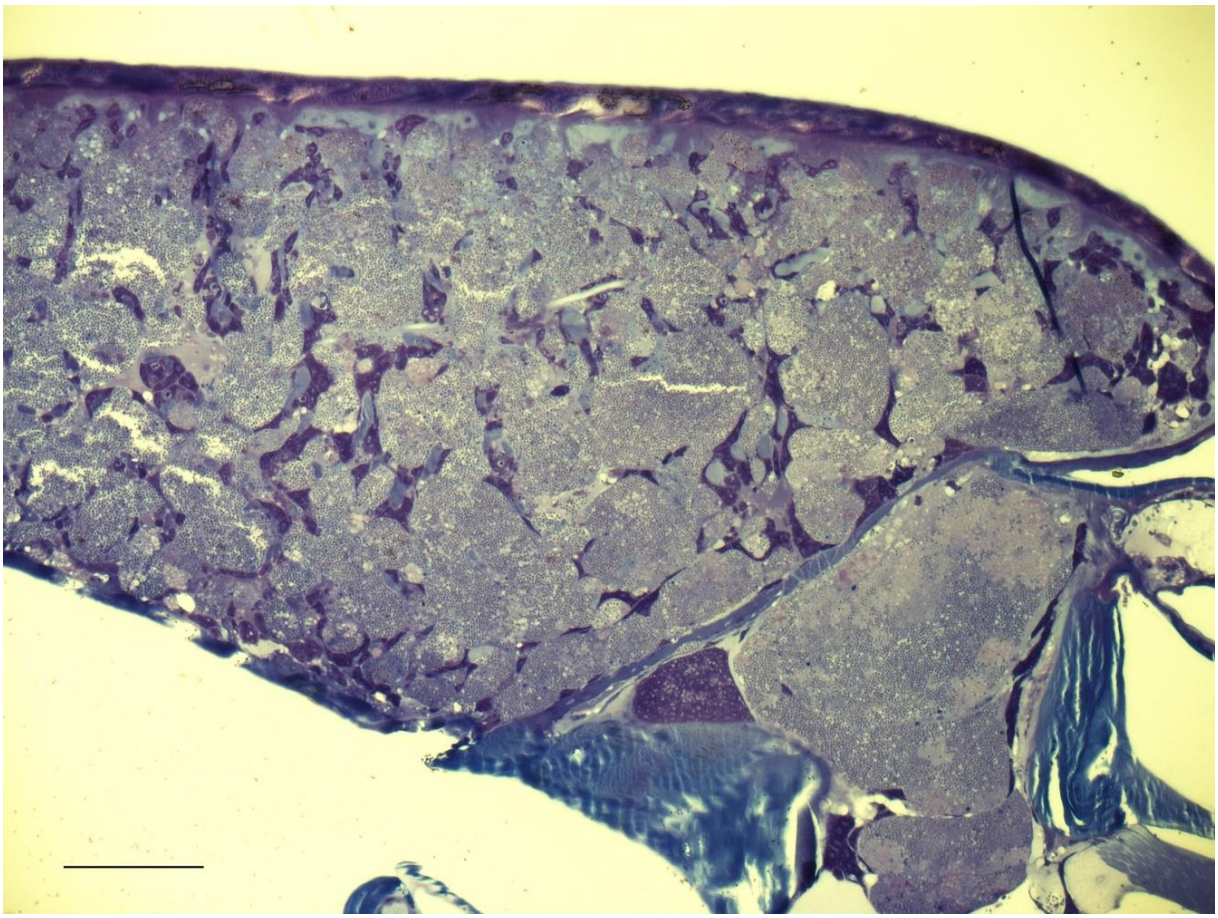

Figure 3.5 Posterior lateral part of the cephalothorax packed with spores and developmental stages of *P. theridion*. Scale bar = 100 µm

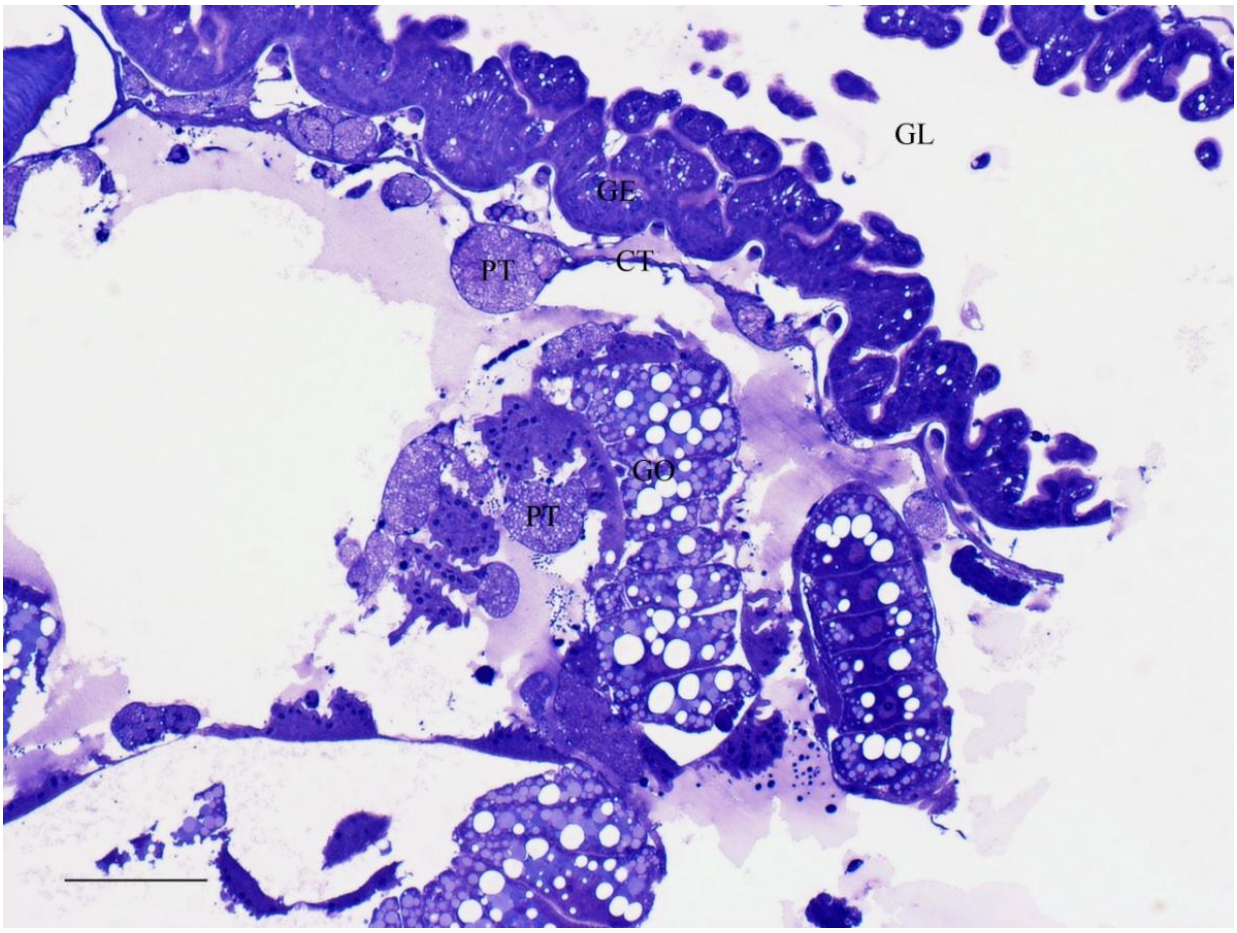

Figure 3.6 Gonadal segment with *P. therdion* infections (PT) in the connective tissue (CT) surrounding the gut and in unidentified cells associated with the gonads. The oocytes (GO), gut epithelium (GE) and the lumen of the gut (GL) are free of *P. theridion*. Scale bar = 100 µm

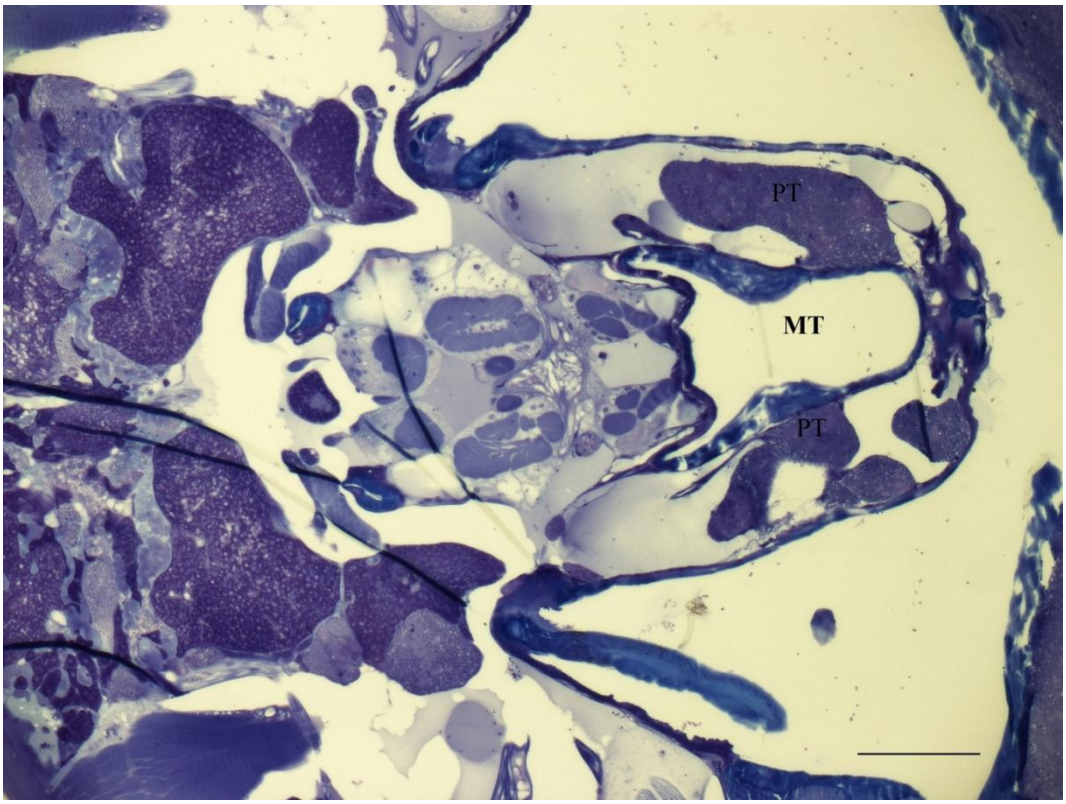

Figure 3.7 The mouth tubule (MT) of an adult female infected with *P. theridion* (PT). Scale bar = 100 µm.

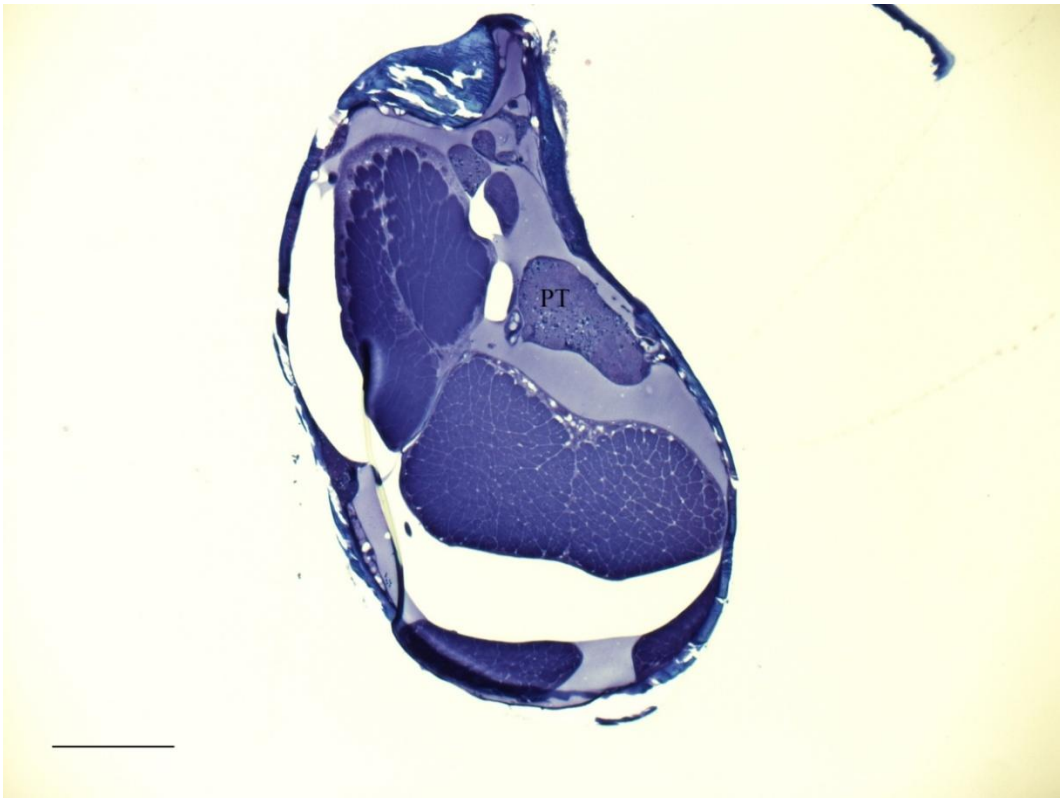

Figure 3.8 An extremity of a salmon louse infected with *P. theridion* (PT). Scale bar = 100 µm.

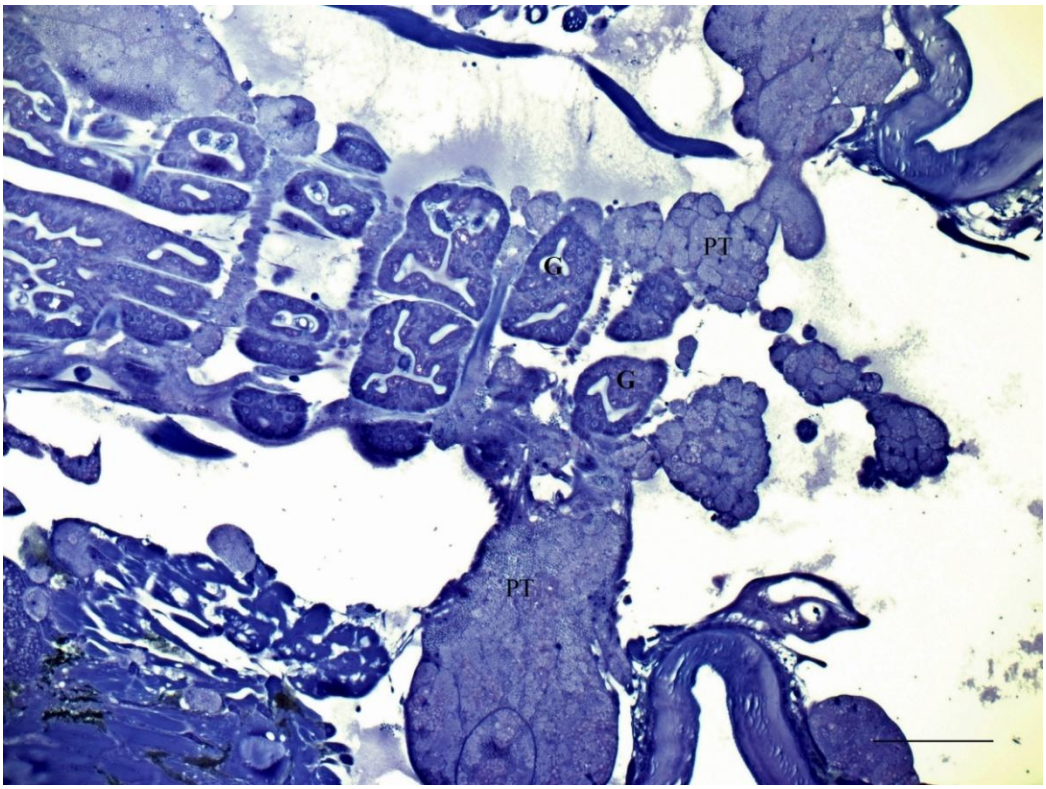

Figure 3.9 The gonadal segment of an adult female louse with large *P. theridion* infections (PT) near the gut (G). Scale bar = 100 µm.

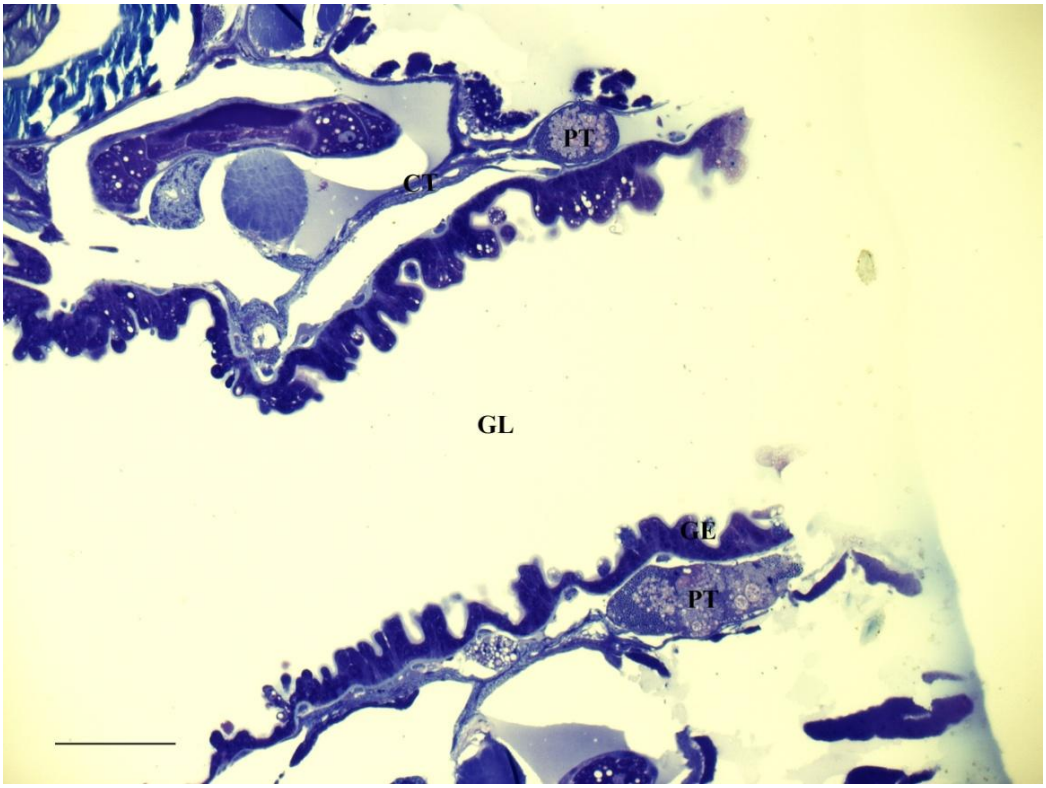

Figure 3.10 *P. theridion* infections (PT) in the connective tissue (CT) surrounding the gut in the cephalothorax of an adult female. The gut lumen (GL) and gut epithelium (GE) are free of *P. theridion*. Scale bar = 100 µm.

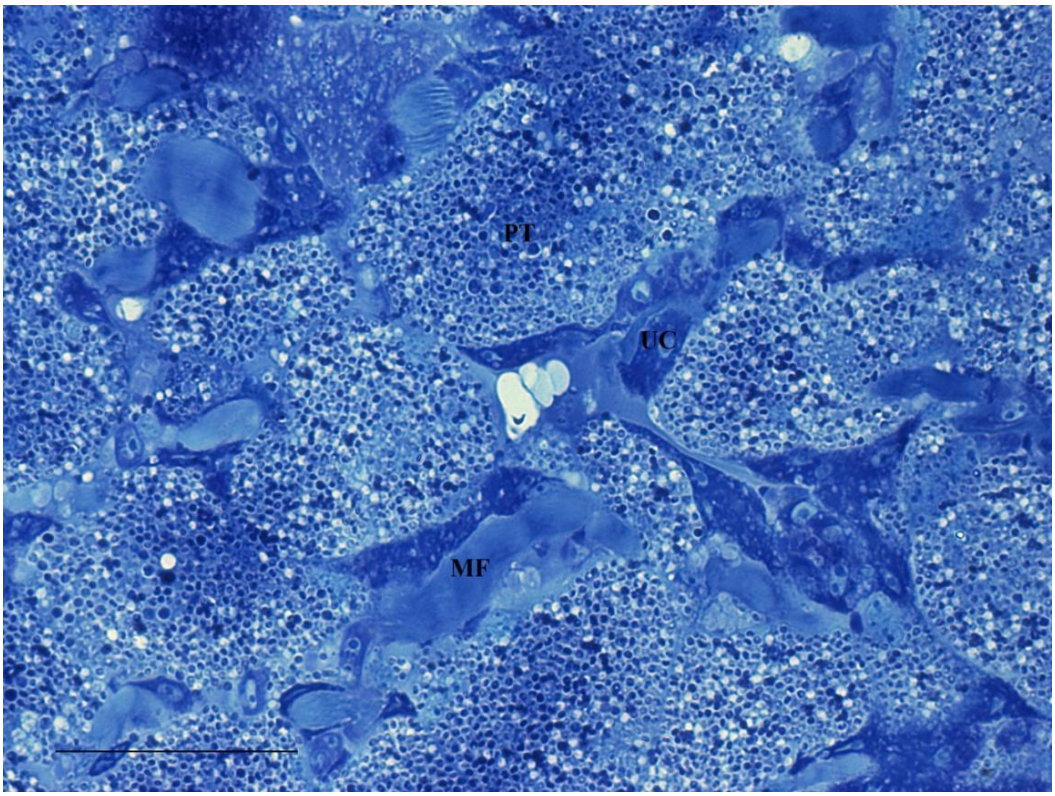

Figure 3.11 Heavily infected area packed with spores of *P. theridion* (PT) in the cephalothorax of an adult female. Few uninfected cells (UC) and muscle fibers (MF) are observed. Scale bar = 50 µm.

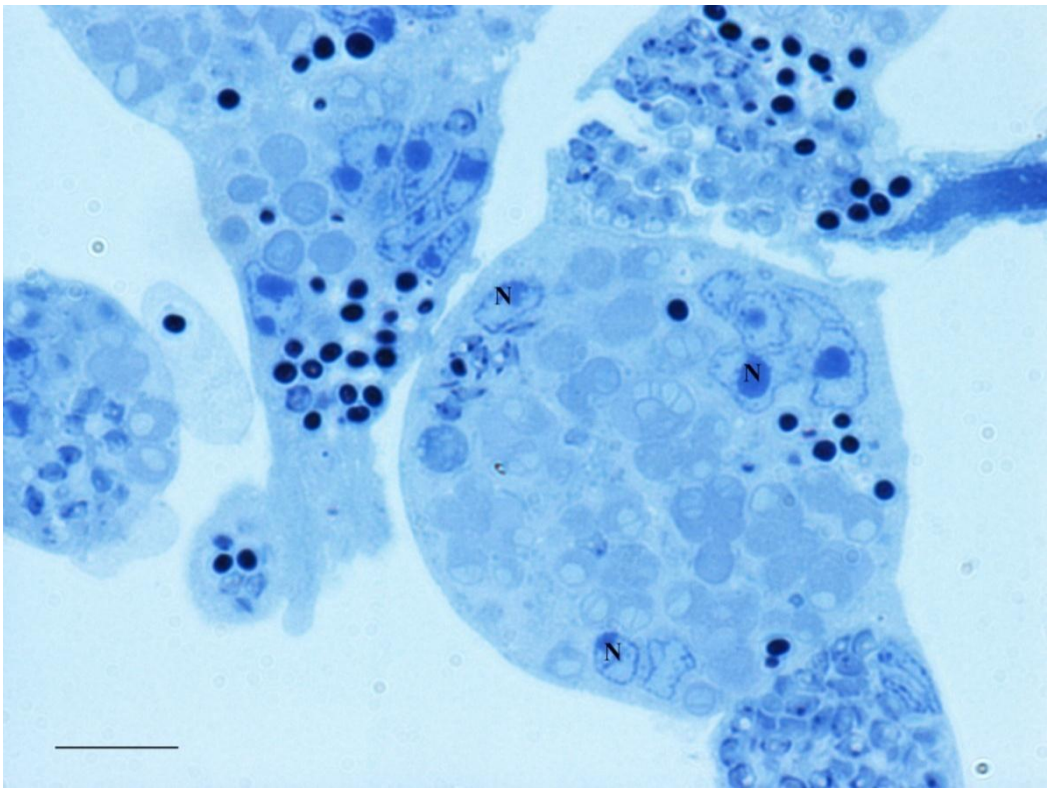

Figure 3.12 Connective tissue cells in the gonadal segment of an adult female infected with *P. theridion*. Multiple nuclei (N) are present in the infected cell**.** Scale bar = 10 µm.

Figure 3.13 Epithelial cell beneath the cuticle (C) infected with a sporont of *P. theridion* (PT). The nucleus (N) is multi lobed and the nucleolus (NU) is condensed compared to the nearby uninfected target cell (UI).

Figure 3.14 Epithelial cell infected with two *P. theridion* meronts in the transition to sporonts (PT). Th cell may contain several nuclei (N) or the nucleus (N) may be hypertrophic and multi lobed compared to the nucleus of the nearby uninfected target cell (UI)

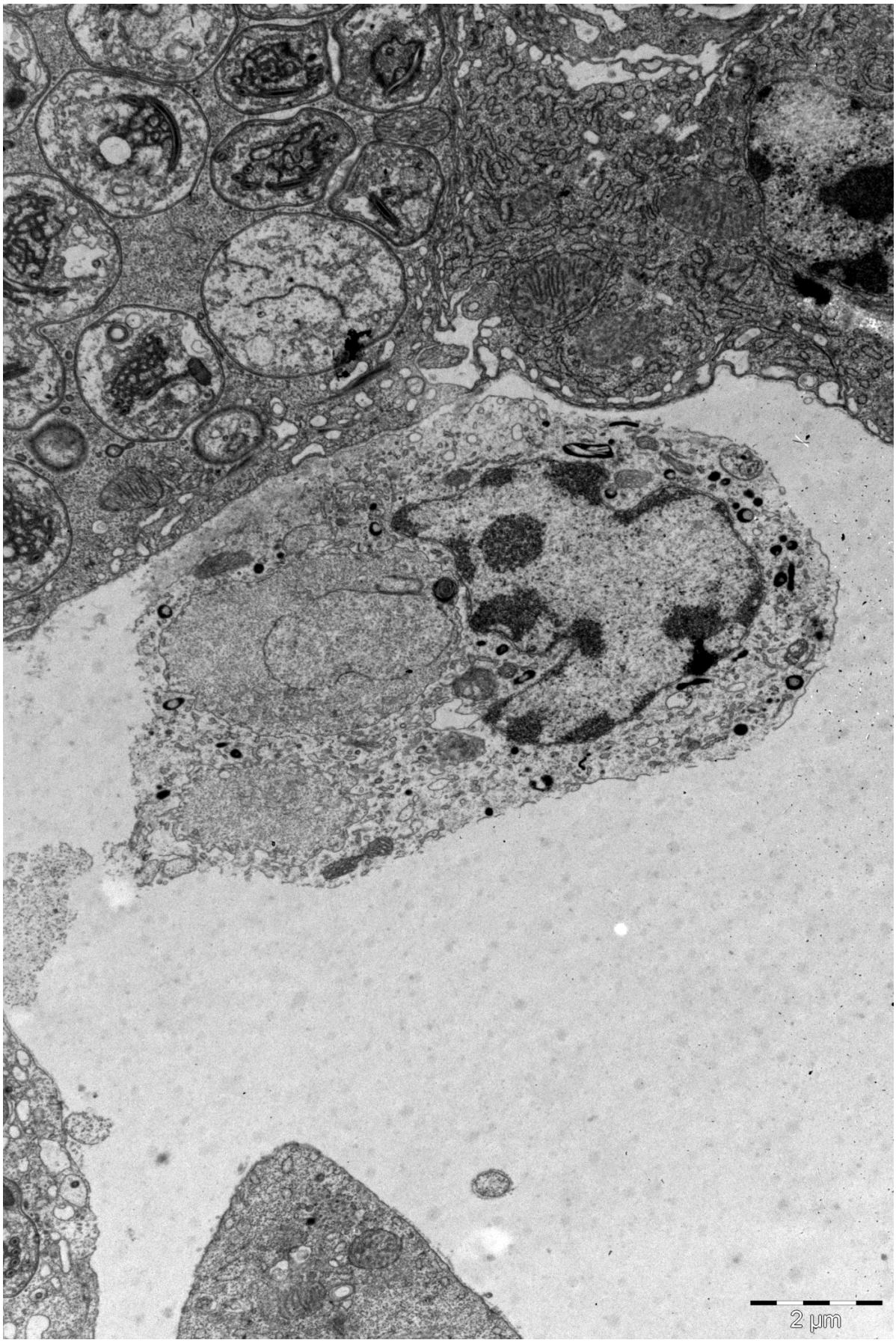

Figure 3.15 Haemocyte infected with a sporont of *P. theriodion*.

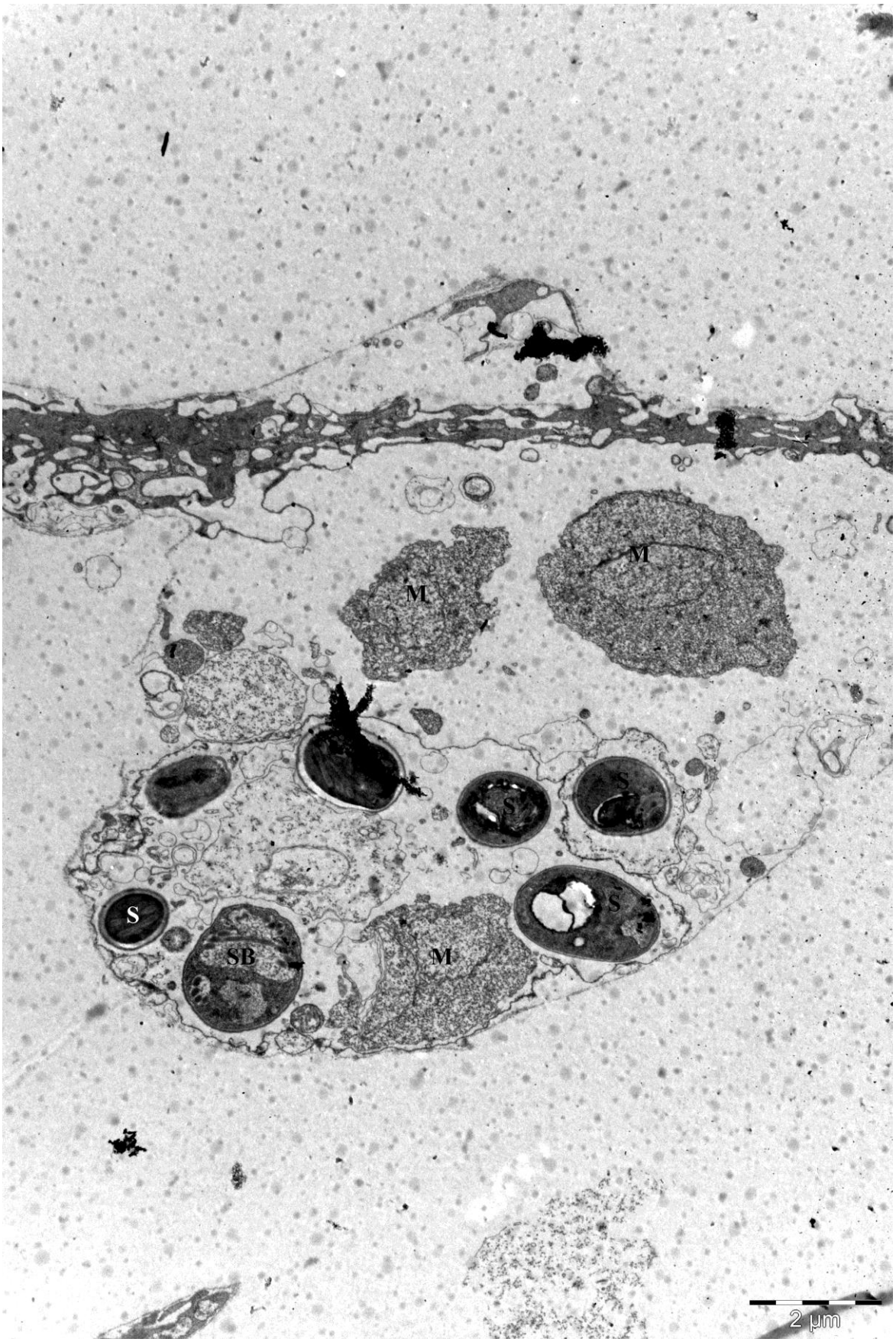

Figure 3.16 Connective tissue cell infected with *P. theridion*. Meronts (M), sporoblasts (SB) and mature spores (S) are observed.

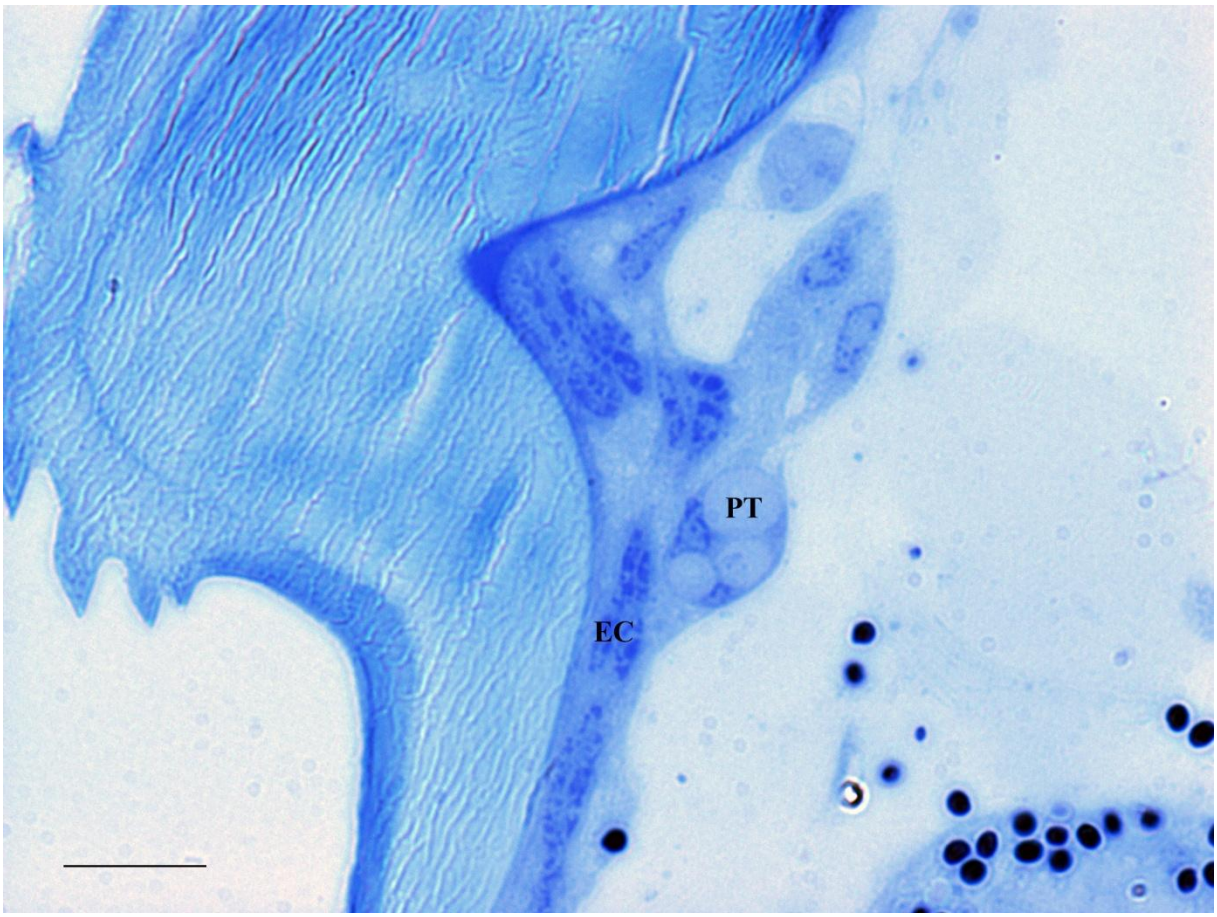

Figure 3.17 *P. theridion* (PT) infecting epithelial cells (EC) in an extremity of an adult female. Scale bar = 10 µm.

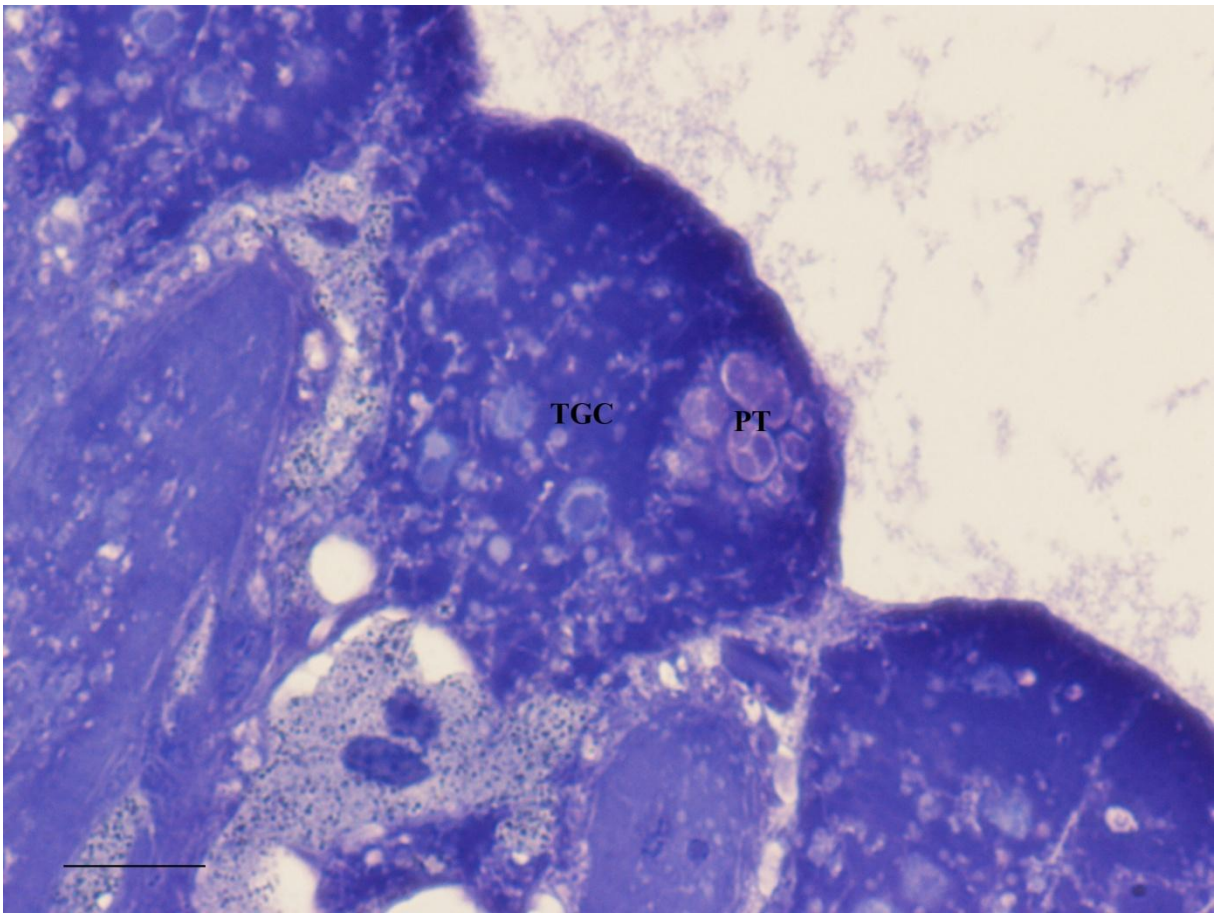

Figure 3.18 Tegmental gland cells (TGC) infected with *P. theridion* (PT). Scale bar = 10 µm.

Development of *P. theridion* in *L .salmonis*

The way of infection is uncertain, but spores have been observed in the lumen of the gut (Fig 3.19). Developmental stages of *P. theridion* are found in the cytoplasm of haemocytes (Fig 3.15), fibroblasts/fibrocytes (Fig 3.16), epithelial cells (Fig 3.17) and tegmental gland cells (Fig 3.18). Infected cells may become hypertrophic and *P. theridion* seems to induce the formation of a syncytium (Fig 3.12, 3.13 and 3.20). An infected cell may contain all the different developmental stages; meront, sporont, sporoblast and spore (Fig 3.21). The first observed developmental stage is meronts. The meronts contain a moderate amount of free ribosomes, a few ER-profiles and a diplokaryon. Their morphology varies from spherical with a single diplokaryon to multilobed plasmodia with several diplokarya (Fig 3.22 and 3.23). The meronts form a merogonial plasmodium by dividing its diplokaryotic nucleus to form several diplokarya. For each diplokaryon there will be formed a lobe and a daughter cell will derive from each lobe (Fig 3.23 and 3.24). During the merogonial stage fission of diplokarya is observed (Fig 3.25 and 3.26). Loss of the nuclear membrane is observed during the sporogonial stages (Fig 3.27 and 3.28) and cells with no visible diplo- or monokaryon have been found (Fig 3.29). Early sporonts are mainly diplokarotic or contain two closely arranged

monokarya and are distinguished from the meronts by an amorph substance on the plasmalemma and rough ER in the cytoplasma (Fig 3.30). Dissociation of diplokaryon is observed in the early sporonts (Fig 3.31 and Fig 3.32). In these cells synaptonemal complexes are observed in the nuclei which may have an incomplete nuclear membrane (Fig 3.28, Fig 3.30 and Fig 3.31). Membrane structures are observed between these dissociating diplokarya (Fig 3.31). Late sporonts are monokaryotic and may contain dense bodies, polar sac primordium, vacuole, polar tube primordium and early elements of golgi (Fig. 3.33). The sporonts may form sporogonial plasmodia and divide by shizogony (Fig. 3.33, 3.34 and 3.35). They may also divide by binary fission (Fig. 3.36). The sporoblasts were not well examined in this study but one could distinguish them from the sporonts by the more developed polar tube and golgi and a more dense sporoplasm (Fig 3.37). Dividing sporoblasts were not observed. The spore structure was not examined during this study.

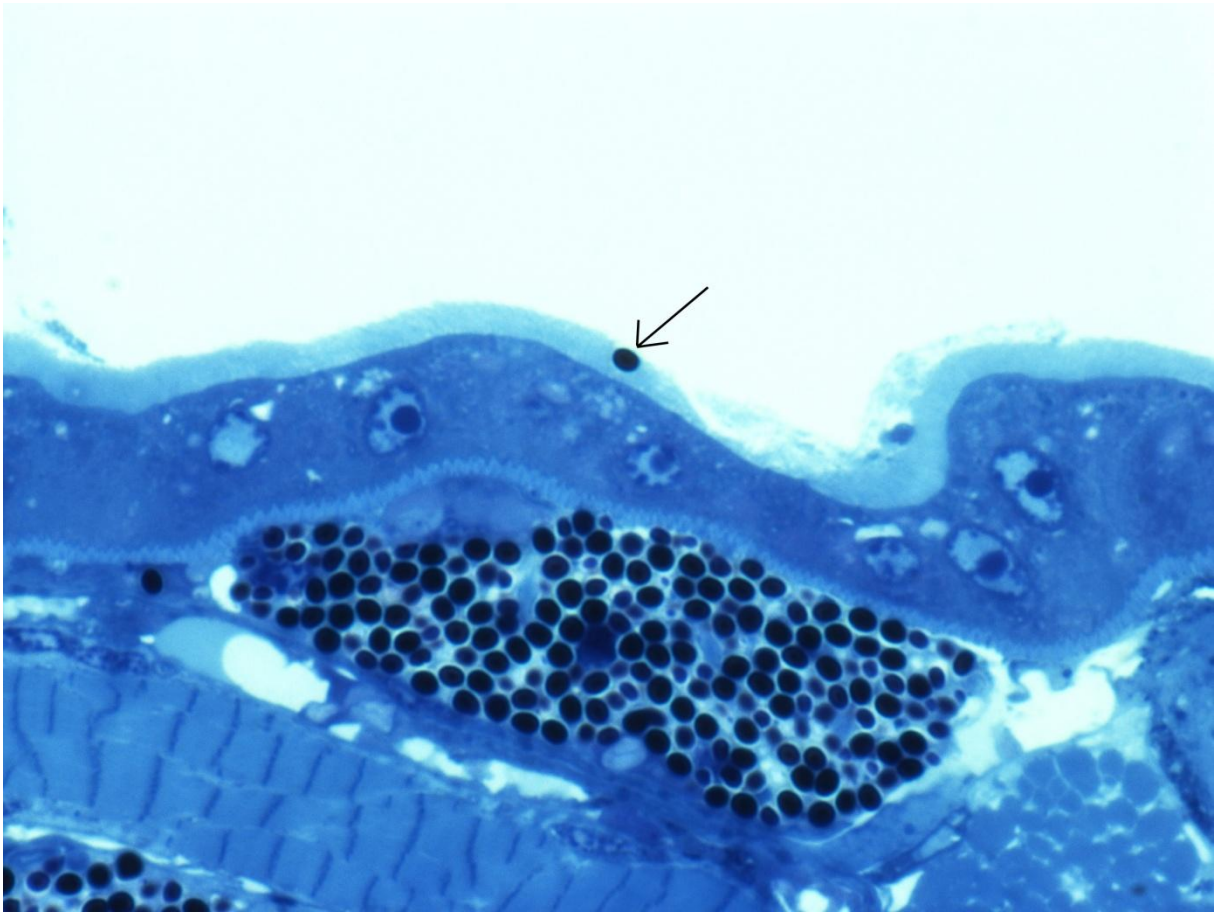

Figure 3.19 Spore located in the microvilli of gut epithelial cells

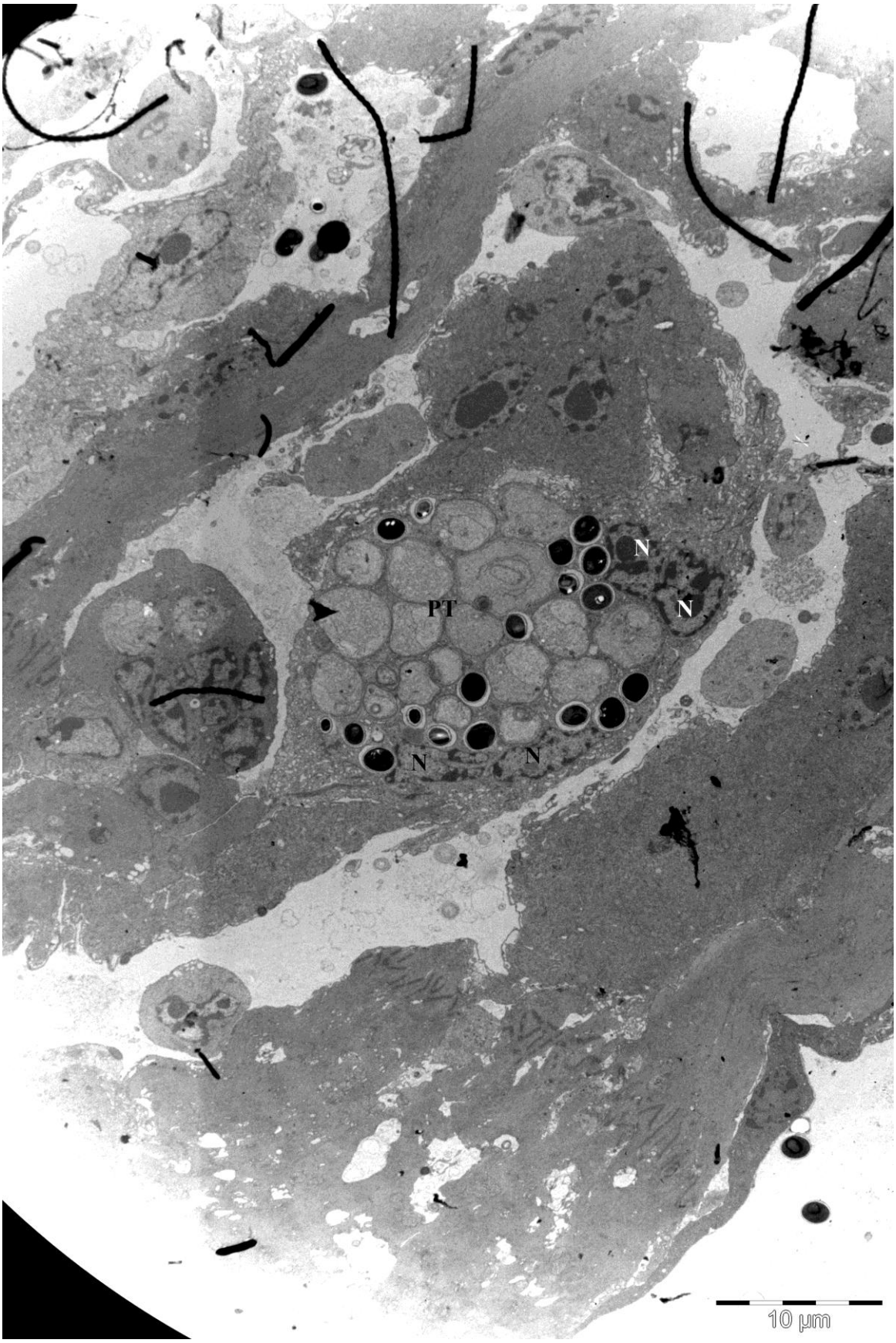

Fig 3.20 A syncytium containing several nuclei (N) caused by *P. theridion* (PT) infection.

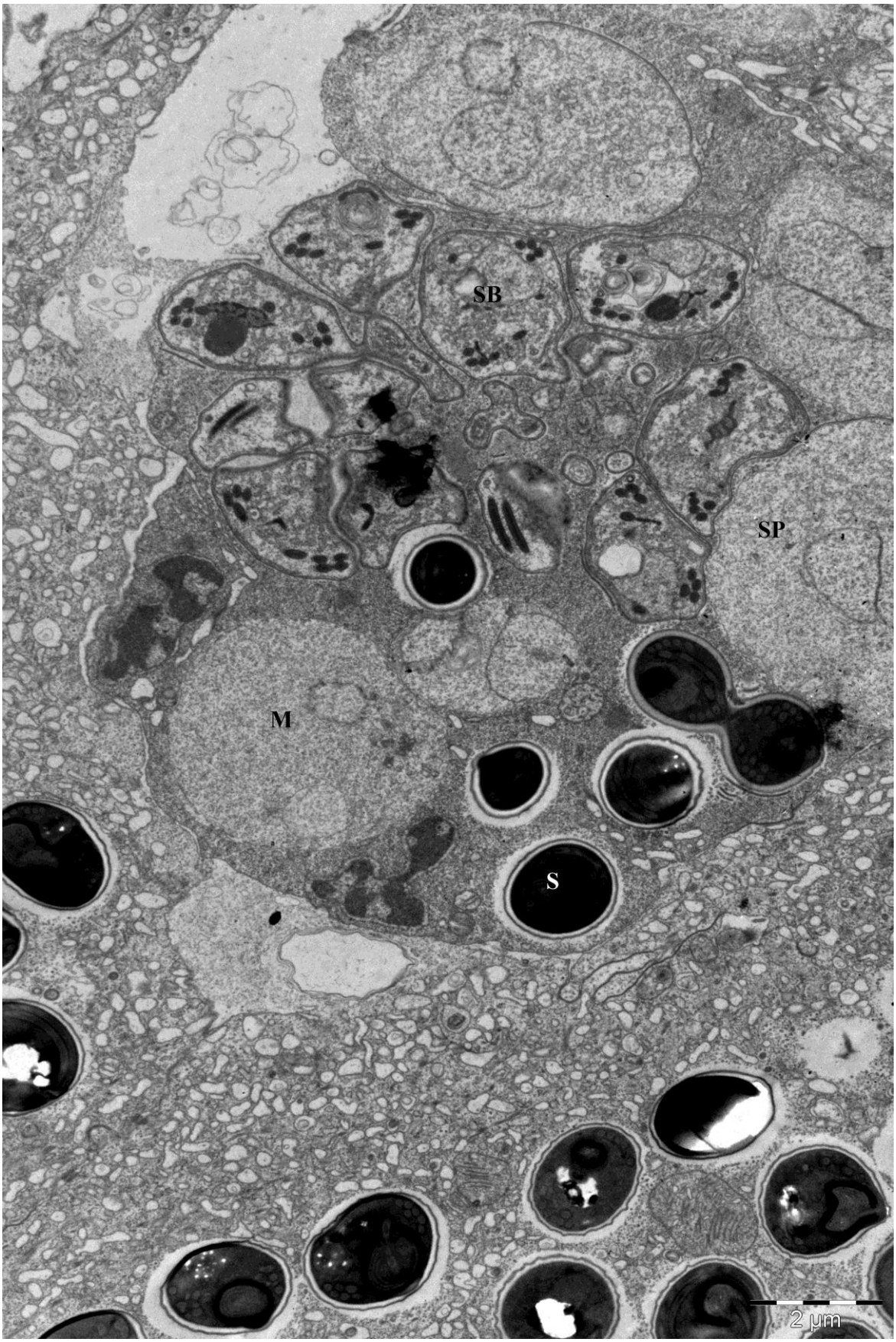

Figure 3.21 A target cell infected with meronts (M), sporonts (SP), sporoblasts (SB) and spores (S) of *P. theridion*.

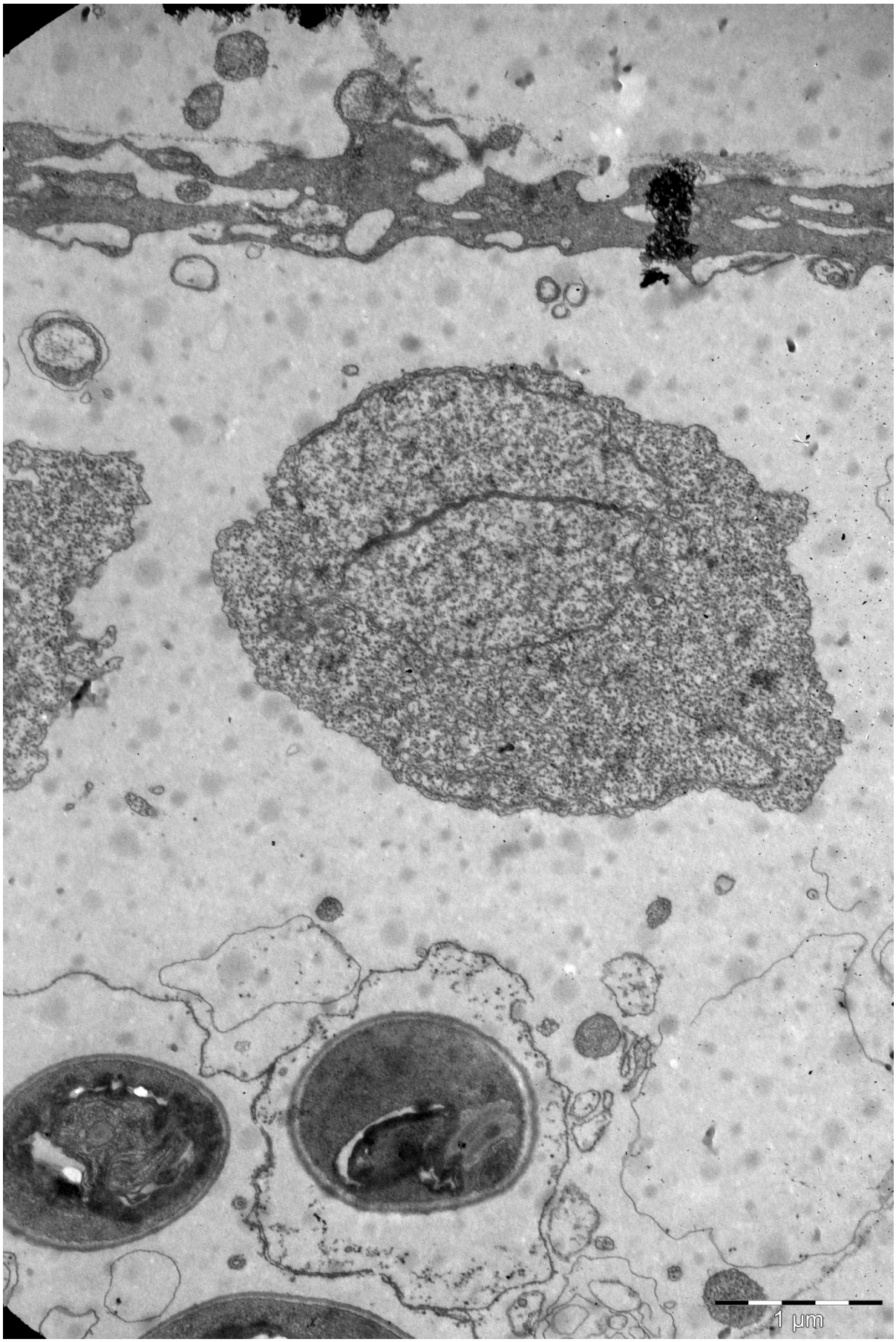

Figure 3.22 A spherical meronts of *P. theridion* containing a single diplokaryon

Figure 3.23 A multilobed plasmodia (MP) of *P.theridion* in the transition between meront and sporont. Diplokarya (DK) are located in the lobes.

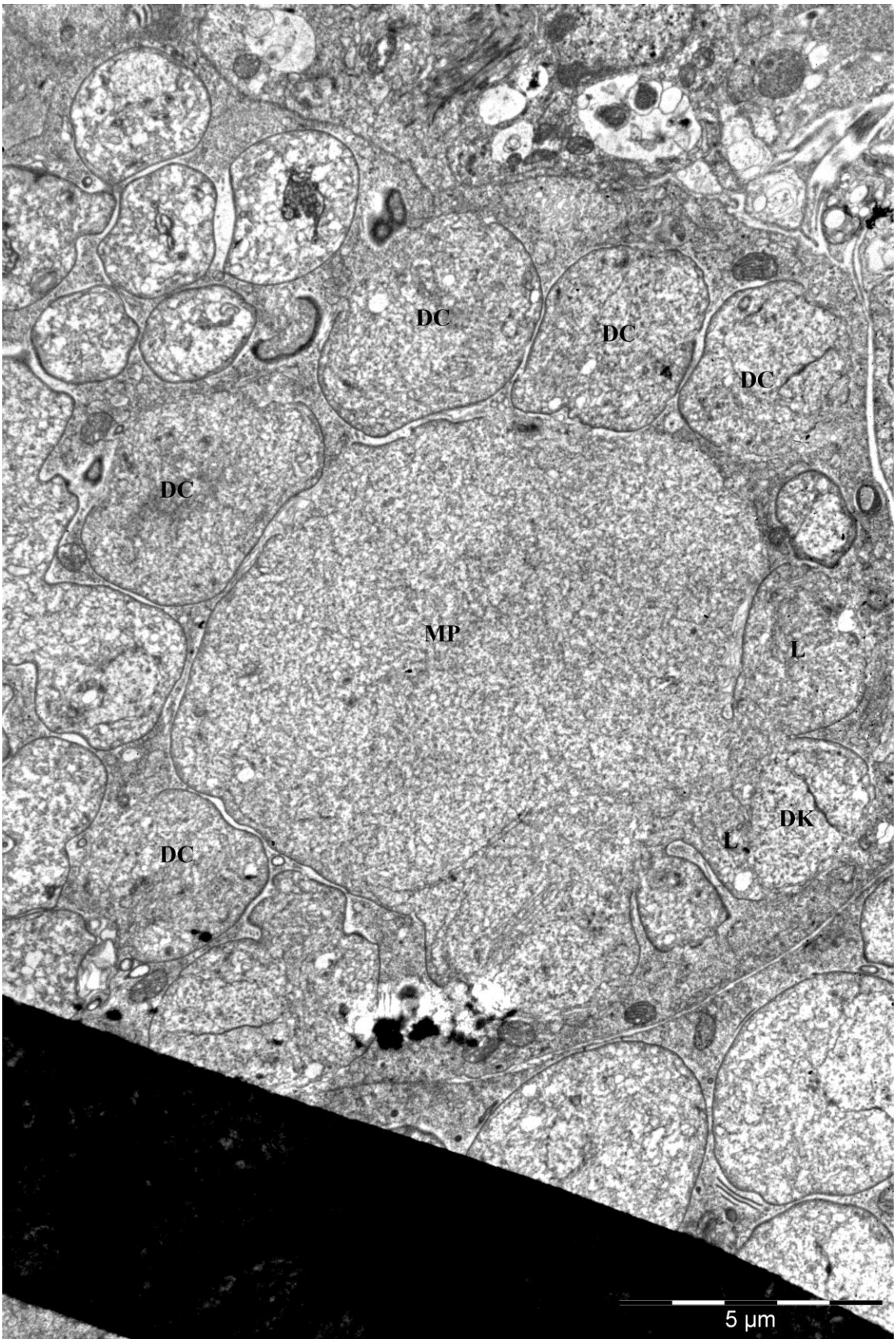

Figure 3.24 A multi lobed plasmodium (MP) of *P. theridion* in the transition between meront and sporont. Lobes (L) with diplokaryon (DK) and nearby daughter cells (DC) are present.

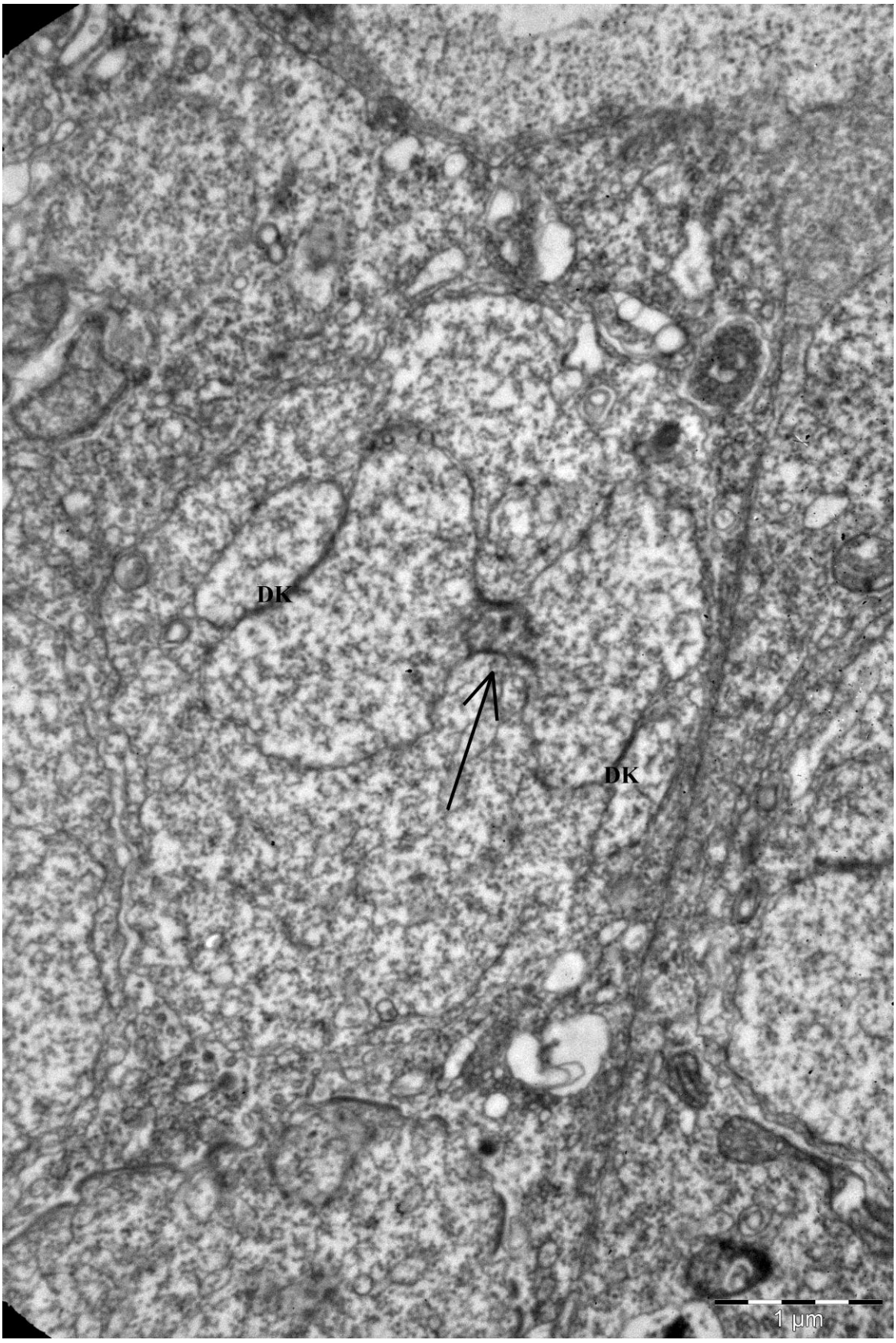

Figure 3.25 A meront of *P. theridion* where fission of diplokarya (DK) occur (arrow).

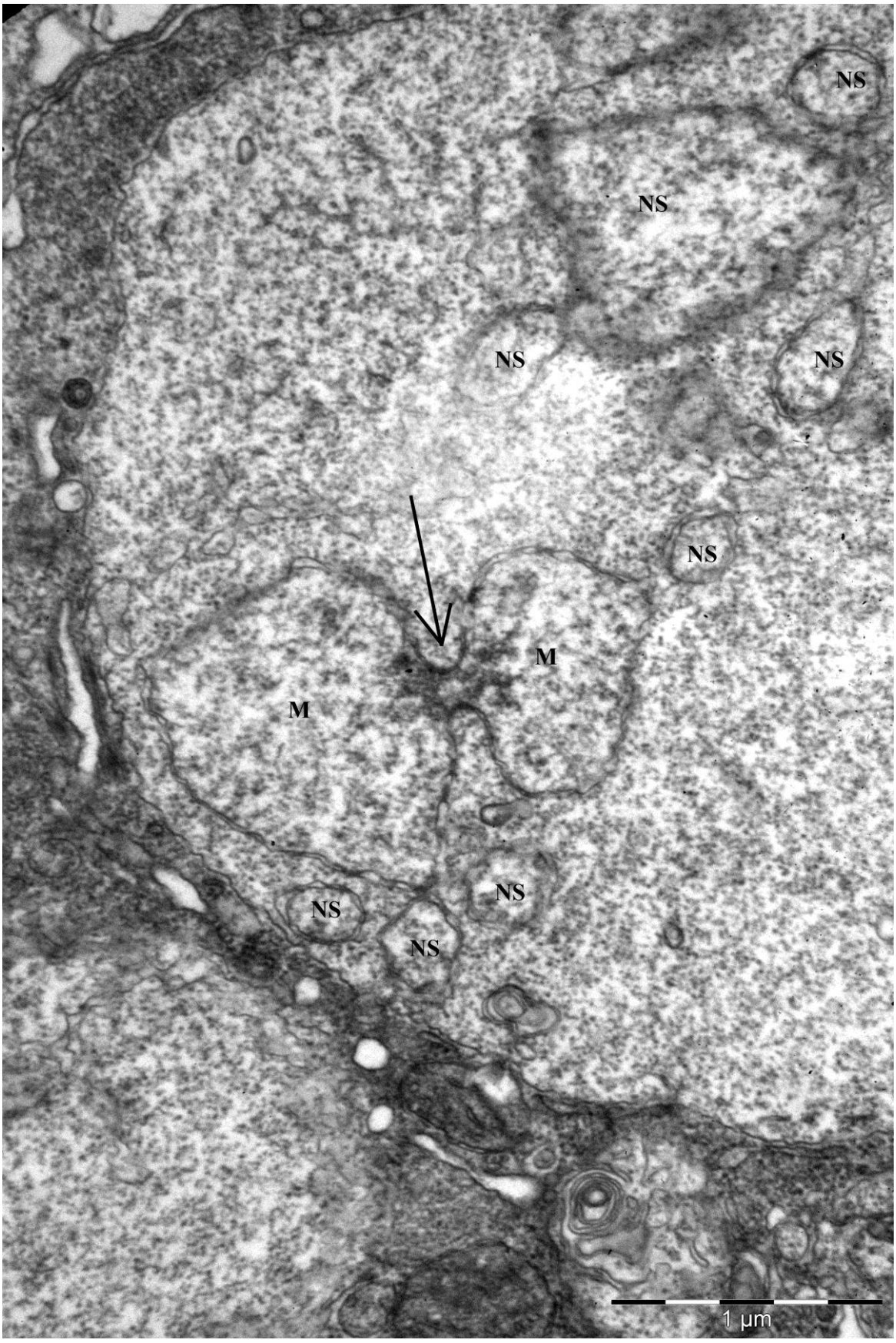

Figure 3.26 Fission (arrow) of a monokaryon (M) or a diplokaryon in a meronts of *P. theridion*. Other nuclear structures (NS) are observed.

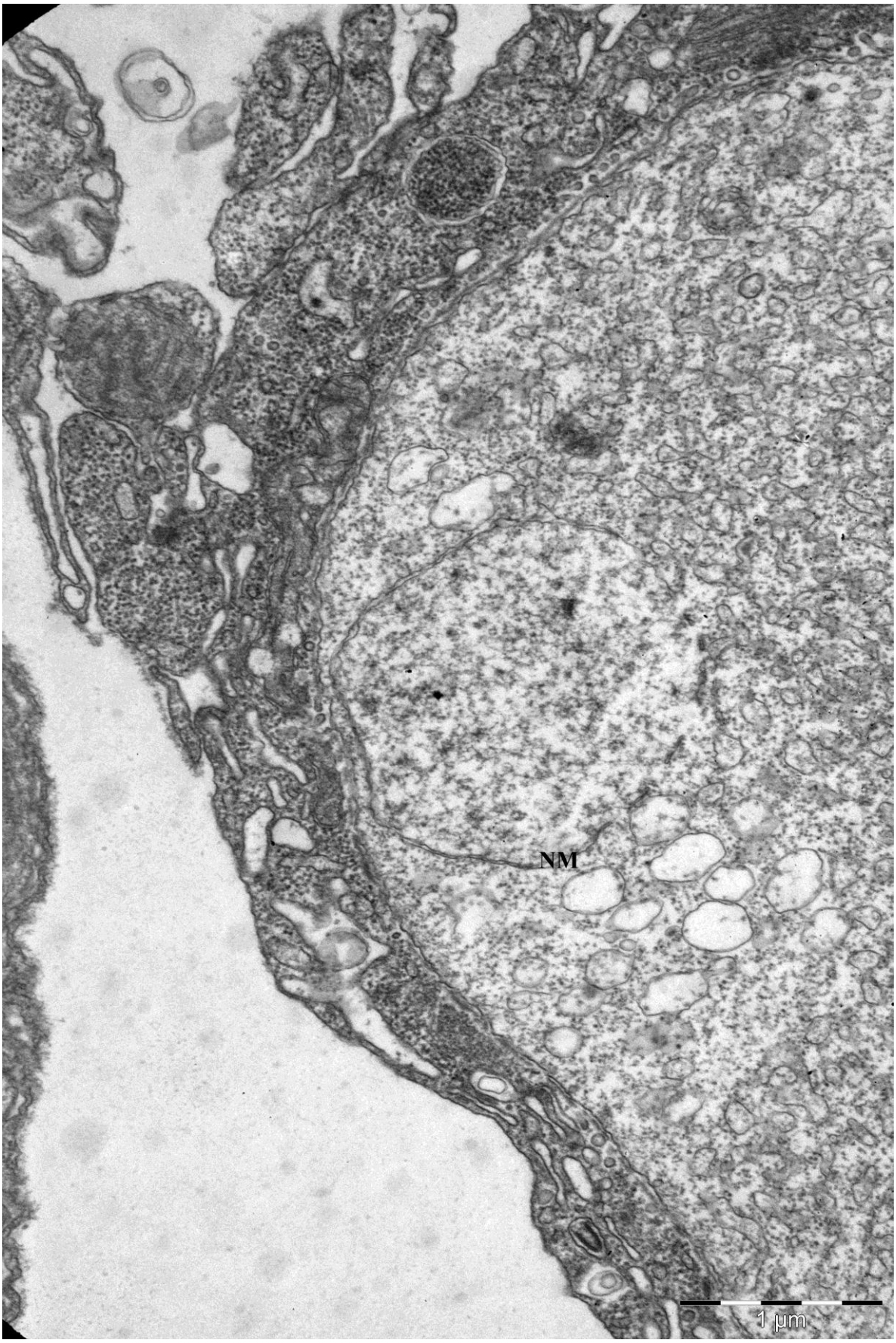

Figure 3.27 Loss of nuclear membrane (NM) in a sporont of *P. theridion*.

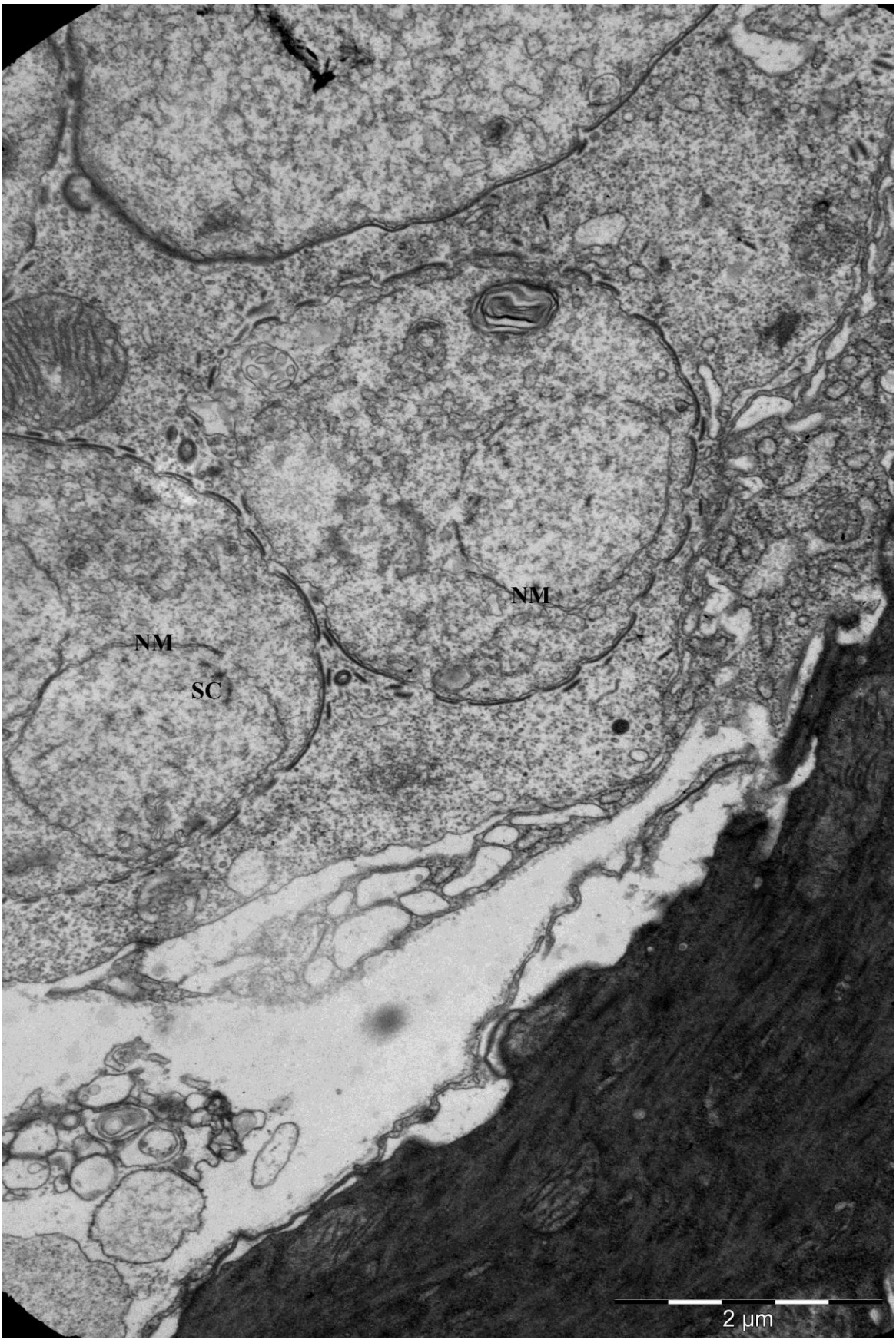

Figure 3.28 Loss of nuclear membrane (NM) in *P. theridion* sporonts. Synaptonemal complexes (SC) are present in the nucleus.

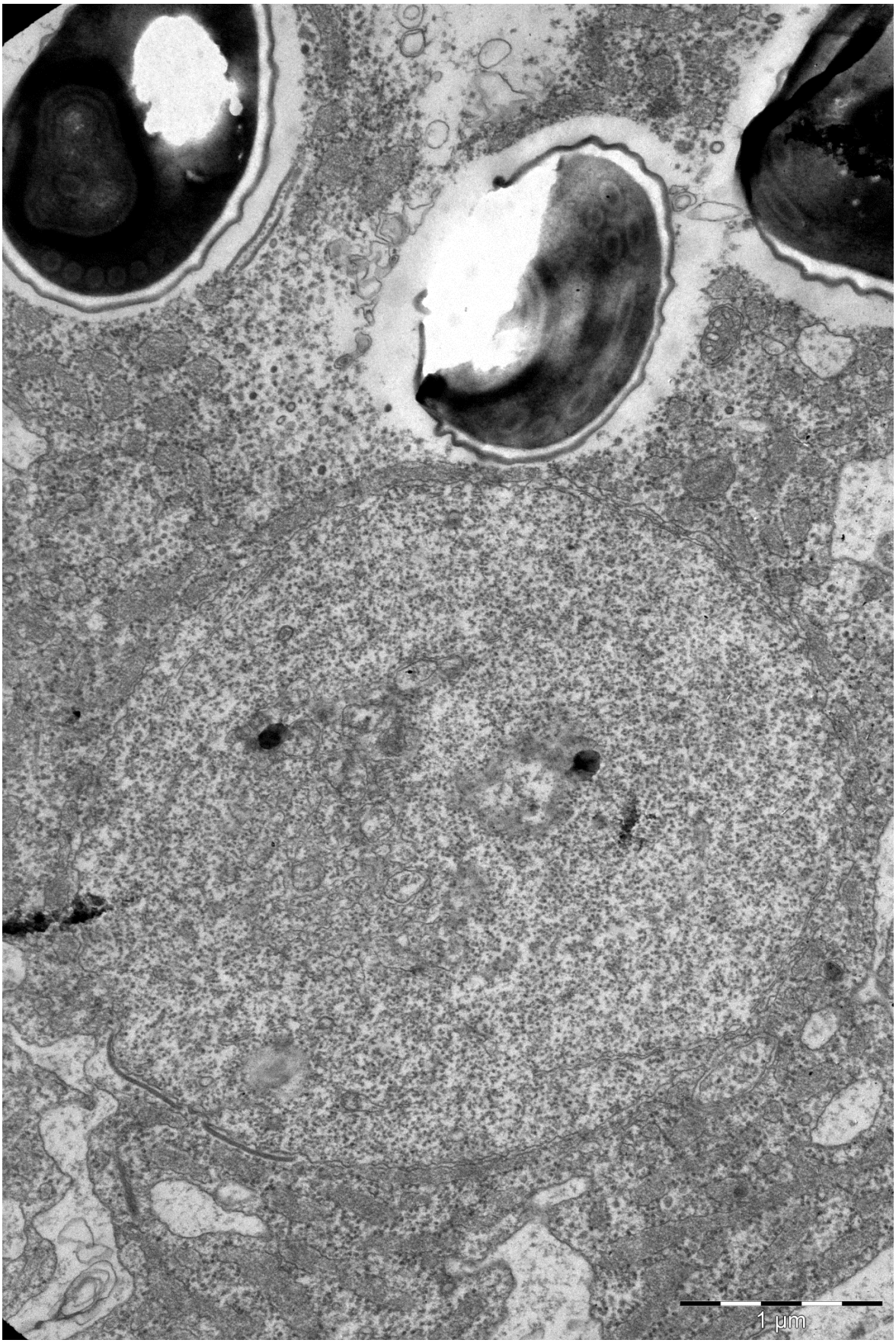

Figure 3.29 A large *P. theridion* cell in the transition between meront and sporont with no visible nuclei.

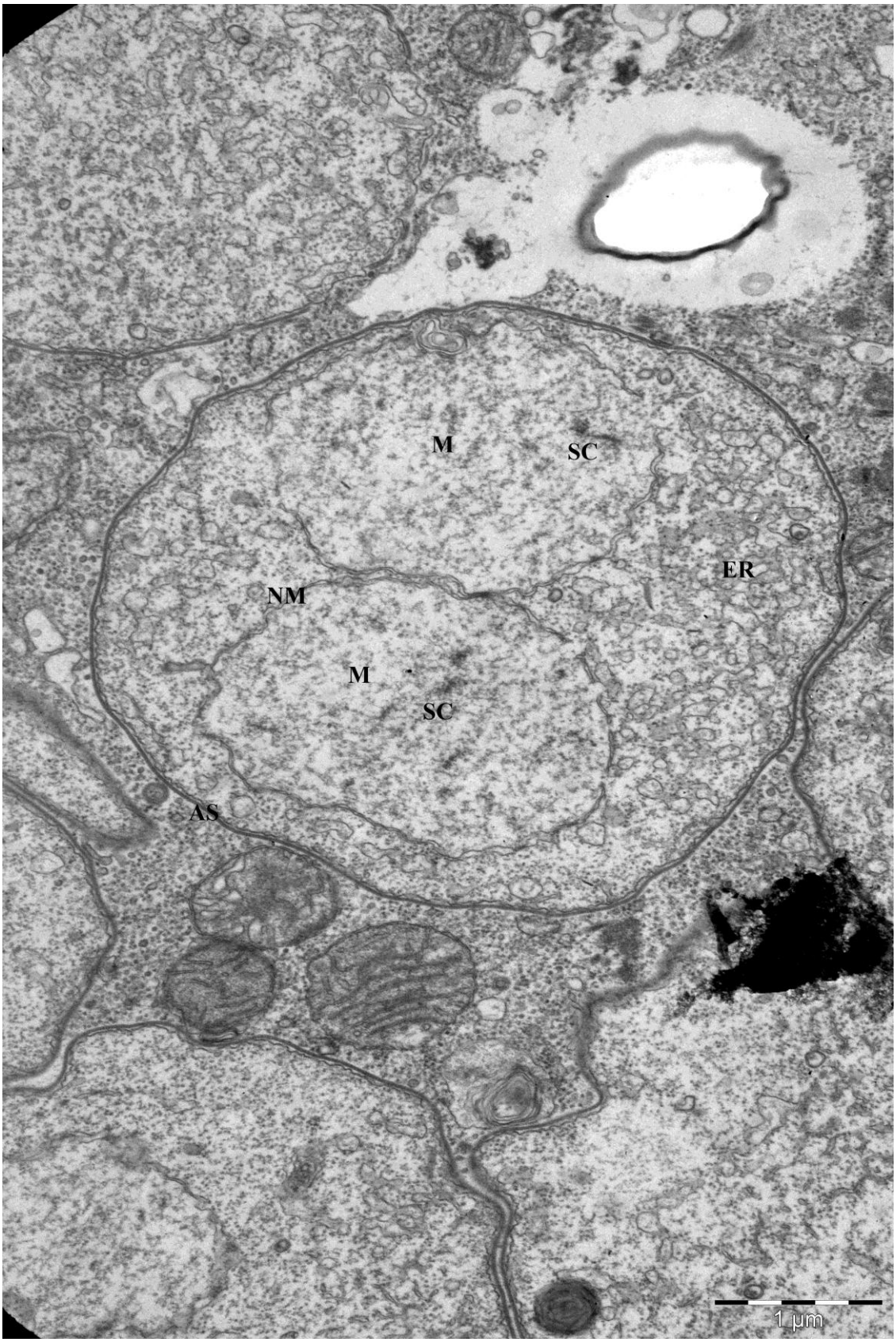

Figure 3.30 An early *P. theridion* sporont with an amorph substance (AS) on the plasmalemma, ER-profiles (ER) and a two closely arranged monokarya (M). The nuclear membrane (NM) is not complete and synaptonemal complexes (SC) are present.

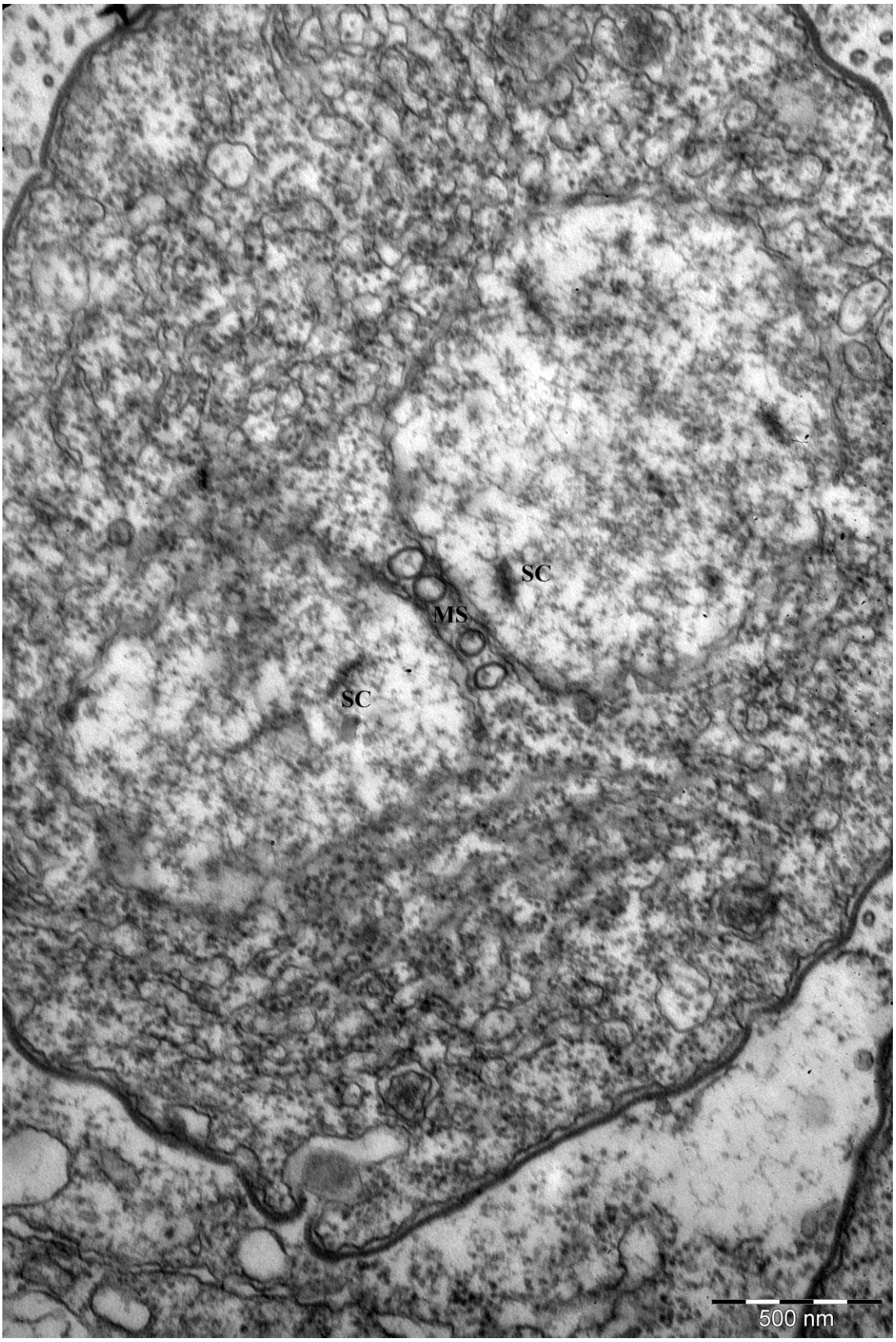

Figure 3.31 Disassociating diplokaryon in an early sporont of *P. theridion*. Membrane structures (MS) are observed between the disassociating diplokaryon. Synaptonemal complexes (SC) are present in the nuclei.

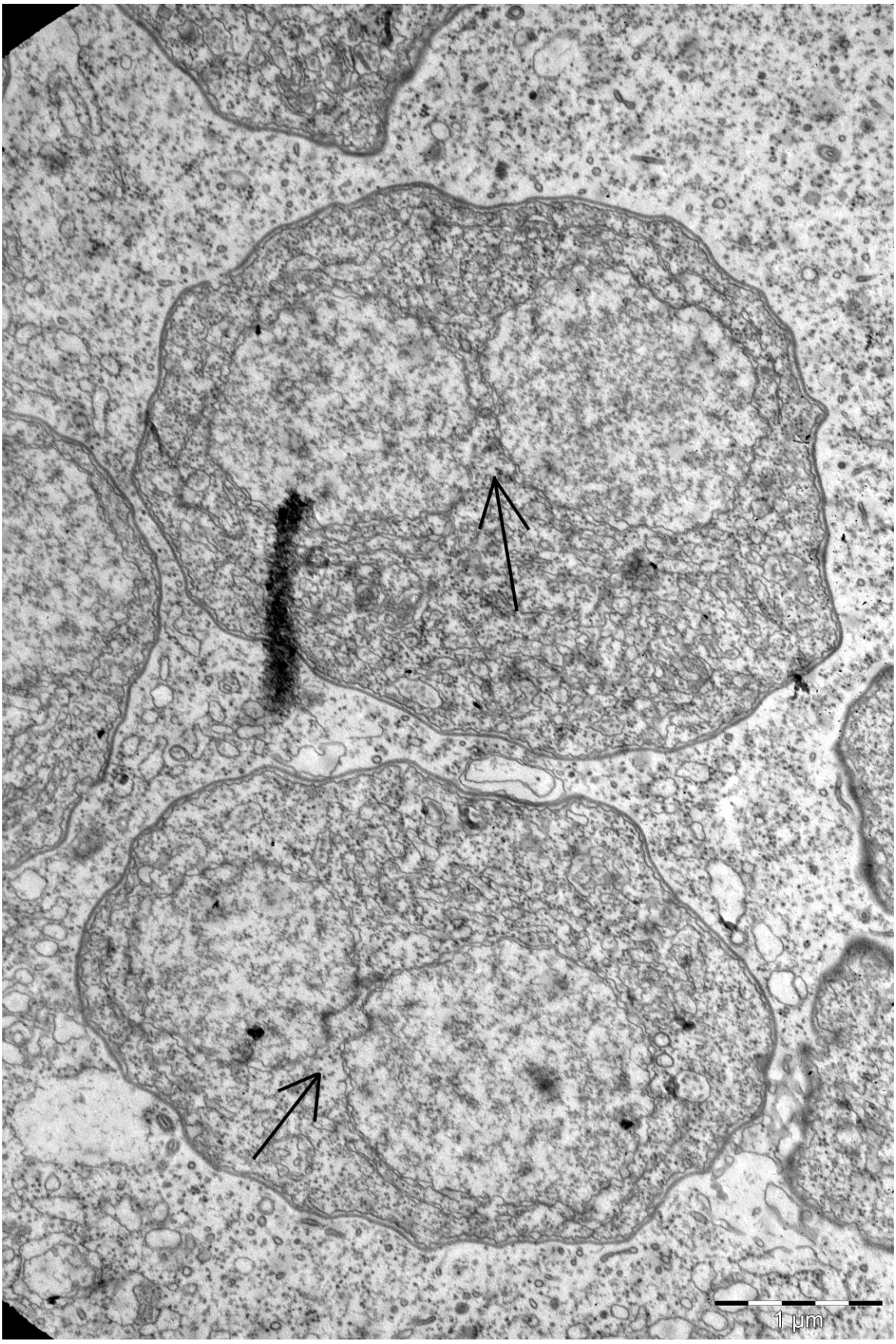

Figure 3.32 Disassociating diplokarya (arrows) in early *P. theridion* sporonts.

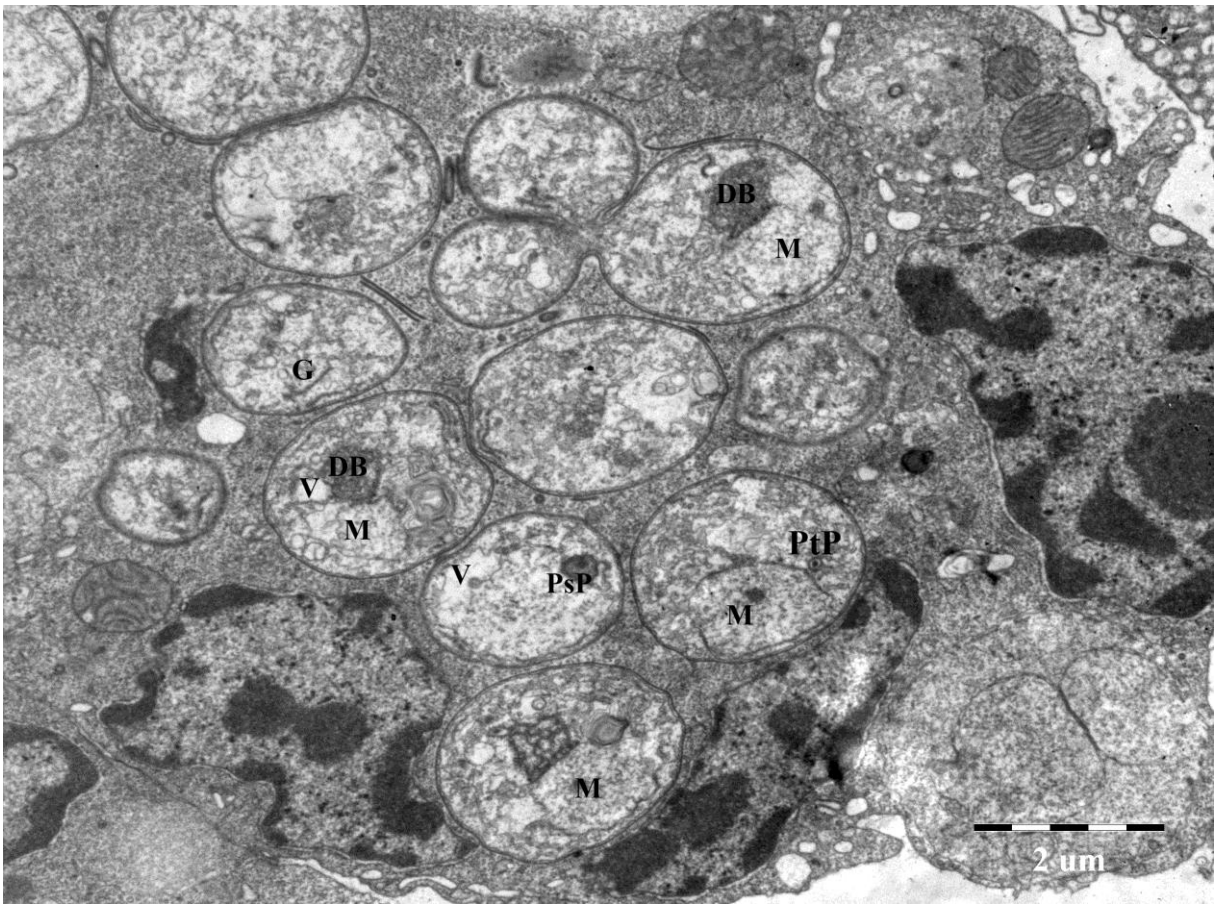

Figure 3.33 Late sporonts of *P. theridion* with a cytoplasm containing a monokaryotic nucleus (M), dense bodies (DB), polar sac primordium (PsP), vacuole (V), polar tube primordium (PtP) and early elements of golgi (G).

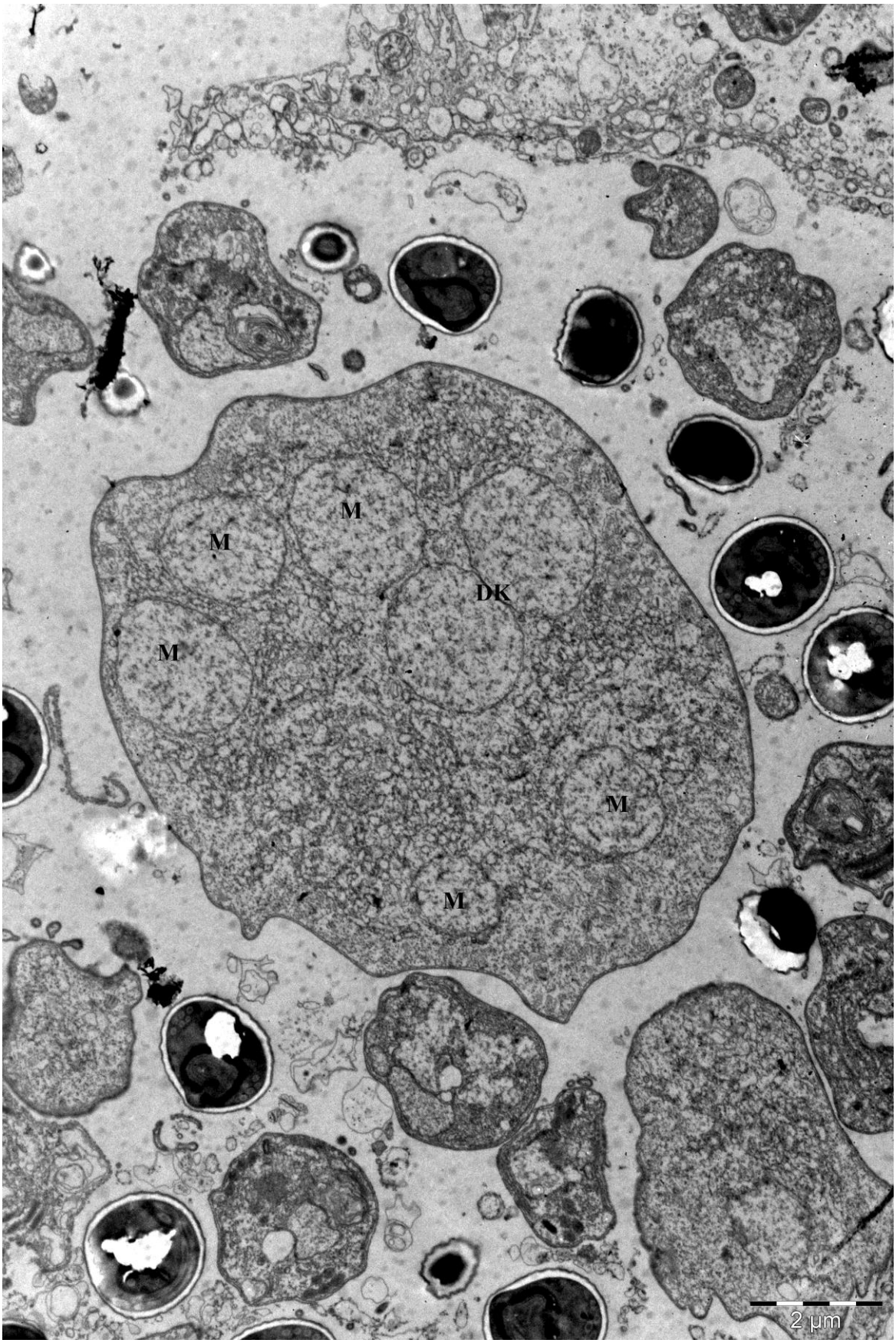

Figure 3.34 Sporogonial plasmodium of *P. theridion* containing several possible monokarya (M) and a single diplokaryon (DK)

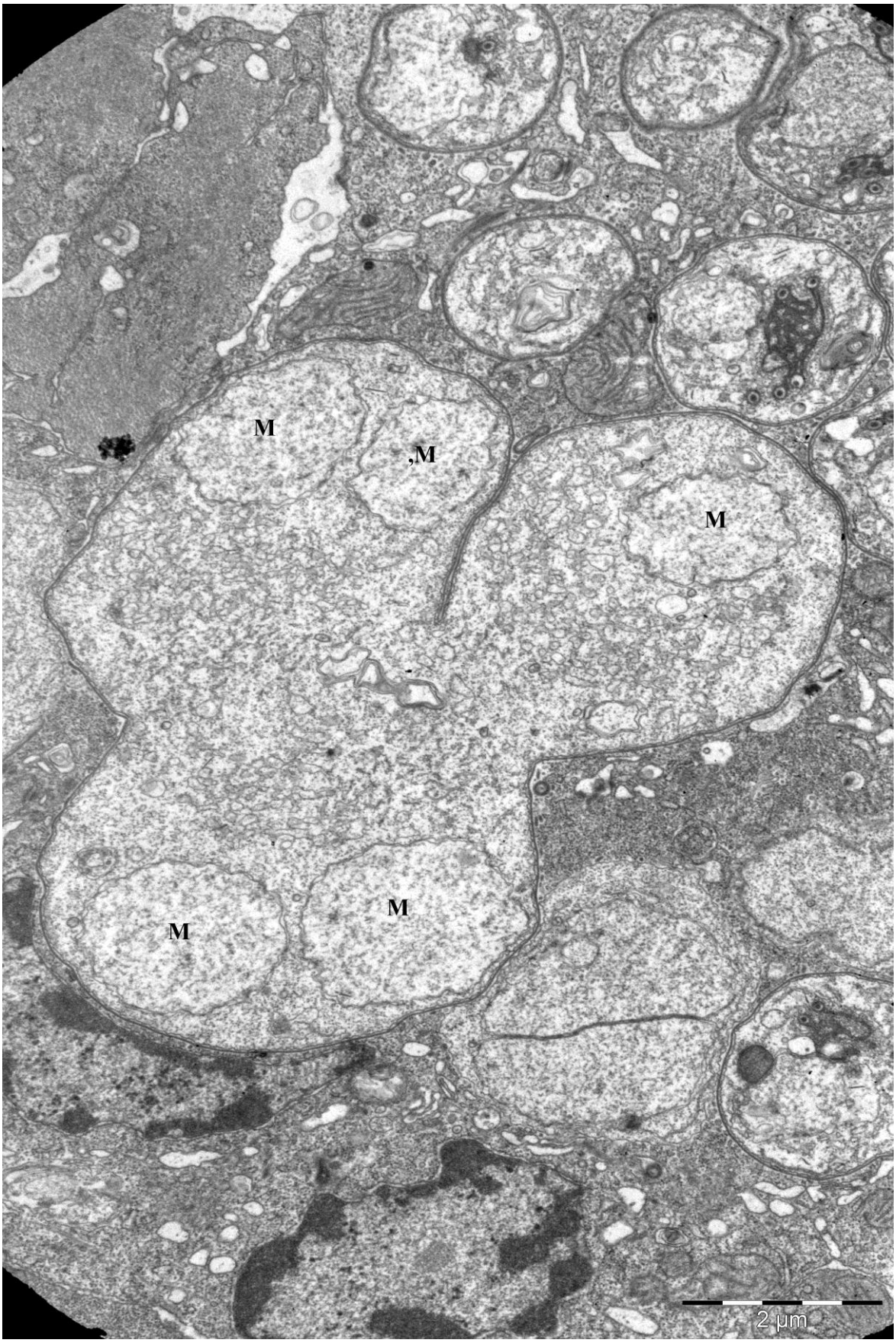

Figure 3.35 A multilobed sporogonial plasmodium of *P. theridion* containing several monokarya (M).

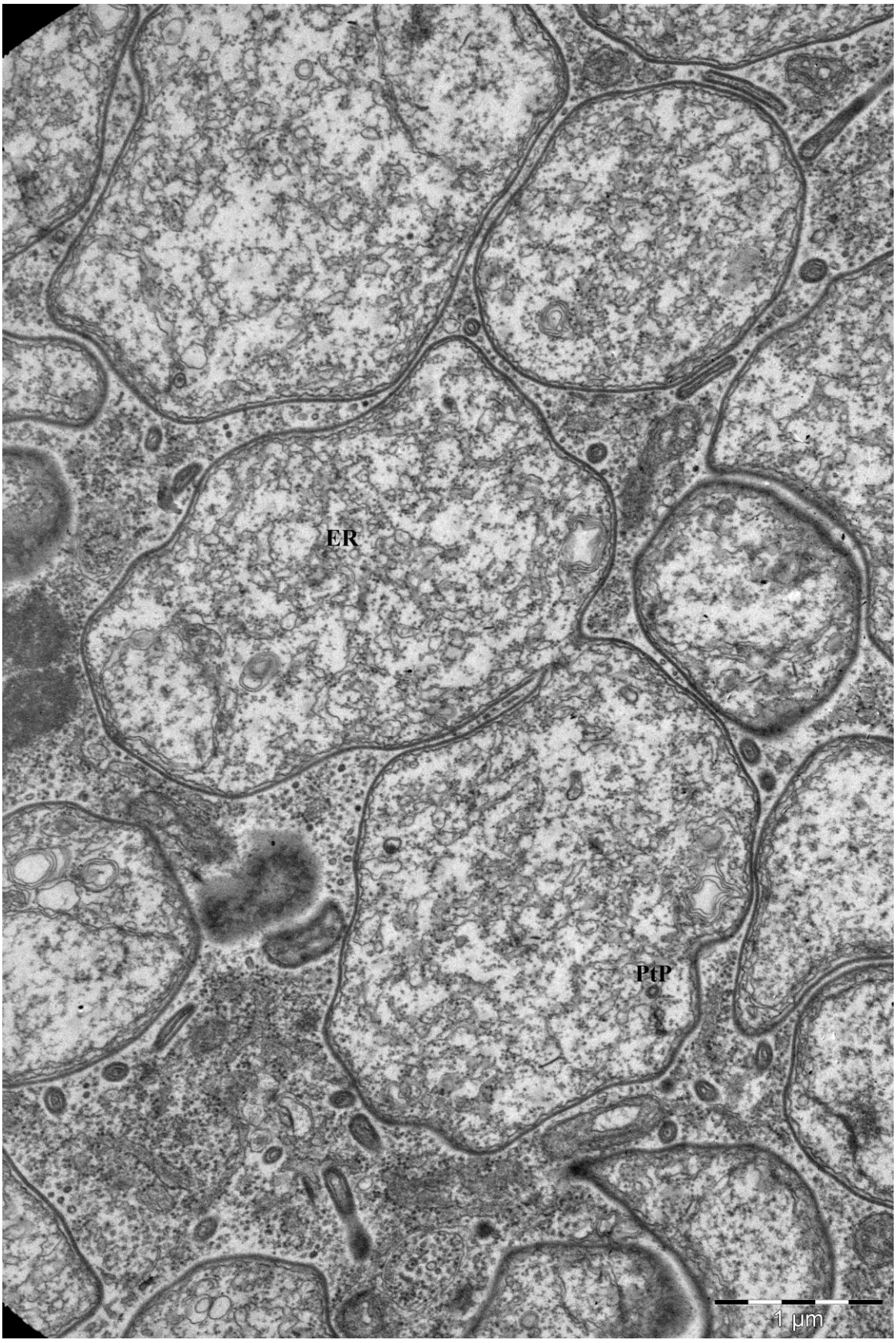

Figure 3.36 Late sporont of *P. theridion* undergoing binary fission. ER (ER) and polar tube primordium (PtP) are observed.

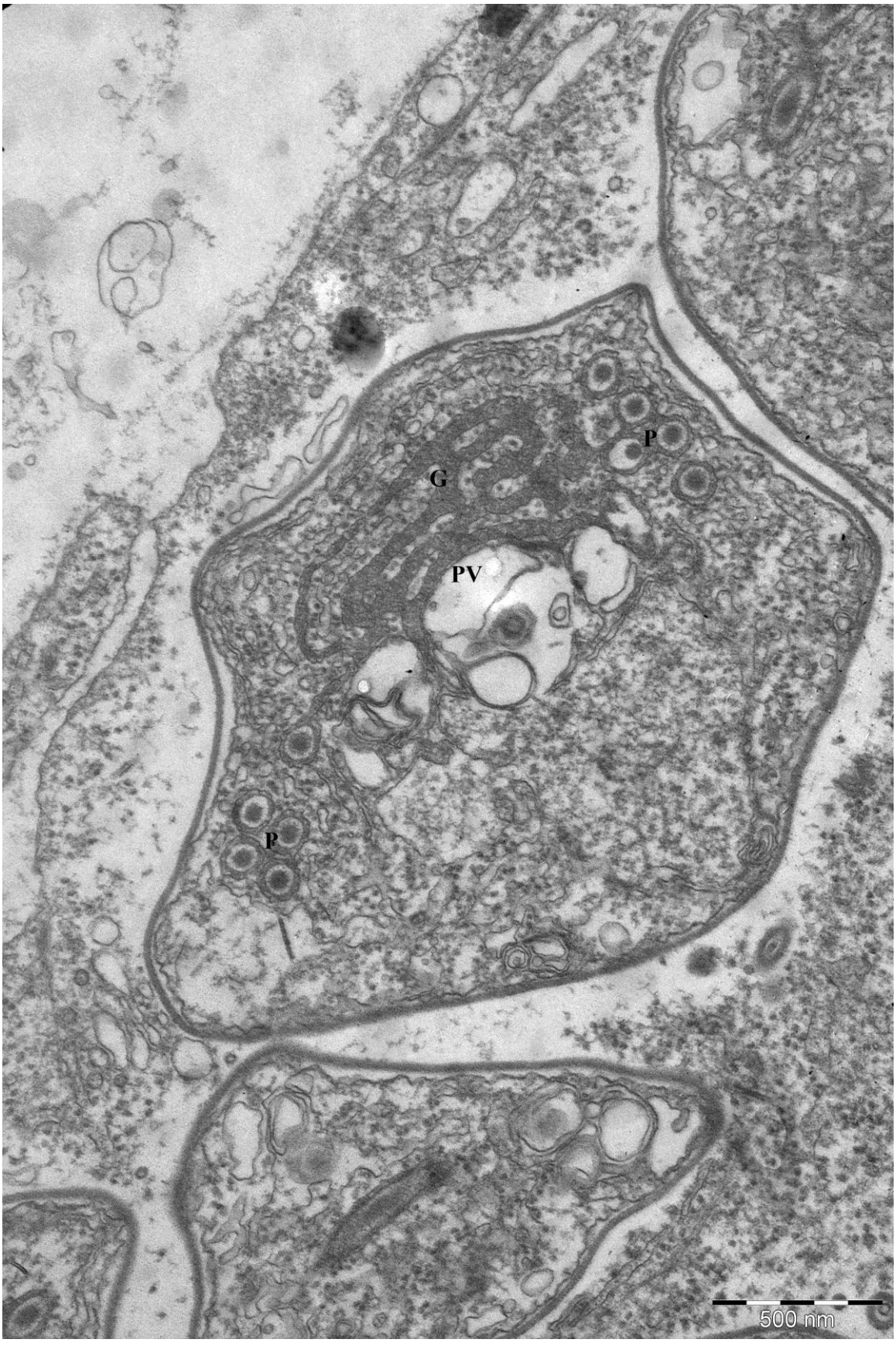

Figure 3.37 A *P. theridion* sporoblast with a dense cytoplasm containing golgi (G), polar tube (P) and a posterior vacuole (PV)

Presence of *P. theridion* in *C. centrodonti* and in *L. salmonis* from rainbow trout

Three *C. centrodonti* tested positive for *P. theridion* with Ct-values of 34,6, 34,0 and 36,8. Sequencing these samples by using *P. theridion* specific primers gave no matching sequence. 19 out of 30 salmon lice obtained from rainbow trout tested positive for *P. theridion*. The intensity of *P.theridion* was Ct= 37.1 (ELF-LS Ct= 12.0).

Other agents associated with *L. salmonis* and *C. centrodonti*

An infection of the gut was observed in a *L. salmonis* in the second preadult stage (Fig 3.38). The infection seems to cause necrosis of the gut epithelial cells (Fig 3.39). Karyorrhexis of the epithelial cell nuclei were observed (Fig 3.40). Bacteria were observed in close vicinity of the necrotic cells (Fig 3.39 and Fig 3.40).

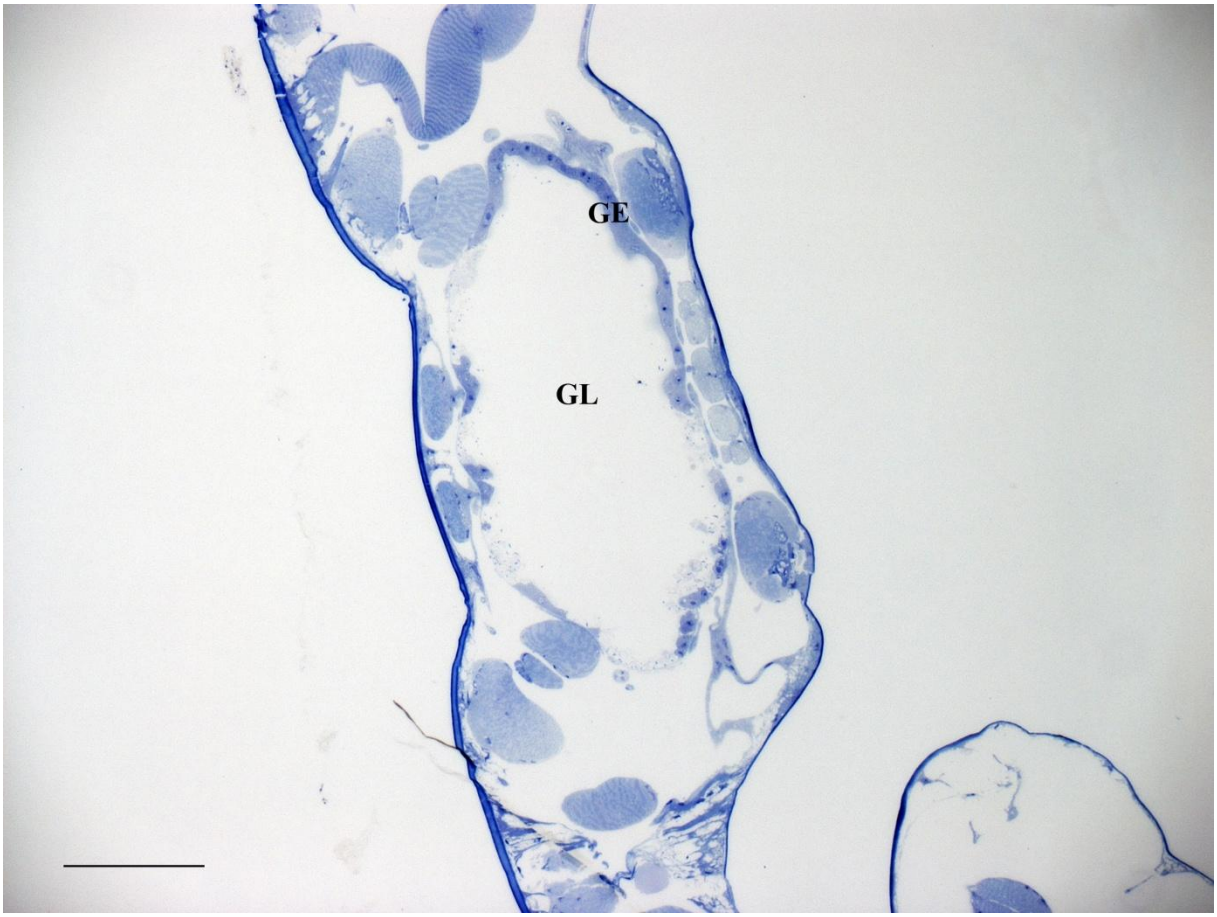

Figure 3.38 An infection of the gut of a second preadult female salmon lice. Only half of the gut epithelium remains. Scale bar= 100µm

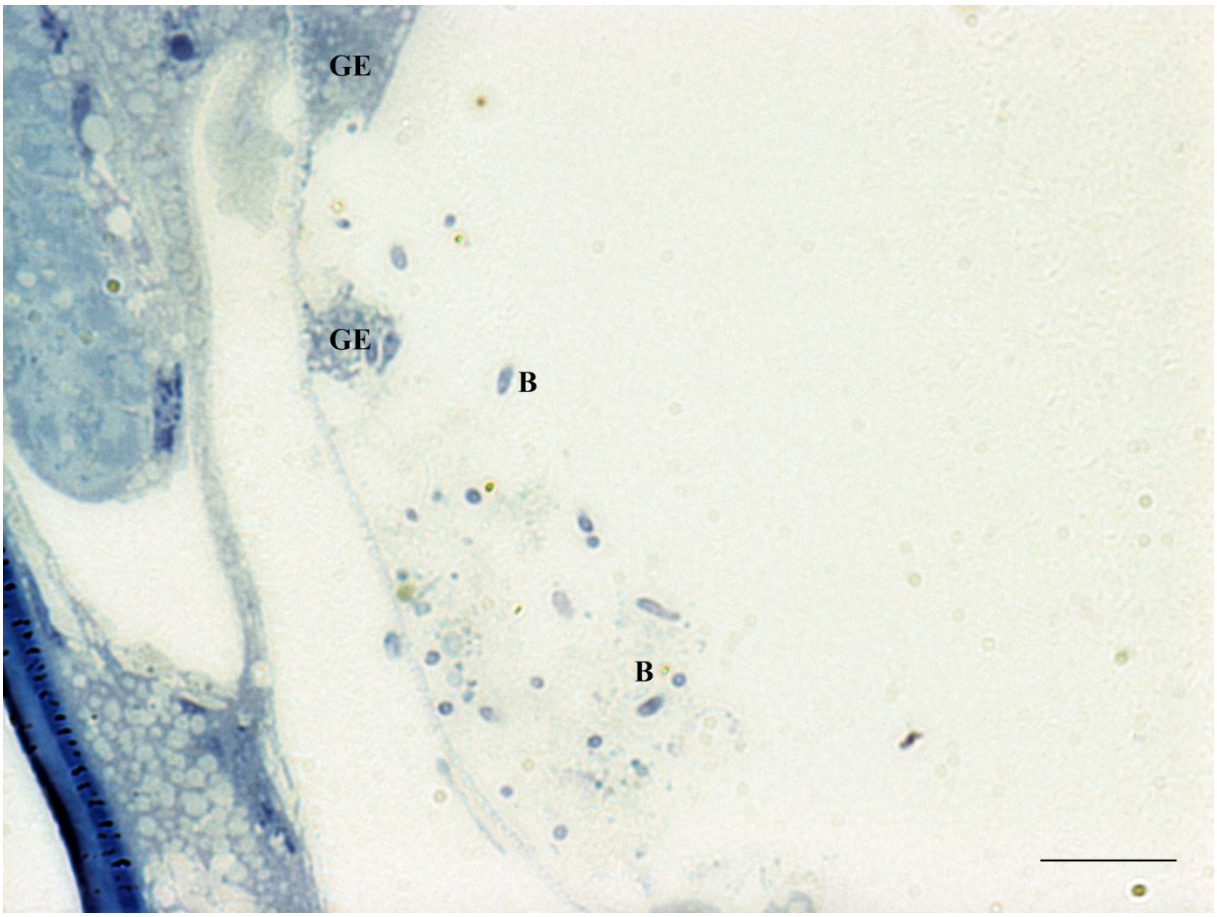

Figure 3.39 Necrosis of gut epithelial cell (GE). Bacteria (B) are observed. Few remaining gut epithelial cells are visible. Scale bar= 10µm

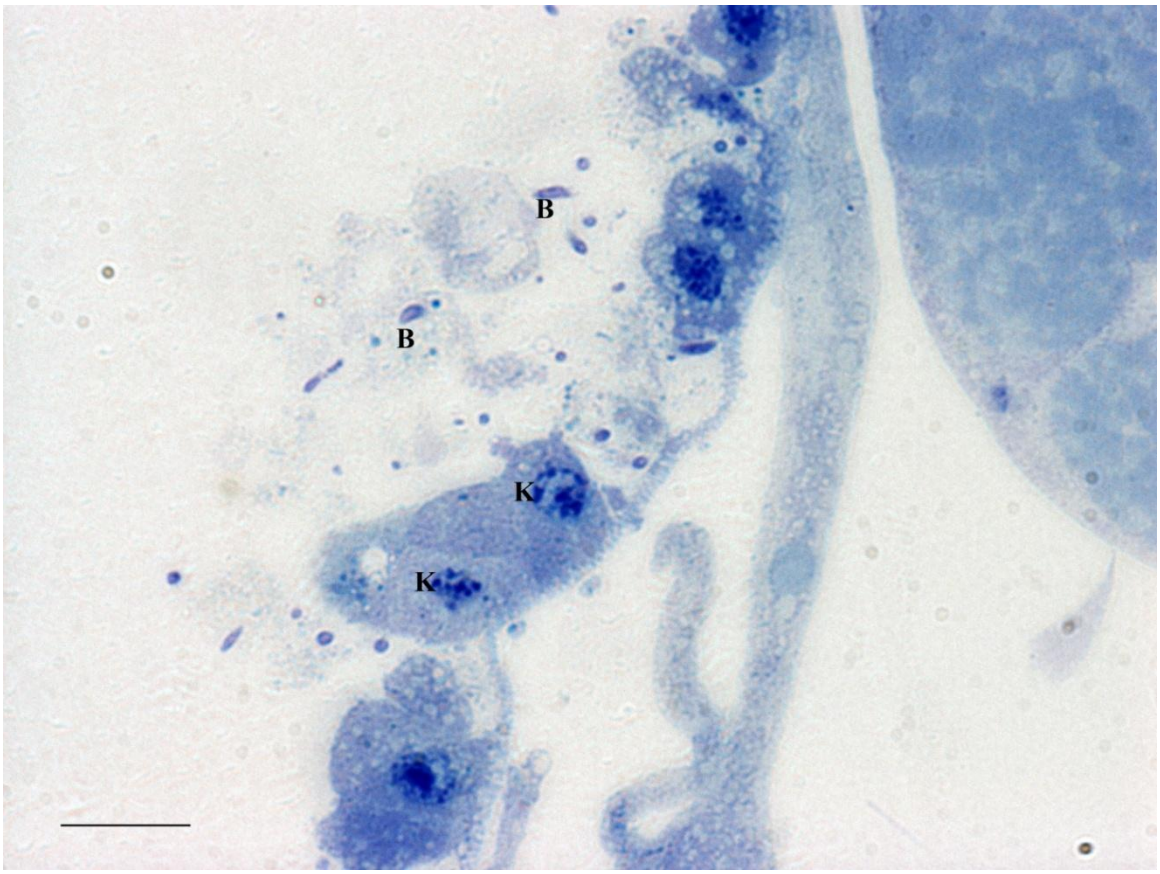

Figure 3.40 Necrosis of gut epithelial cells. Karyorrhexis (K) is observed in the nucleus of necrotic epithelial cells. Bacteria are observed in close vicinity of the necrotic cells. Scale bar = 10µm.

During visual examination of salmon lice for the presence of *P. theridion* inclusions near one or both second antennae were noticed. These inclusions were thought to be caused by *P. theridion* and were therefore registered as weak infections of *P. theridion* in the period from December 2009 to February 2012. Figure 3.41 presents these registrations and they show that the prevalence of these inclusions may be as high as 59,8 % and there is a trend of highest prevalence from December to March. Inclusions from three lice were cut out and tested for the presence of *P. theridion*, however *P.theridion* were not detected in one of the inclusions and the Ct values for *P. theridion* from the two other inclusions were 39.0 and 29.9 (ELF-LS = 14.8 and 13.5). When studied under light microscopy necrosis of gonadal tissue was observed (Fig 3.42 and Fig 3.43). An infiltration of haemocytes is observed and there is an encapsulation of the infected cells. Virus-like particles, viroplasm-like structures and crystalline structures were detected in infected cells (Fig 3.44, Fig 3.45, Fig 3.46 and Fig 3.47). The diameter of the virus-like particles was approximately 40 nm. Later Real time RT-PCR testing of the inclusions showed that these lice tested positive for Piscine Reovirus (PRV) with Ct-values of 35-36.

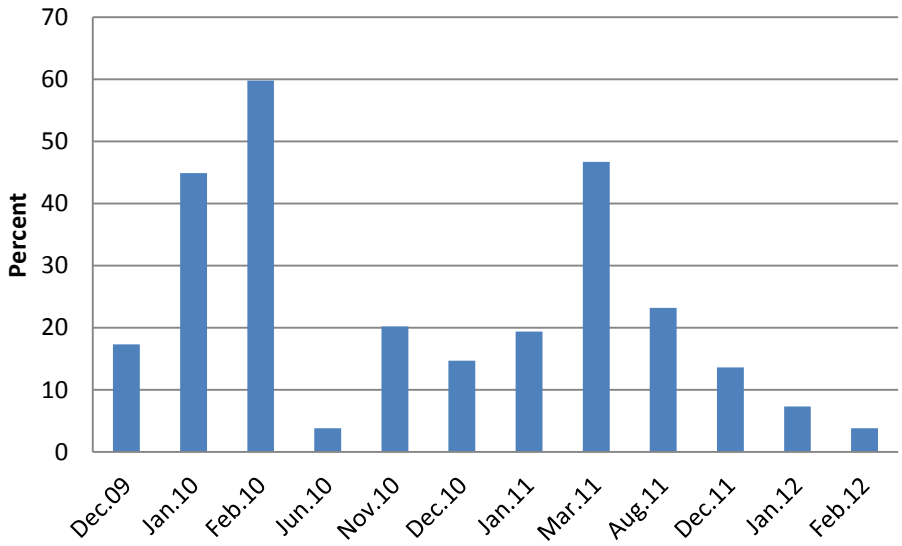

Figure 3.41 Graph showing the prevalence of the inclusions near the second antennae in salmon lice in the period December 2009 to February 2012. The prevalence was highest during the winter 2009-2010.

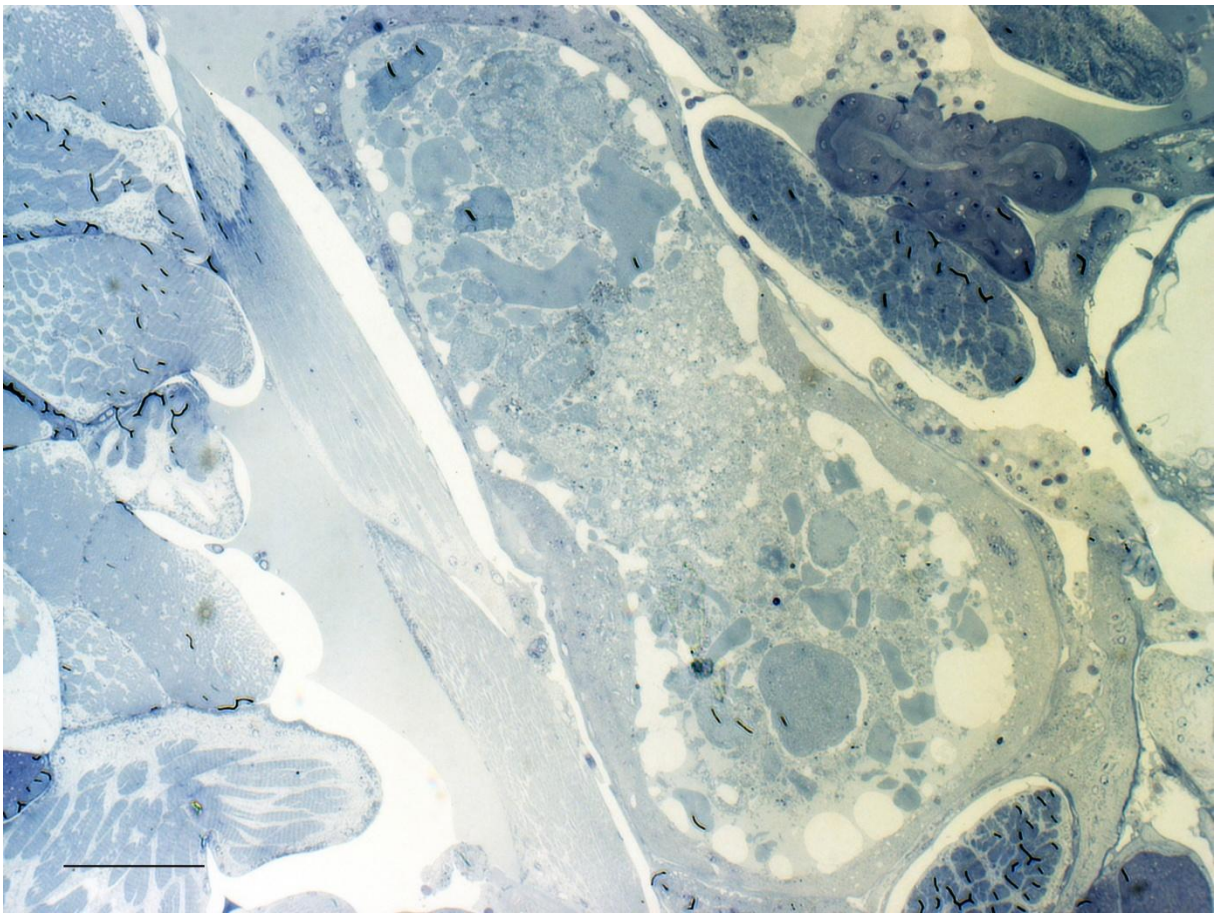

Figure 3.42 Inclusion located near the second antennae of salmon lice. Scale bar = 100 µm.

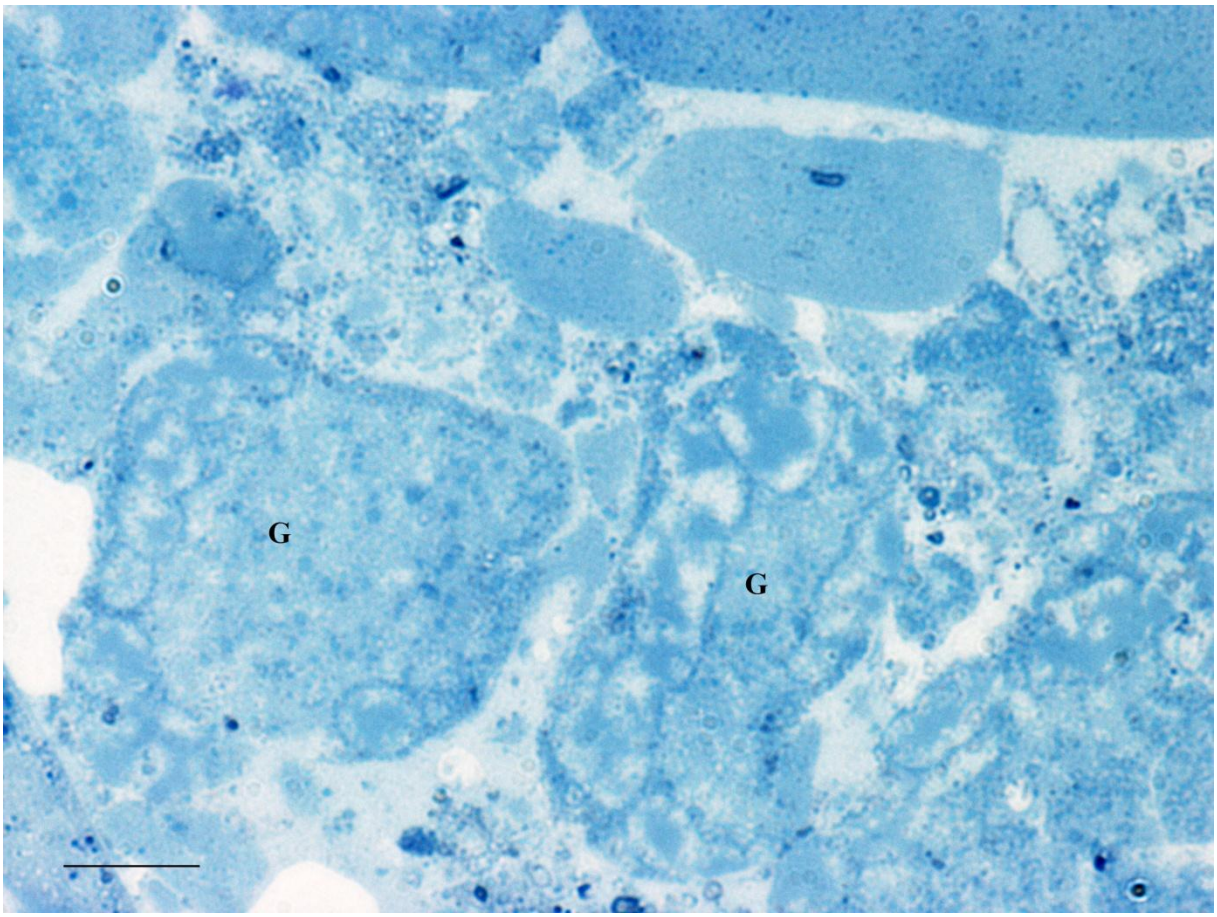

Figure 3.43 The inclusion contains degenerating gonadal cells (G) and cellular debris. Scale bar = 10 µm.

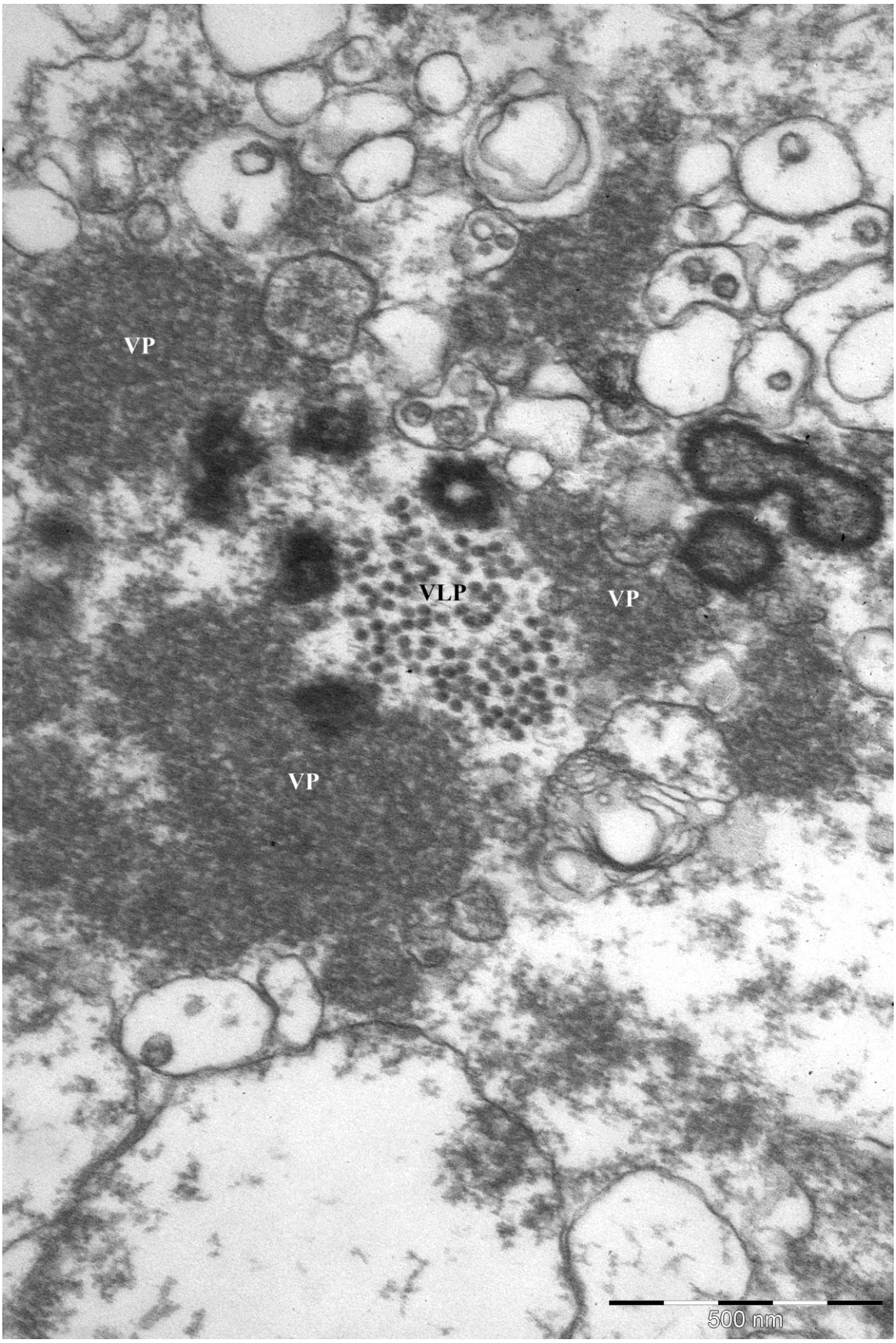

Figure 3.44 Virus-like particles (VLP) surrounded by viroplasm-like structures (VP) located in an inclusion near the second antennae of salmon lice.

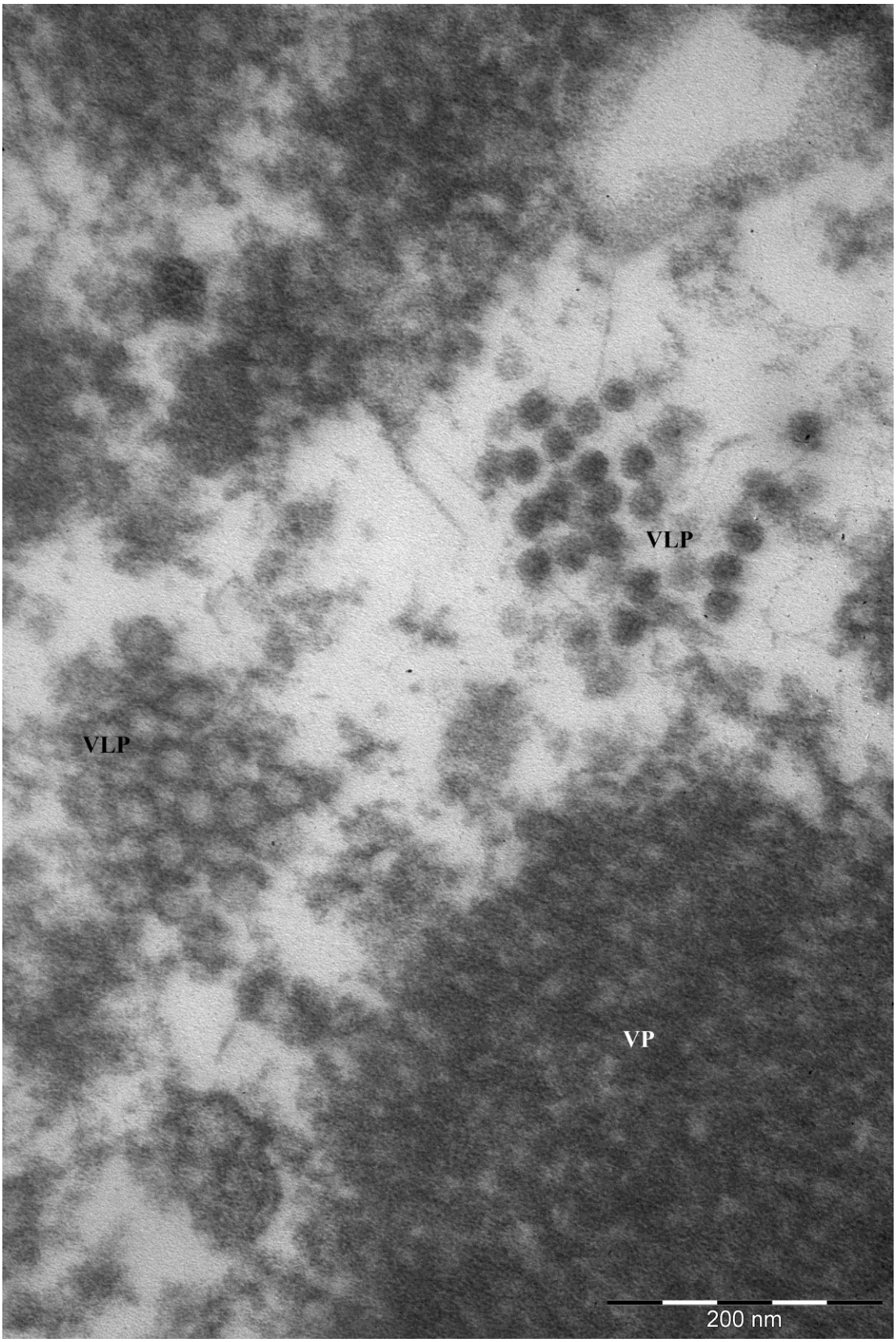

Figure 3.45 An electron micrograph showing virus-like particles (VLP) and a viroplasm-like structure (VP) observed in an inclusion near the second antennae of salmon lice.

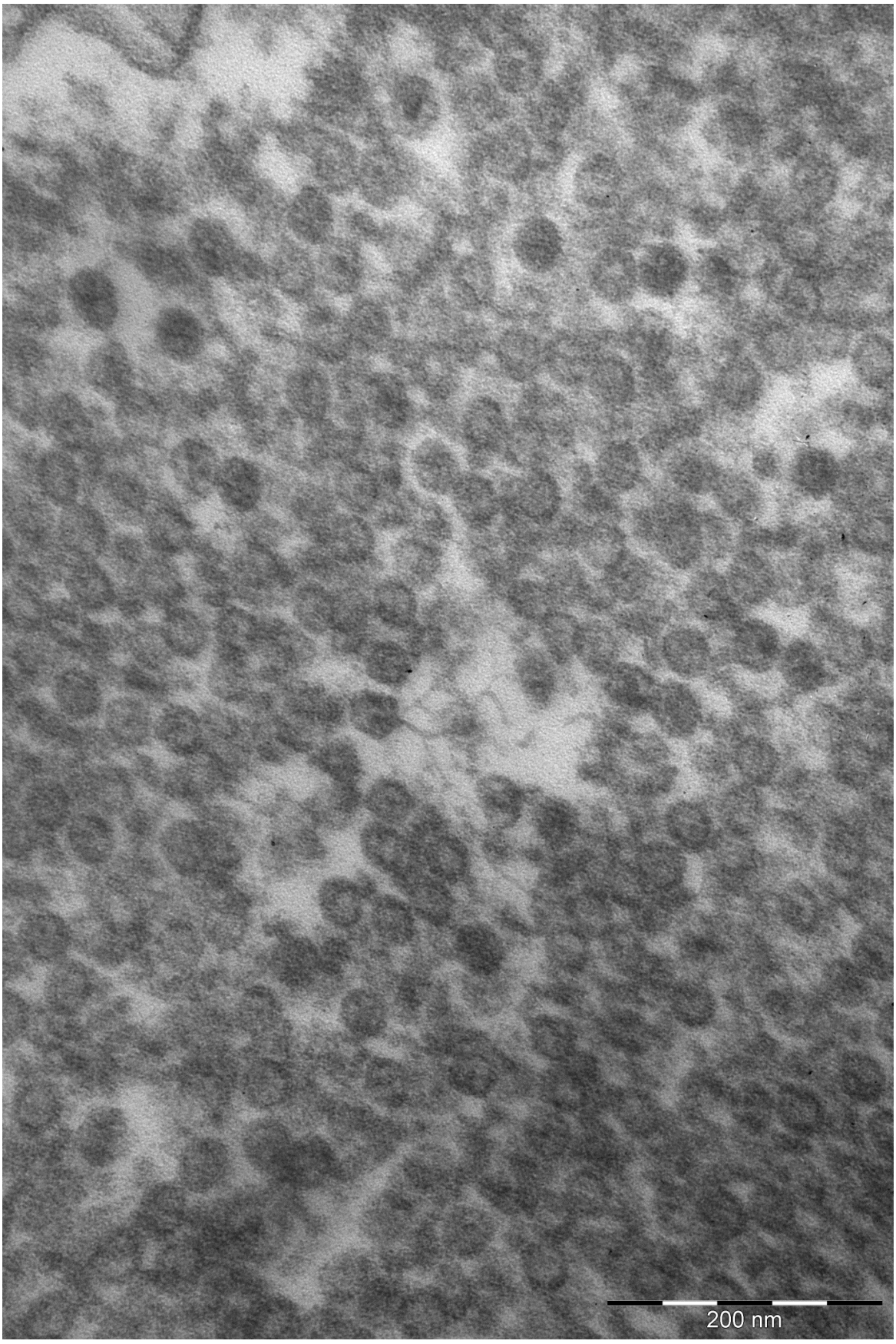

Figure 3.46 An electron micrograph showing virus-like particles located in an inclusion near the second antennae of salmon lice.

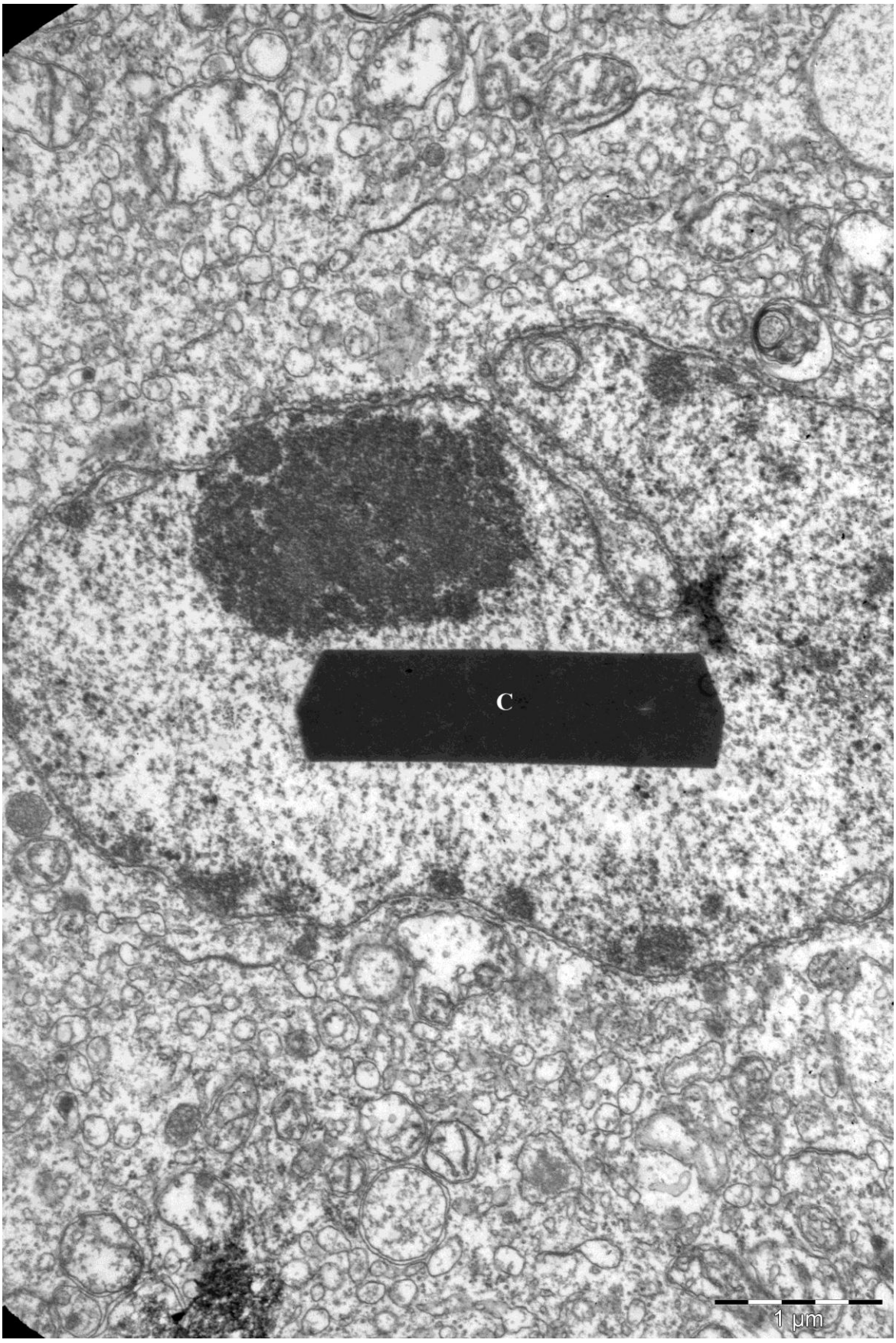

Figure 3.47 A crystalline structure (C) located in the nucleus of an unidentified cell in an inclusion near the second antennae of salmon lice.

A unicellular organism was observed during examination of histological sections of salmon lice from 1990 and was later found in the lice with inclusions near the second antennae. The organism seems to cause pathology in the connective tissue (Fig 3.48, Fig 3.50 and Fig 3.51). When studied under electron microscope the organism seems to distort the arrangement of the connective tissue fibrils (Fig 3.51). The organism is able to attach to and infiltrate the host cells (Fig 3.49, Fig 3.50 and Fig 3.51). The cell cytoplasm is rich in ribosomes and contains several mitochondria, some ER-profiles, tubuline structures and vacuoles beneath the plasma membrane (Fig 3.51, Fig 3.52 and Fig 3.53). The nucleus is large and has a central nucleolus.

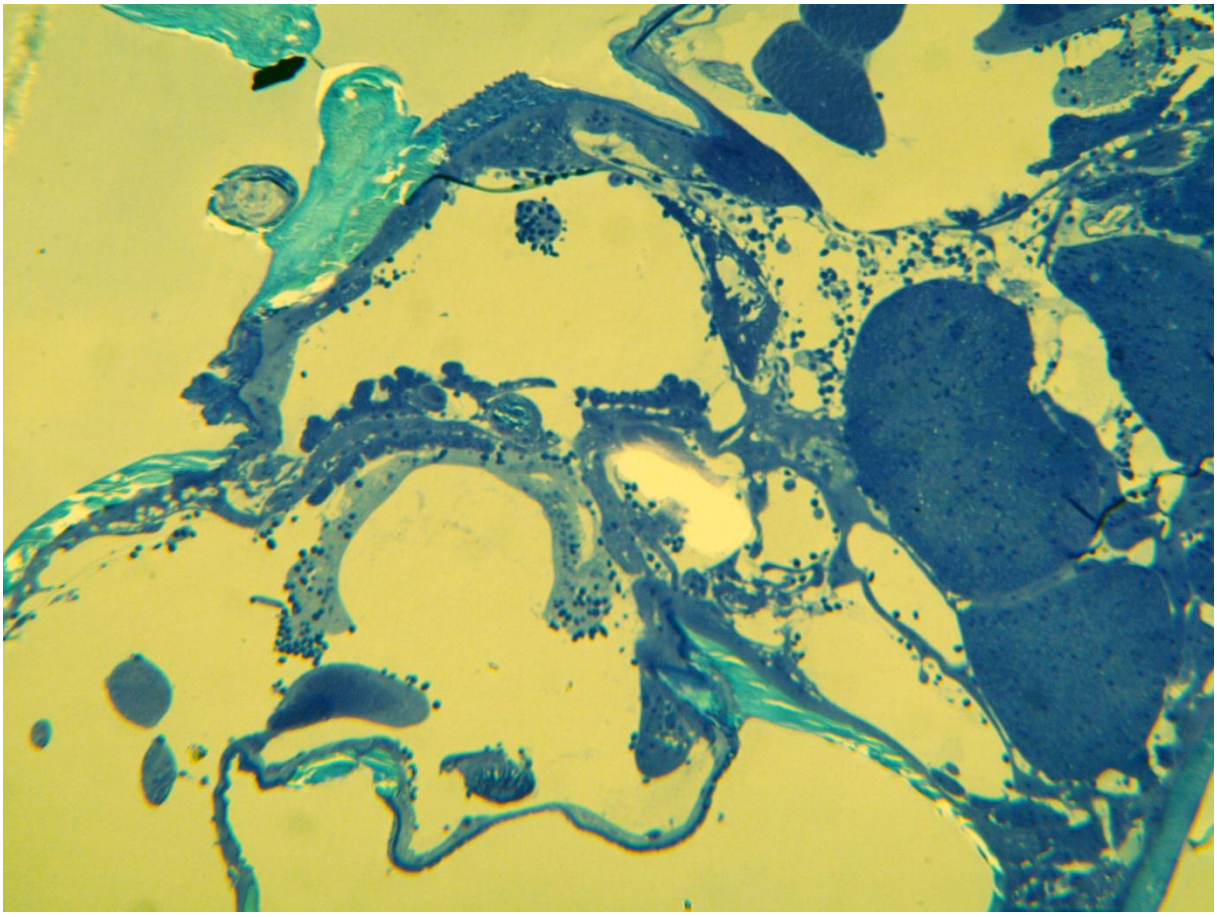

Figure 3.48 A micrograph showing the occurrence of a unicellular organism infecting the connective tissue of salmon lice

Figure 3.49 The unicellular organism attached to connective tissue surrounding muscle fibres. Scale bar = 10 µm

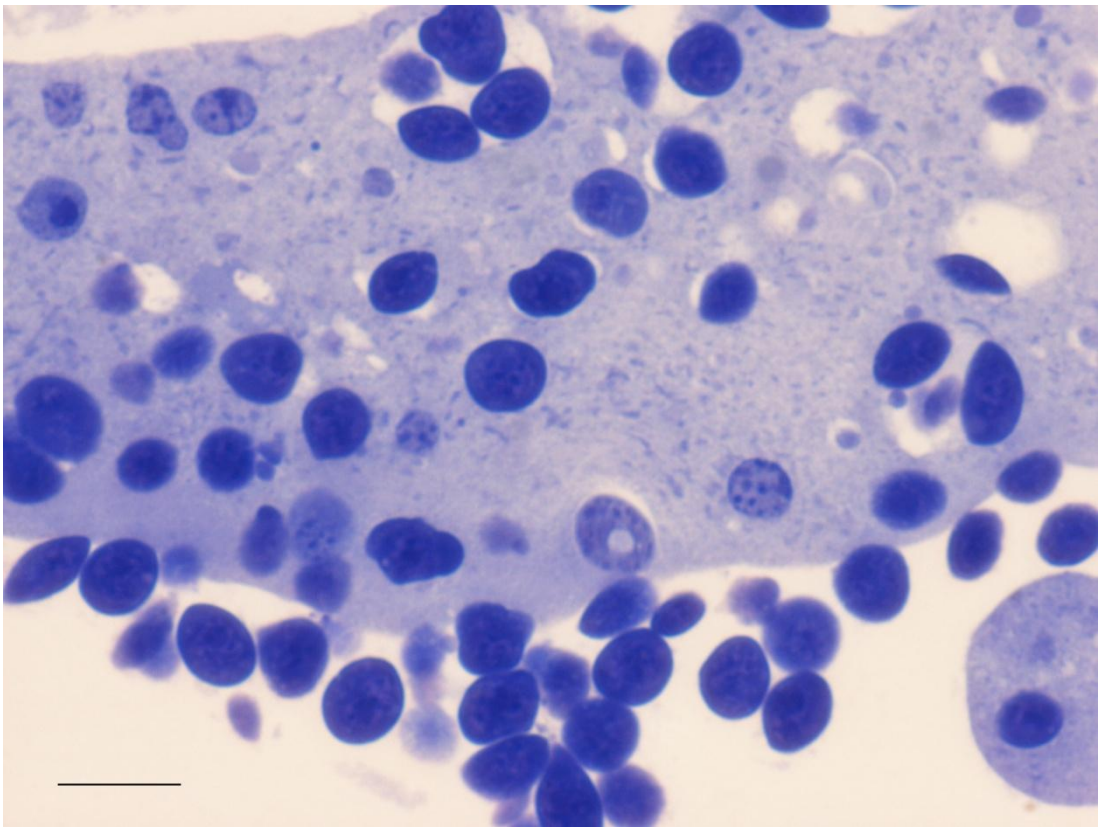

Figure 3.50 The unicellular organism infiltrating connective tissue. Scale bar = 10 µm

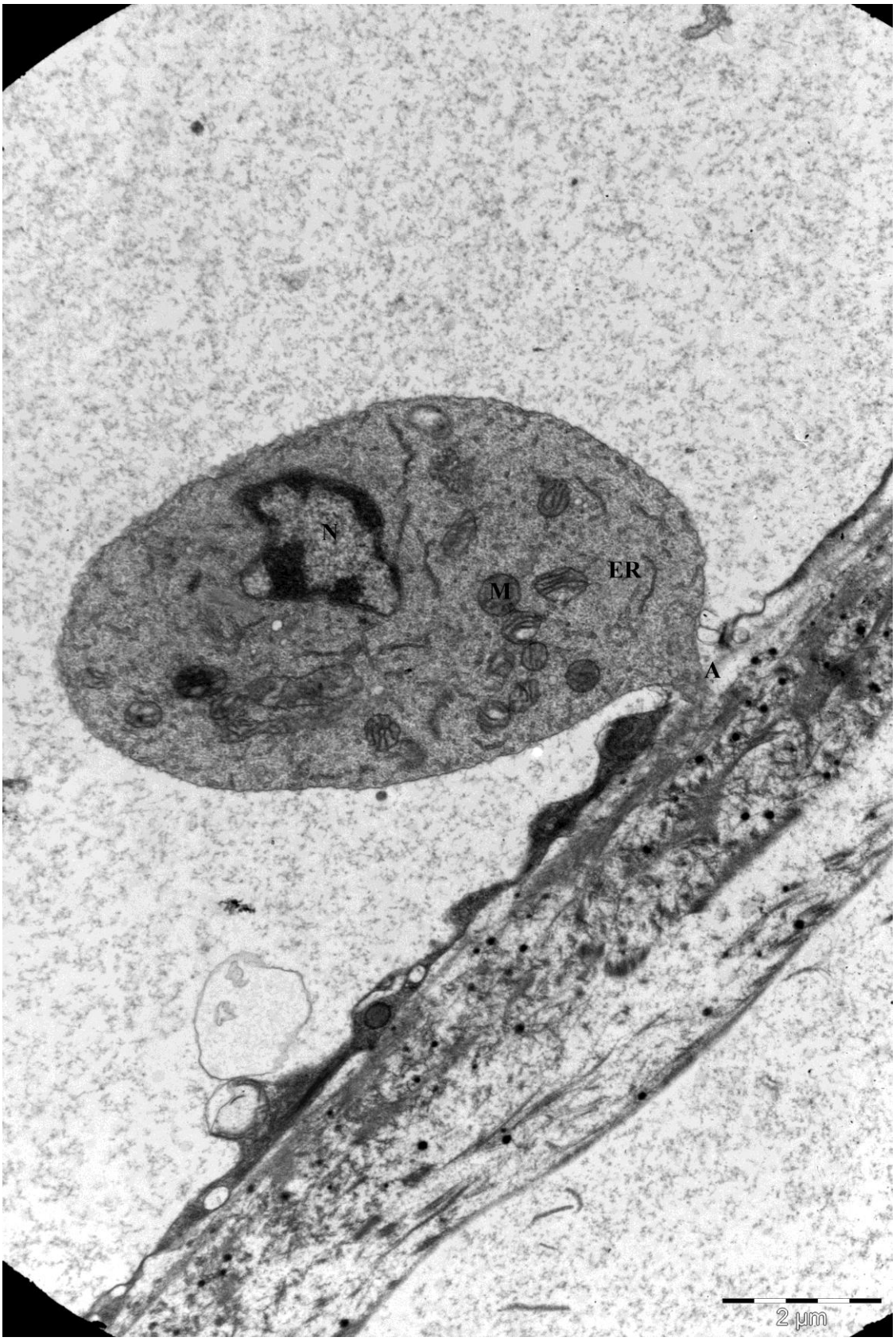

Figure 3.51 A unicellular organism attached (A) to connective tissue. Visible cellular structures are ER profiles (ER), mitochondria (M) and nucleus (N). Distortion of the connective tissue fibrils is observed near the attachment.

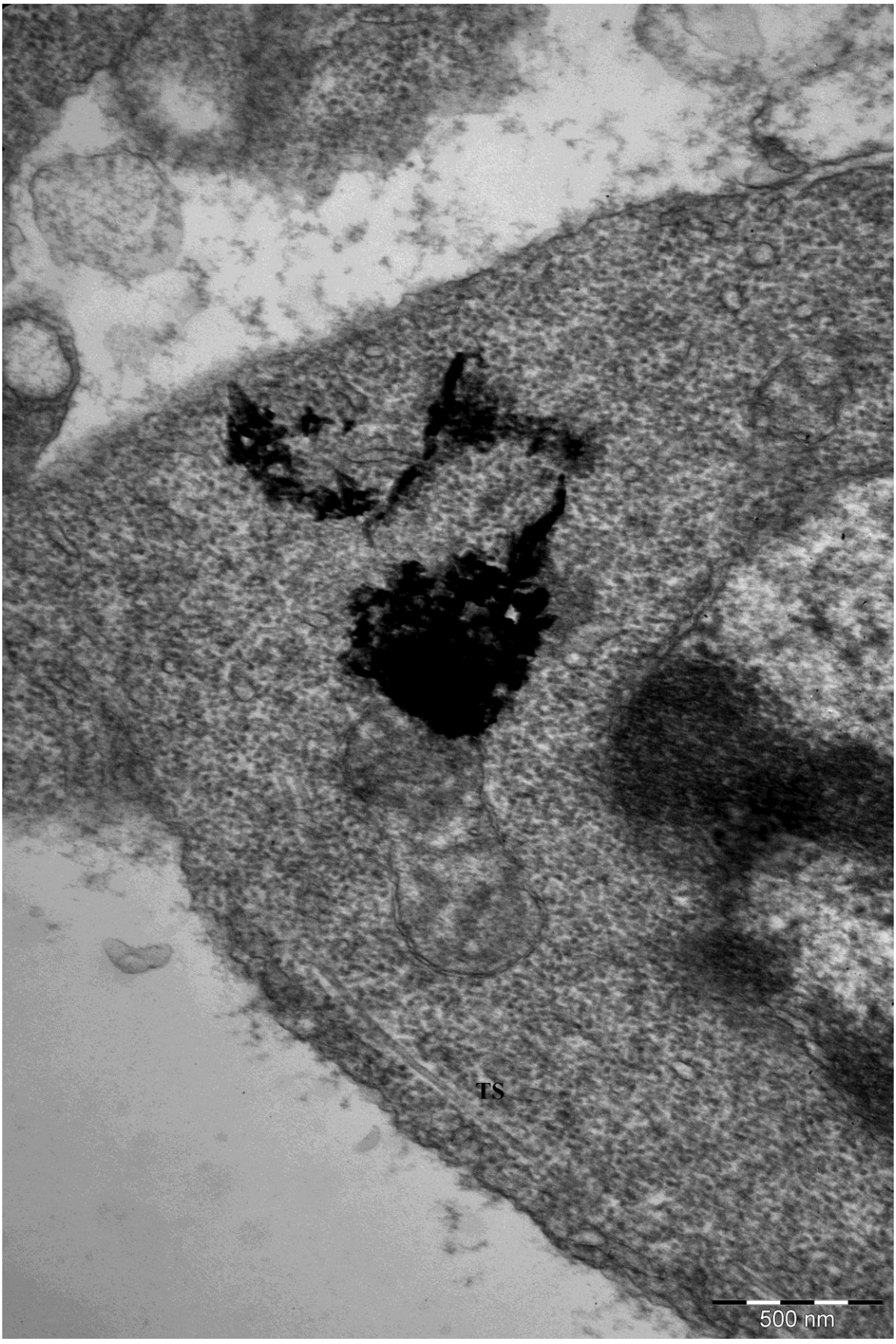

Figure 3.52 Tubuline structures (TS) are observed near the cellular membrane.

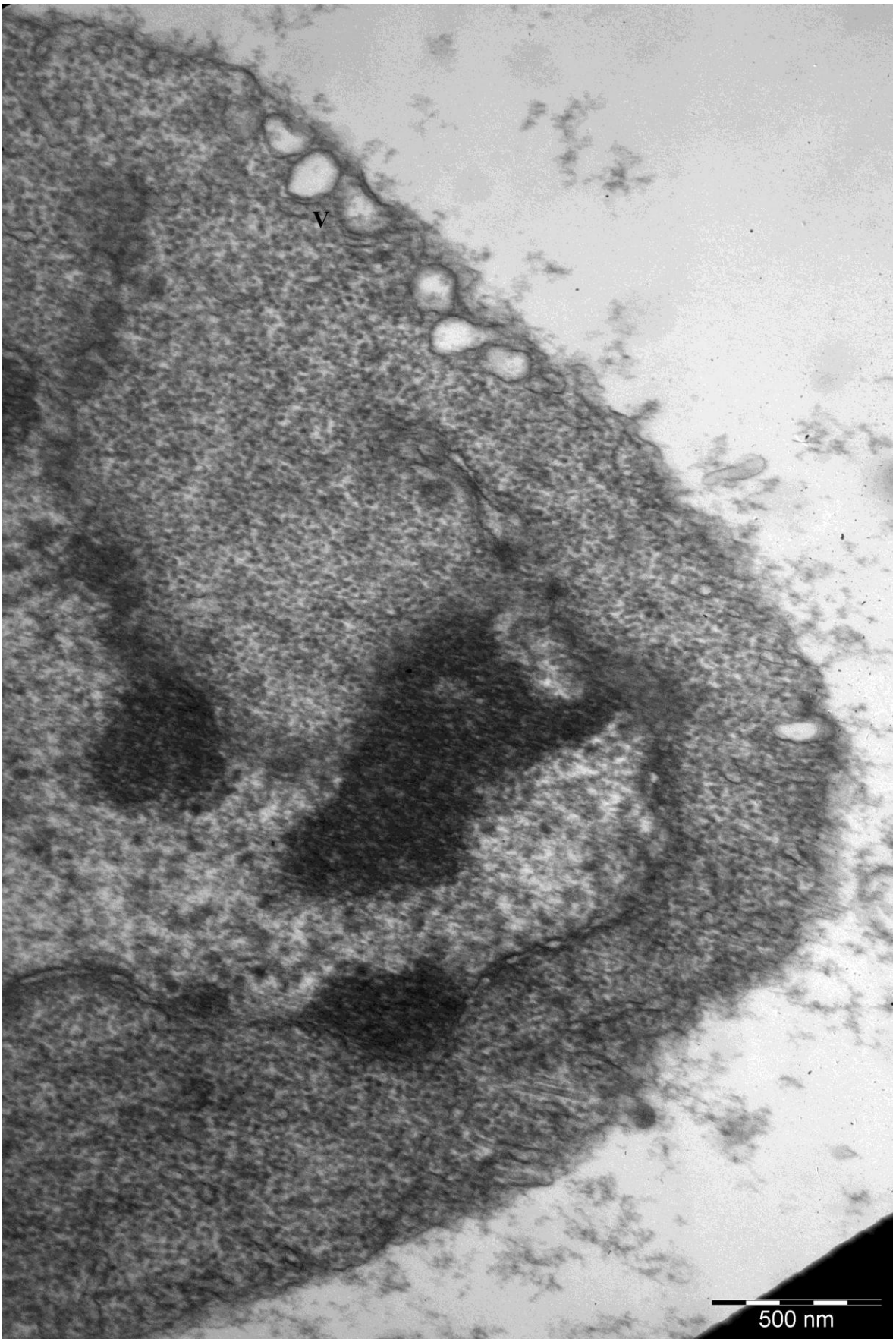

Figure 3.53 Vacuoles (V) are observed beneath the cell membrane.

C. centrodonti were heavily infected by *Udonella sp* (Fig 3.54). The 18S rDNA from *Udonella sp.* from *C. centrodonti* and *L. salmonis* were sequenced. The *Udonella* sp. from *L. salmonis* showed 100% similarity with *Udonella caligorum* from cod and salmon in UK and Norway. The sequence was given the GenBank accession number JX046547. The *Udonella* sp. from *C. centrodonti* had one nucleotide in difference from *Udonella caligorum*. The sequence was given the GenBank accession number JX046546.

In addition an *Ephelota*-like organism was observed on the extremities of *C. centrodonti* (Fig 3.55).

Figure 3.54 *C. centrodonti* heavily infected with *Udonella* sp.

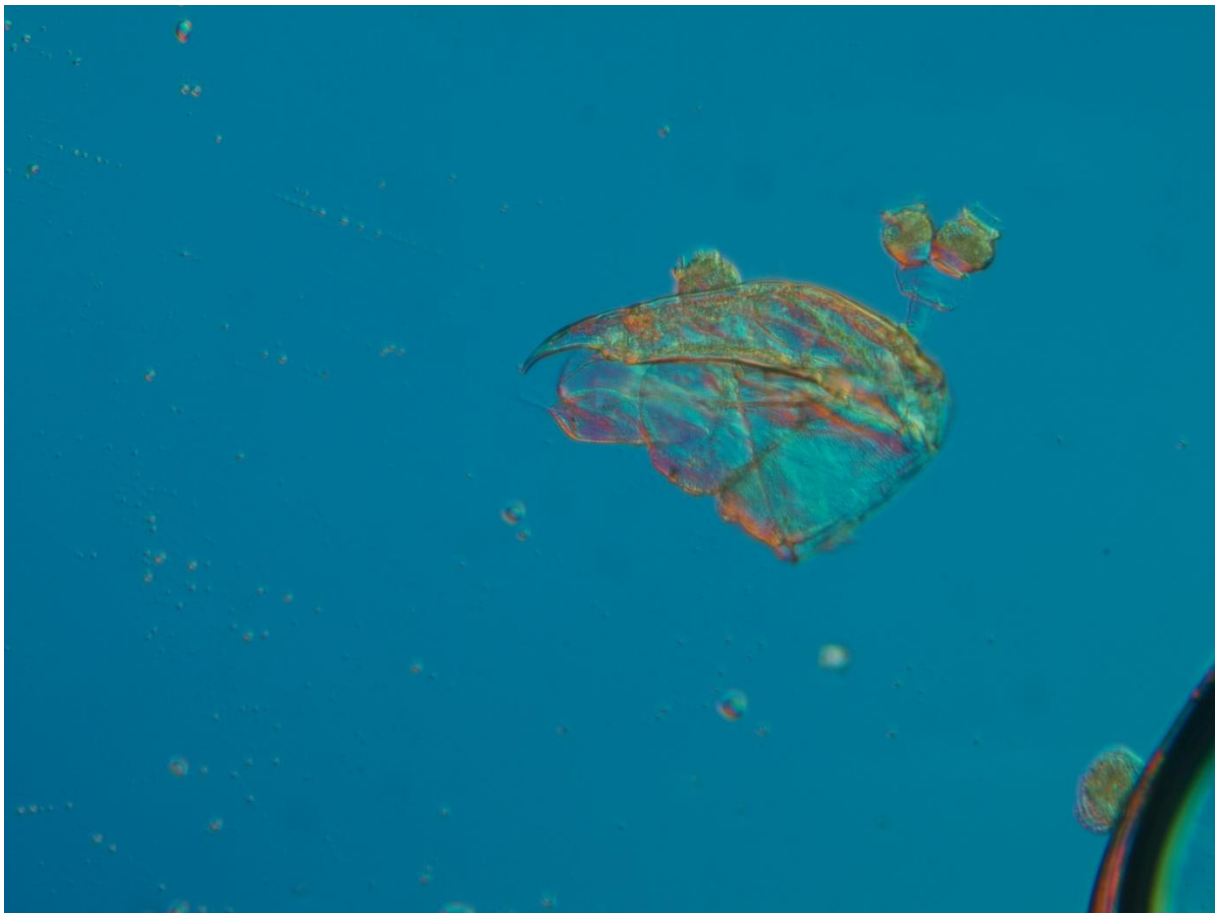

Figure 3.55 Extremity of *C. centrodonti* infected with an *Ephelota*-like organism.

4. Discussion

Prior to the study it was decided to spike all the samples with VHSV to use it as an exogenous control. The ambition was to normalize all the NUC-assays against the ELF-LS assay and the VHSV assay. However, there was made two batches of VHSV-spike and we were unable to obtain the same concentration of VHSV in both batches. The ELF-LS was expressed relatively stable within each developmental stage. Considering this the NUC-assay was only normalized against ELF-LS. The VHSV-spike could however be used as a control of the quality of the RNA extraction as it would give a known Ct-value if the extraction was correctly performed.

The ambition of this study was to use a minimum of 30 individuals from each developmental stage of *Lepeophtheirus salmonis* collected from farmed Atlantic salmon infected with *Paranucleospora theridion*. The lice stages were collected at a time when mature spores of *P. theridion* are known to be present in epithelial cells of infected salmon (Nylund et al., 2009, Nylund et al., 2010). Unfortunately, it was not possible to get enough individuals of chalimi 1 (N = 9), 2 (N = 10) and 4 (N = 26) during the two field sampling periods. The low number of individuals sampled from these two stages may have influenced on the given prevalences and intensities observed. However, there is 100 % prevalence of *P. theridion* in chalimus stage 3 which suggest that the majority of salmon lice on farmed salmon are infected before reaching the free-moving first preadult stage. This supports the assumption made by Nylund et al (2009, 2010) that the salmon louse gets infected when feeding on epithelial cells with intranuclear spores of *P. theridio*n during the chalimi stages allowing enough time for the development of mature spores during the development of *L. salmonis*. This is further supported by the increase in the amount (intensity) of template (16S from *P. theridion*) from chalimus stage 1 until the preadult stages are reached, which may reflect proliferation of *P. theridion* in the lice. A slight drop in intensity is registered in the first preadult stages and in the adult stages which may be due to sampling errors or mortalities of heavily infected lice. Evolution would select for a high parasite burden and virulence in spore producing organisms as this will lead to death of its host and consequential release of spores (Day, 2002). Considering this theory and the evidence of *P. theridion* infecting salmon without the presence of salmon lice (Sveen et al., In press) it is plausible that the drop in intensity in the adult stages of salmon louse could be caused by mortalities in heavy infected lice as this is probably necessary for the release of *P. theridion* spores.

Real-time RT-PCR is a very sensitive method for detecting RNA and Nylund et al. (2011) showed that it is possible to detect RNA and get a Ct value of 35.3 from 1.2 spores. It is therefore probable that some of the positives in this study are false positives caused by contamination of spores on the cuticle and in the lumen of the gut of the lice. To exclude this contamination the results can be presented with a Ct cut-off value at 30 (Figure 4.1). The prevalence will then have a stable increase from 22% at the first chalimus stage to 100% at adult female. This indicate that the lice may not be as rapidly infected as earlier suggested. The intensity show the same trends as earlier presented.

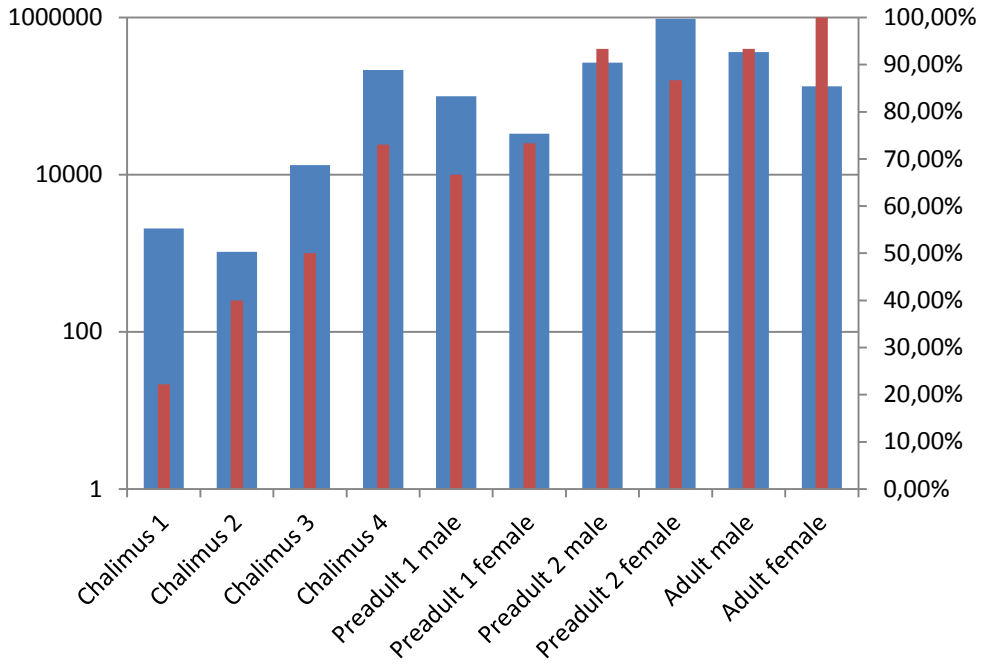

Figure 4.1 The intensity and prevalence of *P. theridion* in salmon lice presented with a Ct cut-off value of 30. The intensity is presented as mean normalized expression (N-fold) and is represented by the blue bar. The red bar represents the prevalence.

There is a clear correlation between the observed infection and measured Ct-values. Only medium to strong *P. theridion* infections were possible to detect visually and the results of visual inspection will therefore not include weak infections. The results do however give a rough overview of the prevalence during the period from December 2009 to February 2012. Sveen et al. (In press) have shown that the prevalence of *P. theridion* in salmon lice increases during the autumn and reaches a maximum in November before it decreases again during the spring. Compared to the results in the present study the development seems similar as the highest prevalences are recorded in December to February. Sveen et al. (In press) suggested that the development of *P. theridion* is temperature dependent. This is supported by the results

in the present study as the prevalence is highest in January and February of 2012 after a warm autumn and winter compared to the previous years. This is further supported by the temperature dependent development of other microsporidians infecting other poikilothermic hosts (Zenke et al., 2005, Antonio and Hedrick, 1995).

In salmon louse the point of entry for *P.theridion* is assumed to be the gut, although *P. theridion* has never been observed in the gut lumen or gut epithelium (Nylund et al., 2010). Observations during this study of spores in the lumen of the gut and *P.theridion* infections in the connective tissue surrounding the gut supports this hypothesis. A similar scenario has been shown for the microsporidian *Glugea stephani* which can infect *Pseudopleuronectes americanus* by oral inoculation. The gut epithelium is not affected but an infection is seen in the connective tissue surrounding the gut (Cali et al., 1986). However, the factors that trigger the polar filament extrusion of *P.theridion* are unknown. Considering the function of the gut epithelial cells; phagocytosis of gut content, intracellular digestion, elimination of the digested content and reabsorption by other gut epithelial cells (Nylund et al., 1992), phagocytosis may be utilized by *P. theridion* to enter the host cells. The phagocytic process may expose the spore to a lower pH which may trigger germination as this is a known triggering factor for germination of other microsporidians (Malone, 1984, Bhat and Nataraju, 2007). This would enable *P. theridion* to infect the nearby connective tissue. Another theory is that the germination may be triggered by adherence to surface proteins on the host cells as suggested by Magaud et al. (1997), Hayman et al. (2005) and Southern et al. (2007). They discovered that spores in the genus *Encephalitozoon* could adhere to host cell surface glycosaminoglycans by a protein located in the endospore, Endospore protein 1 (EnP1). Inhibition of this protein has shown to reduce the success of infection and it is therefore likely that the adherence is involved in the triggering of germination. Adherence of *P. theridion* to gut epithelial cells has not been proved in neither this study nor previous studies (Freeman and Sommerville, 2009, Nylund et al., 2010) and it seems unlikely that germination could be triggered by adherence to non-target cells. As the stimulus for germination is thought to reflect the environment where the spore germinate (Undeen and Epsky, 1990) one could also hypothesize that there are environmental factors in the gut that trigger the germination of *P. theridion*.

The pathology of *P. theridion* in salmon lice indicates autoinfection within the lice. The most affected area in heavily infected lice is beneath the cuticle. However, the point of entry for *P. theridion* is thought to be the gut and this does not correlate unless there is multiplication

followed by autoinfection within the lice. Autoinfection of *P. theridion* has not been observed in the present study nor previous studies (Freeman and Sommerville, 2009, Nylund et al., 2010). However, during the present study and a previous study by Nylund et al. (2010) *P. theridion* infected haemocytes were observed and free spores were present in the haemocoel. Kurtz et al. (2000) has shown that haemocytes may phagocytize spores. This may lead to an infection of the heamocyte and extrusion of the polar filament from intrahaemocytic spores has been observed by David and Weiser (1994). Considering this it is likely that salmon louse heamocytes are involved in the spreading of *P. theridion* within the lice.

Binary fission of meronts was not observed during this study. This was most likely a coincident as binary fission of meronts has been described by both Freeman and Sommerville (2009) and Nylund et al. (2010). During the merontal stage fission of diplokaryoa was observed. In early sporonts there was observed a disassociation of diplokarya, loss of nuclear membrane and synaptonemal complexes in the nuclei. Late sporonts, sporoblasts and spores are monokaryotic. Synaptomental complexes occur during the onset of meiosis and may therefore be used as an indicator of meiosis (Nassonova and Smirnov, 2005, Hazard et al., 1979). A life cycle with sexual reproduction is well described for the genus *Amblyospora*. Canning (1988) has proposed a life cycle for *Amblyospora* spp. with emphasis on the chromosome cycle based on the research by Andreadis (1983), Hazard and Brookbank (1984), Hazard et al. (1985), Sweeney et al. (1985) and Andreadis (1985); *Mosquito larvae are infected by haploid monokaryotic spores produced in copepods. Gametogenesis and plasmotomy lead to the production of diplokaryotic meronts with haploid nuclei. Mitotic division occurs and leads to the production of haploid diplokaryotic spores which infect the ovary of its host. In the F1 generation meronts multiply and produce diplokaryotic sporonts. Loss of the nuclear membrane occurs in the sporonts and this is followed by fusion of the diplokaryon producing a diploid monokaryon. The monokaryon duplicates and form a diploid diplokaryon. The diplokaryon disassociate and meiosis leads to tetraploid mingling of chromosome. Sporonts with two diploid monokaryon are produced. This is followed by meiosis 2 which leads to the production of sporonts with four haploid monokaryon. Mitosis will then follow and haploid octonucleate sporonts are produced. Cytokinesis will then result in eight haploid monokaryotic sporoblasts which develops into spores that are infective to copepods. The development in the copepod is mitotic*.

Hypothesis of development of P. theridion in salmon louse

The observations in the present study indicate sexual reproduction, however no cytoplasmic fusion has been observed. One would expect the occurrence of cytoplasmic fusion as described in the development of *Amblyospora* (Hazard et al., 1985) since the nuclear fusion will give no advantage unless there is mixing of genome derived from different spores (Otto and Gerstein, 2006). This may have been overlooked due to the similarity between fusing and dividing cells. Based on the observations during this study and the development of *Amblyospora* reviewed by Canning (1988) a hypothesis on the development of *P. theridion* in salmon louse is presented in figure 4.2. A target cell for *P. theridion* is infected by several spores. Cytoplasmic fusion occurs and leads to the formation of meronts containing two haploid diplokaryon. Mitotic division of diplokarya leads to the proliferation of diplokarya. In early sporonts the diplokarya disassociate and the nuclear membrane is lost. During formation of new nuclear membrane diploid monokarya are produced. Schizogony will then result in late sporonts containing diploid monokarya. Late sporonts may still have mitotic division. Maturation of the sporonts will lead to the development of sporoblasts and spores which have a diploid monokaryon. Formation of diploid monokaryon may explain the rapid formation of diplokaryon in developmental cycle I in Atlantic salmon (Nylund et al., 2010).

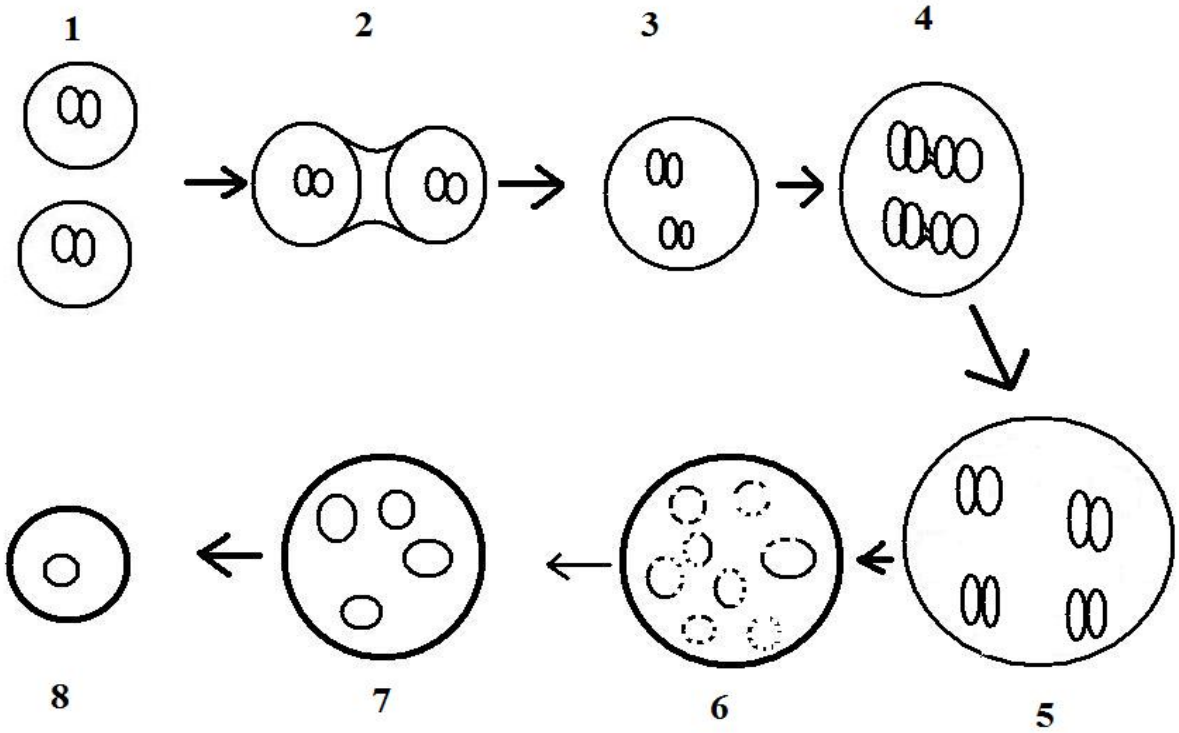

Figure legend presented on next page

Figure 4.2 Suggested development of *P. theridion* in salmon lice. A target cell contains several meronts derived from different spores (1). Cytoplasmic fusion occur (2) which result in a meront containing two diplokarya (3). Mitotic division (4) results in the proliferation of diplokarya (5). In early sporonts the diplokarya disassociate and the nuclear membrane is lost (6). Nuclear fusion will then occur forming diploid monokarya (7). Schizogony will lead to the formation of late sporonts which will develop into diploid monokaryotic sporoblasts and spores (8).

Salmon lice causes severe economic loss to salmonid aquaculture (Costello, 2009). Chemicals applied in bath or incorporated in the feed are the main methods for control of salmon lice (Grave et al., 2004). Cleaner wrasse used as biological control is also common and is cheaper than the use of bath treatments (Costello, 2009). The heavy use of chemical treatments has in the last decade lead to the evolvement of resistant lice (Denholm et al., 2002). The use of biological control has therefore become more attractive as it reduces the use of chemicals and is over time more effective than chemical treatment (Costello, 2009, Treasurer, 2002). Sea lice pathogens used as biological control of sea lice has been reviewed by Treasurer (2002), but at the time there were no known pathogens causing disease in sea lice. David R. Harper applied for the patent "Microbiological control of sea lice" (United Kingdom patent GB2371053, international patent PCT/GB02/00134) during the discovery of a microsporidian causing pathology in salmon lice (Freeman et al., 2003). This parasite was later identified as *P.theridion* which are causing pathology in both salmon and salmon lice (Nylund et al., 2009, Nylund et al., 2010, Nylund et al., 2011) and can therefore be ruled out as a biological approach to control sea lice. During the present study three agents were associated with pathology in salmon lice. Virus-like particles were found in inclusions near the second antennae and may be causing these inclusions. The inclusions contained degenerated gonadal cells and virus-like particles. The inclusions have a high prevalence in salmon lice from cultured Atlantic salmon in the Norwegian county Sogn og Fjordane. The infected lice tested positive for piscine reovirus, however the Ct-values were not low enough to suggest that this is the virus that causes the inclusions. It does however indicate that salmon lice may function as a mechanical vector for piscine reovirus. A unicellular organism and bacteria were also associated with pathology. The unicellular organism seemed to cause pathology in connective tissue and the bacteria were associated with necrosis of the gut epithelial cells. Nylund et al. (1992) have observed bacteria in both the microvilli and epithelial cells of the gut, but no pathology was observed. Due to the pathology associated with these organisms they may be candidates for biological control of salmon lice.

Udonella sp. from *C. centrodonti* showed one nucleotide in difference from *U. caligorum* in the 18S rDNA. This could indicate that this is a new species However if this is the same species as *U. caligorum* or if it is able to infect both *C. centrodonti* and *L .salmonis* it could propose a problem for the use of cleaner wrasse as biological control of salmon lice. Due to the fact that *Udonella* feed on the fish skin and mucus (Sproston, 1946, Freeman and Ogawa, 2010) it may harm the fish in addition to the harm caused by the lice. The use of wild caught cleaner fish could especially propose a problem as there is a greater likelihood of these being infected with *C. centrodonti* infected with *Udonella* sp. than cultured cleaner wrasse.

Conclusions and future perspectives

P. theridion infects the first chalimus stage in salmon lice development on the host. The prevalence and intensity increases during the development of salmon lice and adult lice may be heavily infected were *P. theridion* may fill the entire haemocoelic cavity. The highest prevalence is obtained from December to February. The prevalence indicates that the development is temperature dependent.

The point of entry for *P. theridion* is still unknown, although there are indications that suggest the gut being the point of entry. The pathology of *P. theridion* may suggest several points of entry as the heaviest infections are located beneath the cuticle. It is, however, not likely that the polar filament may penetrate the cuticle. The heavy infections beneath the cuticle are most likely a result of autoinfection.

There are strong indications of sexual reproduction of *P. theridion* during its development in salmon lice. There is however some missing links in its development and the complete mechanism for sexual reproduction is not fully understood. A theory for development have been suggested which includes cytoplasmic fusion of meronts, mitotic division of diplokarya and the fusion of monokarya resulting in diploid monokarya.

Further studies on the infection mechanism and development should be performed. Infection experiments may be a good alternative for a future study as it will give a more controlled scenario and one would be able to study the infection from the first chalimus stage to adult. Further studies should also be performed on the development of prevalence of *P. theridion* in salmon lice over a year with monthly samplings.

Three agents associated with pathology in salmon lice were observed during this study. Further studies should be performed to determine the species and virulence. Their possible use as biological control of salmon lice should also be investigated.

An udonellid was visually detected on *C. centrodonti* and the sequence obtained from its 18S rDNA may indicate that it is a new species. It could be valuable to further sequence its genome and study its morphology to determine its species.

References

AMIGÓ, J. M., GRACIA, M. P., RIUS, M., SALVADÓ, H., MAILLO, P. A. & VIVARÉS, C. P. 1996. Longevity and effects of temperature on the viability and polar-tube extrusion of spores of <i>Glugea stephani , a microsporidian parasite of commercial flatfish. *Parasitology Research,* 82**,** 211-214.

ANDREADIS, T. G. 1983. LIFE-CYCLE AND EPIZOOTIOLOGY OF AMBLYOSPORA SP (MICROSPORA, AMBLYOSPORIDAE) IN THE MOSQUITO, AEDES-CANTATOR. *Journal of Protozoology,* 30**,** 509-518.

ANDREADIS, T. G. 1985. Experimental Transmission of a Microsporidian Pathogen from Mosquitoes to an Alternate Copepod Host. *Proceedings of the National Academy of Sciences of the United States of America,* 82**,** 5574-5577.

ANONYMOUS. 2012. *Fast hydrografisk stasjon Sognesjøen* [Online]. Institute of Marine Research. Available: http://www.imr.no/forskning/forskningsdata/stasjoner/dato.php?page=0&year=2011&stid=5867 [Accessed 24.05. 2012].

ANTONIO, D. B. & HEDRICK, R. P. 1995. EFFECT OF WATER TEMPERATURE ON INFECTIONS WITH THE MICROSPORIDIAN ENTEROCYTOZOON SALMONIS IN CHINOOK SALMON. *Diseases of Aquatic Organisms,* 22**,** 233-236.

AVERY, S. W. & ANTHONY, D. W. 1983. Ultrastructural study of early development of Nosema algerae in anopheles albimanus. *Journal of Invertebrate Pathology,* 42**,** 87-95.

BHAT, S. A. & NATARAJU, B. 2007. A comparative study on artificial germination of two microsporidia under the neutralization method. *Caspian Journal of Environmental Sciences,* 5**,** 105-109.

BRON, J. E., SOMMERVILLE, C., JONES, M. & RAE, G. H. 1991. The settlement and attachment of early stages of the salmon louse, Lepeophtheirus salmonis (Copepoda: Caligidae) on the salmon host, Salmo salar. *Journal of Zoology,* 224**,** 201-212.

CALI, A. & TAKVORIAN, P. M. 1999. Developmental morphology and life cycles of the Microsporida. *In:* WITTNER, M. & WEISS, L. M. (eds.) *The Microsporidia and Microsporidosis.* Washington, DC: ASM press.

CALI, A., TAKVORIAN, P. M., ZISKOWSKI, J. J. & SAWYER, T. K. 1986. Experimental infection of American winter flounder (Pseudopleuronectes americanus) with Glugea stephani (Microsporida). *Journal of Fish Biology,* 28**,** 199-206.

CALI, A. N. N. & OWEN, R. L. 1990. Intracellular Development of Enterocytozoon, A Unique Microsporidian Found in the Intestine of AIDS Patients. *Journal of Eukaryotic Microbiology,* 37**,** 145-155.

CANNING, E. U. 1988. Nuclear division and chromosome cycle in microsporidia. *Biosystems,* 21**,** 333-340.

COSTELLO, M. J. 2006. Ecology of sea lice parasitic on farmed and wild fish. *Trends in Parasitology,* 22**,** 475-483.

COSTELLO, M. J. 2009. The global economic cost of sea lice to the salmonid farming industry. *Journal of Fish Diseases,* 32**,** 115-118.

DAVID, L. & WEISER, J. 1994. Role of Hemocytes in the Propagation of a Microsporidian Infection in Larvae of Galleria mellonella. *Journal of Invertebrate Pathology,* 63**,** 212-213.

DAY, T. 2002. Virulence evolution via host exploitation and toxin production in spore-producing pathogens. *Ecology Letters,* 5**,** 471-476.

DENHOLM, I., DEVINE, G. J., HORSBERG, T. E., SEVATDAL, S., FALLANG, A., NOLAN, D. V. & POWELL, R. 2002. Analysis and management of resistance to chemotherapeutants in salmon lice, Lepeophtheirus salmonis (Copepoda : Caligidae). *Pest Management Science,* 58**,** 528-536.

DEVOLD, M., KROSSOY, B., ASPEHAUG, V. & NYLUND, A. 2000. Use of RT-PCR for diagnosis of infectious salmon anaemia virus (ISAV) in carrier sea trout Salmo trutta after experimental infection. *Diseases of Aquatic Organisms,* 40**,** 9-18.

DOCKER, M. F., KENT, M. L., HERVIO, D. M. L., KHATTRA, J. S., WEISS, L. M., CALI, A. N. N. & DEVLIN, R. H. 1997. Ribosomal DNA Sequence of Nucleospora salmonis Hedrick, Groff and Baxa, 1991 (Microsporea: Enterocytozoonidae): Implications for Phylogeny and Nomenclature. *Journal of Eukaryotic Microbiology,* 44**,** 55-60.

DRAGHI, A., POPOV, V. L., KAHL, M. M., STANTON, J. B., BROWN, C. C., TSONGALIS, G. J., WEST, A. B. & FRASCA, S. 2004. Characterization of "Candidatus Piscichlamydia salmonis" (Order Chlamydiales), a Chlamydia-Like Bacterium Associated With Epitheliocystis in Farmed Atlantic Salmon (Salmo salar). *Journal of Clinical Microbiology,* 42**,** 5286-5297.

DUESUND, H., NYLUND, S., WATANABE, K., OTTEM, K. F. & NYLUND, A. 2010. Characterization of a VHS virus genotype III isolated from rainbow trout (Oncorhychus mykiss) at a marine site on the west coast of Norway. *Virology Journal,* 7.

DUNN, A. M. & SMITH, J. E. 2001. Microsporidian life cycles and diversity: the relationship between virulence and transmission. *Microbes and Infection,* 3**,** 381-388.

FRANZEN, C. 2005. How do microsporidia invade cells? *Folia Parasitologica,* 52**,** 36-40.

FREEMAN, M. A., BELL, A. S. & SOMMERVILLE, C. 2003. A hyperparasitic microsporidian infecting the salmon louse, Lepeophtheirus salmonis: an rDNA-based molecular phylogenetic study. *Journal of Fish Diseases,* 26**,** 667-676.

FREEMAN, M. A. & OGAWA, K. 2010. Variation in the small subunit ribosomal DNA confirms that Udonella (Monogenea: Udonellidae) is a species-rich group. *International Journal for Parasitology,* 40**,** 255-264.

FREEMAN, M. A. & SOMMERVILLE, C. 2009. Desmozoon lepeophtherii n. gen., n. sp., (Microsporidia: Enterocytozoonidae) infecting the salmon louse Lepeophtheirus salmonis (Copepoda: Caligidae). *Parasites & Vectors,* 2.

FROST, P. & NILSEN, F. 2003. Validation of reference genes for transcription profiling in the salmon louse, Lepeophtheirus salmonis, by quantitative real-time PCR. *Veterinary Parasitology,* 118**,** 169-174.

GRAVE, K., HORSBERG, T. E., LUNESTAD, B. T. & LITLESKARE, I. 2004. Consumption of drugs for sea lice infestations in Norwegian fish farms: methods for assessment of treatment patterns and treatment rate. *Diseases of Aquatic Organisms,* 60**,** 123-131.

HAYMAN, J. R., SOUTHERN, T. R. & NASH, T. E. 2005. Role of sulfated glycans in adherence of the microsporidian Encephalitozoon intestinalis to host cells in vitro. *Infection and Immunity,* 73**,** 841-848.

HAZARD, E. I., ANDREADIS, T. G., JOSLYN, D. J. & ELLIS, E. A. 1979. Meiosis and Its Implications in the Life Cycles of Amblyospora and Parathelohania (Microspora). *The Journal of Parasitology,* 65**,** 117-122.

HAZARD, E. I. & BROOKBANK, J. W. 1984. Karyogamy and meiosis in an Amblyospora sp. (Microspora) in the mosquito Culex salinarius. *Journal of Invertebrate Pathology,* 44**,** 3-11.

HAZARD, E. I., FUKUDA, T. & BECNEL, J. J. 1985. GAMETOGENESIS AND PLASMOGAMY IN CERTAIN SPECIES OF MICROSPORA. *Journal of Invertebrate Pathology,* 46**,** 63-69.

HEUCH, P. A. & KARLSEN, H. E. 1997. Detection of infrasonic water oscillations by copepodids of Lepeophtheirus salmonis (Copepoda: Caligida). *Journal of Plankton Research,* 19**,** 735-747.

HEUCH, P. A., NORDHAGEN, J. R. & SCHRAM, T. A. 2000. Egg production in the salmon louse Lepeophtheirus salmonis (Kroyer) in relation to origin and water temperature. *Aquaculture Research,* 31**,** 805-814.

ISHIHARA, R. & HAYASHI, Y. 1968. Some properties of ribosomes from the sporoplasm of Nosema bombycis. *Journal of Invertebrate Pathology,* 11**,** 377-385.

JOHNSON, S. C. & ALBRIGHT, L. J. 1991a. DEVELOPMENT, GROWTH, AND SURVIVAL OF LEPEOPHTHEIRUS-SALMONIS (COPEPODA, CALIGIDAE) UNDER LABORATORY CONDITIONS. *Journal of the Marine Biological Association of the United Kingdom,* 71**,** 425-436.

JOHNSON, S. C. & ALBRIGHT, L. J. 1991b. THE DEVELOPMENTAL STAGES OF LEPEOPHTHEIRUS-SALMONIS (KROYER, 1837) (COPEPODA, CALIGIDAE). *Canadian Journal of Zoology-Revue Canadienne De Zoologie,* 69**,** 929-950.

JONES, M. W., SOMMERVILLE, C. & BRON, J. 1990. The histopathology associated with the juvenile stages of Lepeophtheirus salmonis on the Atlantic salmon, Salmo salar L. *Journal of Fish Diseases,* 13**,** 303-310.

KARLSEN, M., NYLUND, A., WATANABE, K., HELVIK, J. V., NYLUND, S. & PLARRE, H. 2008. Characterization of 'Candidatus Clavochlamydia salmonicola': an intracellular bacterium infecting salmonid fish. *Environmental Microbiology,* 10**,** 208-218.

KEELING, P. J. & FAST, N. M. 2002. MICROSPORIDIA: Biology and Evolution of Highly Reduced Intracellular Parasites. *Annual Review of Microbiology,* 56**,** 93-116.

KEOHANE, E. M. & WEISS, L. M. 1999. The structure, function, and composition of the microsporidian polar tube. *In:* WITTNER, M. & WEISS, L. M. (eds.) *The Microsporidia and Microsporidosis.* Washington, DC: ASM press.

KUBISTA, M., ANDRADE, J. M., BENGTSSON, M., FOROOTAN, A., JONAK, J., LIND, K., SINDELKA, R., SJOBACK, R., SJOGREEN, B., STROMBOM, L., STAHLBERG, A. & ZORIC, N. 2006. The real-time polymerase chain reaction. *Molecular Aspects of Medicine,* 27**,** 95-125.

KURTZ, J., NAHIF, A. A. & SAUER, K. P. 2000. Phagocytosis of Vairimorpha sp. (Microsporida, Nosematidae) Spores by Plutella xylostella and Panorpa vulgaris Hemocytes. *Journal of Invertebrate Pathology,* 75**,** 237-239.

KVELLESTAD, A., FALK, K., NYGAARD, S. M. R., FLESJÅ, K. & HOLM, J. A. 2005. Atlantic salmon paramyxovirus (ASPV) infection contributes to proliferative gill inflammation (PGI) in seawater-reared Salmo salar. *Diseases of Aquatic Organisms,* 67**,** 47-54.

LARSSON, R. 1986. Ultrastructure, function, and classification of Microsporidia. *Progress in Protistology,* 1**,** 325-390.

LEE, S. C., CORRADI, N., BYRNES III, E. J., TORRES-MARTINEZ, S., DIETRICH, F. S., KEELING, P. J. & HEITMAN, J. 2008. Microsporidia Evolved from Ancestral Sexual Fungi. *Current Biology,* 18**,** 1675-1679.

LOM, J. & NILSEN, F. 2003. Fish microsporidia: fine structural diversity and phylogeny. *International Journal for Parasitology,* 33**,** 107-127.

MAGAUD, A., ACHBAROU, A. & DESPORTES-LIVAGE, I. 1997. Cell Invasion by the Microsporidium Encephalitozoon intestinalis. *Journal of Eukaryotic Microbiology,* 44**,** 81s-81s.

MALONE, L. A. 1984. Factors controlling in vitro hatching of Vairimorpha plodiae (Microspora) spores and their infectivity to Plodia interpunctella, Heliothis virescens, and Pieris brassicae. *Journal of Invertebrate Pathology,* 44**,** 192-197.

MULLER, P. Y., JANOVJAK, H., MISEREZ, A. R. & DOBBIE, Z. 2002. Processing of gene expression data generated by quantitative real-time RT-PCR. *Biotechniques,* 32**,** 1372-+.

NASSONOVA, E. S. & SMIRNOV, A. V. 2005. Synaptonemal complexes as evidence for meiosis in the life cycle of the monomorphic diplokaryotic microsporidium Paranosema grylli. *European Journal of Protistology,* 41**,** 175-181.

NILSEN, F. 2000. Small Subunit Ribosomal DNA Phylogeny of Microsporidia with Particular Reference to Genera That Infect Fish. *The Journal of Parasitology,* 86**,** 128-133.

NYLUND, A., HOVLAND, T., WATANABE, K. & ENDRESEN, C. 1995. Presence of infectious salmon anaemia virus (ISAV) in tissues of Atlantic salmon, Salmo salar L., collected during three separate outbreaks of the disease. *Journal of Fish Diseases,* 18**,** 135-145.

NYLUND, A., WATANABE, K., NYLUND, S., ARNESEN, C. E. & KARLSBAKK, E. 2009. "Nytt" patogen - "gammel" sykdom. *Norsk Fiskeoppdrett,* 34**,** 44-49.

NYLUND, A., WATANABE, K., NYLUND, S., KARLSEN, M., SÆTHER, P., ARNESEN, C. & KARLSBAKK, E. 2008. Morphogenesis of salmonid gill poxvirus associated with proliferative gill disease in farmed Atlantic salmon (<i>Salmo salar) in Norway. *Archives of Virology,* 153**,** 1299-1309.

NYLUND, A., ØKLAND, S. & BJØRKNES, B. 1992. Anatomy and Ultrastructure of the Alimentary Canal in Lepeophtheirus salmonis (Copepoda: Siphonostomatoida). *Journal of Crustacean Biology,* 12**,** 423-437.

NYLUND, S., ANDERSEN, L., SAEVAREID, I., PLARRE, H., WATANABE, K., ARNESEN, C. E., KARLSBAKK, E. & NYLUND, A. 2011. Diseases of farmed Atlantic salmon Salmo salar associated with infections by the microsporidian Paranucleospora theridion. *Diseases of Aquatic Organisms,* 94**,** 41-57.

NYLUND, S., NYLUND, A. R. E., WATANABE, K., ARNESEN, C. E. & KARLSBAKK, E. 2010. Paranucleospora theridion n. gen., n. sp. (Microsporidia, Enterocytozoonidae) with a Life Cycle in the Salmon Louse (Lepeophtheirus salmonis, Copepoda) and Atlantic Salmon (Salmo salar). *Journal of Eukaryotic Microbiology,* 57**,** 95-114.

OTTO, S. P. & GERSTEIN, A. C. 2006. Why have sex? The population genetics of sex and recombination. *Biochemical Society Transactions,* 34**,** 519-522.

PFAFFL, M. W. 2004. Quantification strategies in real-time PCR. *In:* BUSTIN, S. A. (ed.) *A-Z of quantitative PCR.* CA, USA: International University line (IUL).

POPPE, T. T. & HÅSTEIN, T. 1982. Costiasis på laksesmolt (Salmo salar L.) i sjøoppdrett. *Norsk Veterinærtidsskr,* 94**,** 259-262.

REPSTAD, O. 2011. *KARTLEGGING AV PATOGENDYNAMIKKEN HOS OPPDRETTSLAKS (Salmo salar L.) MED DIAGNOSEN PANKREASSYKDOM (PD).* Master Master, University of Bergen.

RITCHIE, G., MORDUE, A. J., PIKE, A. W. & RAE, G. H. 1996. Observations on mating and reproductive behaviour of Lepeophtheirus salmonis, Krøyer (Copepoda: Caligidae). *Journal of Experimental Marine Biology and Ecology,* 201**,** 285-298.

SOUTHERN, T. R., JOLLY, C. E., LESTER, M. E. & HAYMAN, J. R. 2007. EnP1, a microsporidian spore wall protein that enables spores to adhere to and infect host cells in vitro. *Eukaryotic Cell,* 6**,** 1354-1362.

SPROSTON, N. G. 1946. A Synopsis of the Monogenetic Trematodes. *The Transactions of the Zoological Society of London,* 25**,** 185-600.

STEINUM, T., KVELLESTAD, A., RØNNEBERG, L. B., NILSEN, H., ASHEIM, A., FJELL, K., NYGÅRD, S. M. R., OLSEN, A. B. & DALE, O. B. 2008. First cases of amoebic gill disease (AGD) in Norwegian seawater farmed Atlantic salmon, Salmo salar L., and phylogeny of the causative amoeba using 18S cDNA sequences. *Journal of Fish Diseases,* 31**,** 205-214.

SVEEN, S., ØVERLAND, H., KARLSBAKK, E. & NYLUND, A. In press. *Paranucleospora theridion* (Microspora) infection dynamics in farmed Atlantic salmon (*Salmo salar*) put to sea in spring and autumn.

SWEENEY, A. W., HAZARD, E. I. & GRAHAM, M. F. 1985. Intermediate host for an Amblyospora sp. (Microspora) infecting the mosquito, Culex annulirostris. *Journal of Invertebrate Pathology,* 46**,** 98-102.

TREASURER, J. W. 2002. A review of potential pathogens of sea lice and the application of cleaner fish in biological control. *Pest Management Science,* 58**,** 546-558.

TUCKER, C. S., NORMAN, R., SHINN, A. P., BRON, J. E., SOMMERVILLE, C. & WOOTTEN, R. 2002. A single cohort time delay model of the life-cycle of the salmon louse Lepeophtheirus salmonis on Atlantic salmon Salmo salar. *Fish Pathology,* 37**,** 107-118.

UNDEEN, A. H. & EPSKY, N. D. 1990. In vitro and in vivo germination of Nosema locustae (Microspora: Nosematidae) spores. *Journal of Invertebrate Pathology,* 56**,** 371-379.

VAVRA, J. & LARSSON, J. I. R. 1999. Structure of the Microsporidia. *In:* WITTNER, M. & WEISS, L. M. (eds.) *The Microsporidia and Microsporidosis.* Washington, DC: ASM press.

WITTNER, M. 1999. Historic perspective on the Microsporida: Expanding horizons. *In:* WITTNER, M. & WEISS, L. M. (eds.) *The Microsporidia and Microsporidosis.* Washington, DC: ASM press.

ZENKE, K., URAWA, S., FUJIYAMA, I., YOKOYAMA, H. & OGAWA, K. 2005. Effects of water temperature on infection of the microsporidian Kabatana takedai in salmonids. *Fish Pathology,* 40**,** 119-123.

Appendix

Recipes

1 % AGROSE GEL
4.0 g SeaKem® LA Agrose (Cambrex) dissolved in 400 ml 1x TAE, heated 10 min in microwave oven. Stored at 60 °C.

50x TAE (Tris-Acetate-EDTA)
242 g Tris Base (Merck)
57,1 ml "Glacial actetic acid"
100 ml 0,5 EDTA (pH=8.0)
Add ddH2O up to 1 liter

1x TAE
200 ml 50x TAE buffer added ddH2O, total 10 liter

6x LOADINGBUFFER
35 ml glycerol
200 µl bromine phenol blue
200 µl xylencyanol
200 µl Tris-HCL (pH=8.5)
14,4 ml ddH2O

Modified Karnovskys Fixative (100 ml)
80 ml Ringers solution a
10 ml 25 % glutaraldehyde
10 ml 10% paraformaldehyde b
4 g sucrose

a Ringers solution (including 0,2M phosphate buffer) (1.000 ml):
NaH2PO4H2O: 1,65 g
Na2HPO42H20: 6,76 g
NaCl: 6,75 g
KCl: 0,12 g
NaHCO3: 0,15 g
Glucose: 1,65 g
ddH2O: 1000 ml

b 10 % paraformaldehyde:
2 g formaldehyde to 20 g dH2O (1:10)
Heated 70°C. Added 2 drops 1 M NaOH until the fluid is transparent.

Washing of Karnovsky:

Washed with Ringers solution 4 times (on ice)

1. 10-15 seconds
2. 30 minutes
3. Over night
4. 30 minutes

Dehydration:

First sampling 020911

- 60 % acetone for 15 minutes (on ice)
- 90 % acetone for 15 minutes (on ice)
- 100 % acetone for 15 minutes x 3 (room temperature)

Second sampling 101111

- 60 % acetone for 15 minutes (on ice)
- 90 % acetone for 15 minutes (on ice)
- 100 % acetone for 15 minutes (room temperature)
- 100 % propylene oxide for 15 minutes x 2 (room temperature)

Infiltration:

- 2:1, 100 % acetone: Epon Embed 812 for 1 hour
- 1:1, 100 % acetone: Epon Embed 812 for 1 hour
- 2:3, 100 % acetone: Epon Embed 812 for 1 hour
- 1:2, 100 % acetone: Epon Embed 812 over night
- 100% Epon Embed 812 for 2,5 hours

Real time RT-PCR data

Table 1 Chalimus 1 data. Ct- values for *P. theridion* (NUC), lice elongation factor (ELF-LS) and viral heamorrhagic syndrome virus (VHSV). Normalized expression for NUC vs ELF-LS and NUC vs VHSV are presented.

Stage/date	NUC	ELF-LS	VHSV	NE ELF-LS	NE VHSV	N-Fold ELF-LS	N-Fold VHSV
C1101111-1	32,9	23,2	26,0	0,0006690	0,0111476	145,4	61,1
C1101111-2	neg	32,4	29,4	-	-	0,0	0,0
C1101111-3	28,6	23,6	24,3	0,0156509	0,0660564	3402,4	362,3
C1101111-4	37,6	24,5	25,0	0,0000604	0,0002243	13,1	1,2
C1101111-5	neg	22,6	24,9	-	-	0,0	0,0
C1101111-6	34,3	20,7	24,7	0,0000517	0,0017663	11,2	9,7
C1101111-7	neg	24,1	27,8	-	-	0,0	0,0
C1101111-8	28,7	21,4	24,6	0,0034010	0,0725697	739,3	398,1
C1101111-9	38,1	22,9	25,1	0,0000155	0,0001823	3,4	1,0

Table 2 Chalimus 2 data. Ct- values for *P. theridion* (NUC), lice elongation factor (ELF-LS) and viral heamorrhagic syndrome virus (VHSV). Normalized expression for NUC vs ELF-LS and NUC vs VHSV are presented.

Stage/date	NUC	ELF-LS	VHSV	NE ELF-LS	NE VHSV	N-Fold ELF-LS	N-Fold VHSV
C2101111-1	27,0	18,4	23,2	0,0016234	0,0896121	352,9	491,6
C2101111-2	34,0	22,4	25,9	0,0001817	0,0049525	39,5	27,2
C2101111-3	39,2	22,6	25,3	0,0000061	0,0000955	1,3	0,5
C2101111-4	34,4	17,4	23,7	0,0000059	0,0008745	1,3	4,8
C2101111-5	29,3	18,8	23,8	0,0004388	0,0280428	95,4	153,8
C2101111-6	24,2	19,2	24,1	0,0169273	1,0886240	3679,8	5971,6
C2101111-7	34,7	20,1	24,5	0,0000256	0,0012509	5,6	6,9
C2101111-8	neg	neg	30,9	-	-	0,0	0,0
C2 020911-1	30,0	18,7	25,6	0,0002455	0,0589204	53,4	323,2
C2 020911-2	30,7	17,2	23,9	0,0000612	0,0117048	13,3	64,2

Table 3 Chalimus 3 data. Ct- values for *P. theridion* (NUC), lice elongation factor (ELF-LS) and viral heamorrhagic syndrome virus (VHSV). Normalized expression for NUC vs ELF-LS and NUC vs VHSV are presented.

Stage/date	NUC	ELF-LS	VHSV	NE ELF-LS	NE VHSV	N-Fold ELF-LS	N-Fold VHSV
C3 101111-1	21,0	16,4	28,1	0,0264690	160,6870967	5754,1	881443,2
C3 101111-2	29,9	16,9	29,2	0,0000828	0,7408104	18,0	4063,7
C3 101111-3	26,1	15,9	29,0	0,0006067	9,0293861	131,9	49530,4
C3 101111-4	26,4	15,6	27,9	0,0004061	3,4128371	88,3	18721,0
C3 101111-5	30,2	15,9	28,2	0,0000352	0,3239137	7,7	1776,8
C3 101111-6	32,3	15,1	29,6	0,0000052	0,1965061	1,1	1077,9
C3 101111-7	32,4	15,6	29,1	0,0000065	0,1321990	1,4	725,2
C3 101111-8	19,2	15,5	28,7	0,0495647	750,2042385	10774,9	4115218,0
C3 101111-9	30,6	15,2	27,5	0,0000174	0,1464065	3,8	803,1
C3 101111-10	30,9	15,6	28,3	0,0000183	0,2062189	4,0	1131,2
C3 101111-11	33,7	16,4	29,0	0,0000046	0,0502047	1,0	275,4
C3 101111-12	25,8	15,6	29,2	0,0005876	11,7605946	127,7	64512,3
C3 101111-13	21,7	15,3	27,4	0,0075287	58,3883497	1636,7	320287,2
C3 101111-14	32,1	15,5	28,5	0,0000075	0,1056867	1,6	579,7
C3 101111-15	35,6	20,5	33,9	0,0000184	0,3935141	4,0	2158,6
C3 101111-16	23,9	20,8	34,6	0,0607056	1 771,5761503	13196,9	9717916,3
C3 101111-17	29,6	16,2	29,0	0,0000651	0,8301681	14,2	4553,9
C3 101111-18	31,8	15,5	29,1	0,0000091	0,1906096	2,0	1045,6
C3 101111-19	24,3	17,0	29,8	0,0041338	51,7697039	898,7	283980,8
C3 101111-20	29,7	16,3	27,9	0,0000658	0,3558209	14,3	1951,8
C3 101111-21	31,1	16,6	29,0	0,0000323	0,2968510	7,0	1628,4
C3 101111-22	19,1	14,5	27,6	0,0287915	386,0512140	6259,0	2117669,9
C3 101111-23	27,2	15,1	27,6	0,0001708	1,6113818	37,1	8839,2
C3 101111-24	28,1	15,9	27,7	0,0001494	0,9526977	32,5	5226,0
C3 101111-25	30,1	16,1	28,4	0,0000457	0,3802172	9,9	2085,7
C3 101111-26	30,9	14,8	27,8	0,0000113	0,1563829	2,4	857,8
C3 020911-1	32,0	17,4	25,6	0,0000276	0,0153044	6,0	84,0
C3 020911-2	33,9	20,9	27,9	0,0000731	0,0209807	15,9	115,1
C3 020911-3	18,9	19,4	26,6	0,7356318	222,5468206	159920,0	1220772,5
C3 020911-4	34,5	21,1	26,3	0,0000551	0,0045843	12,0	25,1

Table 4 Chalimus 4 data. Ct- values for *P. theridion* (NUC), lice elongation factor (ELF-LS) and viral heamorrhagic syndrome virus (VHSV). Normalized expression for NUC vs ELF-LS and NUC vs VHSV are presented.

Stage/date	NUC	ELF-LS	VHSV	NE ELF-LS	NE VHSV	N-Fold ELF-LS	N-Fold VHSV
C4 101111-1	13,2	18,3	20,9	17,3904360	210,0073738	3780529,6	1151987,8
C4 101111-2	31,7	20,0	28,2	0,0001851	0,1112398	40,2	610,2
C4 101111-3	26,6	14,2	22,4	0,0001415	0,0676935	30,8	371,3
C4 101111-4	11,3	12,4	21,3	1,3904037	978,7843881	302261,7	5369086,1
C4 101111-5	26,9	13,3	21,8	0,0000634	0,0377710	13,8	207,2
C4 101111-6	26,7	13,9	22,0	0,0001126	0,0477842	24,5	262,1
C4 101111-7	20,6	15,0	23,2	0,0139489	6,7694173	3032,4	37133,4
C4 101111-8	24,3	13,9	22,5	0,0005424	0,3379144	117,9	1853,6
C4 101111-9	28,0	14,9	22,8	0,0000841	0,0360583	18,3	197,8
C4 101111-10	19,7	13,0	21,7	0,0069327	4,6168319	1507,1	25325,5
C4 101111-11	27,2	13,8	21,8	0,0000723	0,0315457	15,7	173,0
C4 101111-12	30,1	13,7	21,7	0,0000094	0,0038574	2,0	21,2
C4 101111-13	30,3	13,3	21,7	0,0000064	0,0034094	1,4	18,7
C4 101111-14	29,0	13,5	21,9	0,0000183	0,0098423	4,0	54,0
C4 101111-15	25,6	12,7	21,4	0,0001049	0,0685287	22,8	375,9
C4 101111-16	29,2	13,0	21,4	0,0000110	0,0058671	2,4	32,2
C4 101111-17	28,2	13,6	22,2	0,0000325	0,0207733	7,1	114,0
C4 101111-18	23,9	12,8	21,5	0,0003495	0,2217390	76,0	1216,3
C4 101111-19	29,3	13,4	22,3	0,0000139	0,0101986	3,0	55,9
C4 101111-20	26,4	14,9	21,8	0,0002614	0,0536408	56,8	294,2
C4 101111-21	26,2	12,7	21,8	0,0000701	0,0618741	15,2	339,4
C4 101111-22	17,9	13,7	22,5	0,0368139	27,7481354	8003,0	152211,4
C4 020911-1	32,3	25,1	26,6	0,0033322	0,0253729	724,4	139,2
C4 020911-2	30,4	16,4	25,1	0,0000460	0,0344344	10,0	188,9
C4 020911-3	30,6	20,9	25,9	0,0006905	0,0467785	150,1	256,6
C4 020911-4	31,8	17,6	26,0	0,0000372	0,0241879	8,1	132,7

Table 5 Preadult 1 male data. Ct- values for *P. theridion* (NUC), lice elongation factor (ELF-LS) and viral heamorrhagic syndrome virus (VHSV). Normalized expression for NUC vs ELF-LS and NUC vs VHSV are presented.

Stage/date	NUC	ELF-LS	VHSV	NE ELF-LS	NE VHSV	N-Fold ELF-LS	N-Fold VHSV
PA1M 101111-1	30,1	13,9	27,0	0,0000102	0,1409189	2,2	773,0
PA1M 101111-2	27,0	13,4	27,0	0,0000624	1,1836611	13,6	6492,9
PA1M 101111-3	18,1	13,7	27,4	0,0320139	669,4916606	6959,5	3672472,1
PA1M 101111-4	28,7	13,8	27,4	0,0000263	0,5381719	5,7	2952,1
PA1M 101111-5	22,0	13,6	26,8	0,0022103	32,4593754	480,5	178054,7
PA1M 101111-6	10,6	13,9	27,1	5,6474908	85 025,7982139	1227715,4	466405914,5
PA1M 101111-7	26,8	15,1	27,9	0,0002063	2,4265208	44,9	13310,6
PA1M 101111-8	30,6	14,7	27,6	0,0000127	0,1628672	2,8	893,4
PA1M 101111-9	28,5	14,0	27,3	0,0000340	0,5473871	7,4	3002,7
PA1M 101111-10	29,3	13,8	27,0	0,0000180	0,2647193	3,9	1452,1
PA1M 101111-11	30,0	13,4	27,1	0,0000083	0,1778032	1,8	975,3
PA1M 101111-12	29,0	16,6	27,4	0,0001288	0,4117032	28,0	2258,4
PA1M 101111-13	11,5	13,2	26,9	2,0905356	40 222,2622469	454464,3	220637752,3
PA1M 101111-14	25,8	14,1	27,6	0,0002178	4,1875799	47,3	22970,8
PA1M 101111-15	14,0	13,9	26,9	0,6181562	7 839,2774455	134381,8	43002070,5
PA1M 101111-16	25,4	13,8	neg	0,0002424	-	52,7	0,0
PA1M 101111-17	14,8	13,3	31,4	0,2342495	96 152,8282693	50923,8	527442832,0
PA1M 101111-18	18,9	13,7	27,5	0,0180115	396,3218582	3915,5	2174009,1
PA1M 101111-19	18,5	18,3	32,1	0,4562390	12 328,3909065	99182,4	67626938,6
PA1M 101111-20	26,0	13,8	27,3	0,0001553	2,8196447	33,8	15467,1
PA1M 020911-1	29,5	23,1	28,6	0,0059926	0,6665403	1302,7	3656,3
PA1M 020911-2	28,3	25,4	29,6	0,0589163	2,9546708	12807,9	16207,7
PA1M 020911-3	34,5	22,7	30,7	0,0001580	0,0963225	34,4	528,4
PA1M 020911-4	32,9	24,2	30,3	0,0012395	0,2185566	269,5	1198,9
PA1M 020911-5	40,3	25,9	30,7	0,0000257	0,0018729	5,6	10,3
PA1M 020911-6	32,0	22,4	29,3	0,0007405	0,1998619	161,0	1096,3
PA1M 020911-7	34,9	22,2	30,3	0,0000872	0,0535314	19,0	293,6
PA1M 020911-8	35,5	24,5	29,7	0,0002646	0,0241221	57,5	132,3
PA1M 020911-9	38,4	23,8	30,8	0,0000239	0,0073102	5,2	40,1
PA1M 020911-10	32,6	26,1	30,8	0,0053258	0,3848353	1157,8	2111,0

Table 6 Preadult 1 female data. Ct- values for *P. theridion* (NUC), lice elongation factor (ELF-LS) and viral heamorrhagic syndrome virus (VHSV). Normalized expression for NUC vs ELF-LS and NUC vs VHSV are presented.

Stage/date	NUC	ELF-LS	VHSV	NE ELF-LS	NE VHSV	N-Fold ELF-LS	N-Fold VHSV
PA1F 020911-1	27,2	16,1	26,9	0,0003098	0,9506016	67,4	5214,5
PA1F 020911-2	24,8	15,1	24,3	0,0008860	0,8726725	192,6	4787,0
PA1F 020911-3	27,9	13,8	24,4	0,0000452	0,1118153	9,8	613,4
PA1F 020911-4	30,7	27,9	25,9	0,0625873	0,0477289	13605,9	261,8
PA1F 020911-5	30,4	16,0	25,4	0,0000320	0,0398676	6,9	218,7
PA1F 020911-6	31,5	17,6	26,3	0,0000443	0,0346279	9,6	190,0
PA1F 020911-7	33,1	17,6	28,5	0,0000157	0,0563488	3,4	309,1
PA1F 020911-8	35,3	21,6	26,8	0,0000430	0,0038108	9,3	20,9
PA1F 020911-9	26,6	15,6	24,8	0,0003255	0,3335938	70,8	1829,9
PA1F 020911-10	28,4	17,0	24,6	0,0002525	0,0908967	54,9	498,6
PA1F 020911-11	28,1	14,4	24,6	0,0000563	0,1115192	12,2	611,7
PA1F 020911-12	33,5	28,8	25,6	0,0157506	0,0056963	3424,0	31,2
PA1F 020911-13	27,5	20,3	26,0	0,0038629	0,4166340	839,8	2285,4
PA1F 020911-14	29,7	15,6	25,7	0,0000434	0,0805535	9,4	441,9
PA1F 020911-15	36,0	30,1	26,2	0,0068344	0,0015033	1485,7	8,2
PA1F 101111-1	25,3	11,5	24,6	0,0000585	0,7507484	12,7	4118,2
PA1F 101111-2	26,2	21,3	27,8	0,0183908	3,7815602	3998,0	20743,6
PA1F 101111-3	24,0	11,3	23,5	0,0001269	0,8731356	27,6	4789,6
PA1F 101111-4	22,1	12,2	23,7	0,0008632	3,6138469	187,6	19823,6
PA1F 101111-5	22,7	10,7	23,2	0,0002117	1,7203418	46,0	9436,9
PA1F 101111-6	20,8	12,2	24,2	0,0019429	12,2189595	422,4	67026,7
PA1F 101111-7	25,0	11,7	23,5	0,0000830	0,4396291	18,0	2411,6
PA1F 101111-8	25,6	13,6	24,4	0,0001952	0,5279336	42,4	2896,0
PA1F 101111-9	26,4	13,4	24,4	0,0000951	0,2983119	20,7	1636,4
PA1F 101111-10	25,2	11,6	24,3	0,0000685	0,6306127	14,9	3459,2
PA1F 101111-11	13,7	16,3	24,7	3,3373589	2 113,2093925	725512,8	11591933,0
PA1F 101111-12	22,7	14,9	26,5	0,0030114	15,5958001	654,7	85550,2
PA1F 101111-13	25,2	12,4	24,9	0,0001119	0,9772676	24,3	5360,8
PA1F 101111-14	23,7	11,9	24,9	0,0002171	2,6894670	47,2	14753,0
PA1F 101111-15	34,4	31,1	27,2	0,0373081	0,0091066	8110,5	50,0

Table 7 Preadult 2 male data. Ct- values for *P. theridion* (NUC), lice elongation factor (ELF-LS) and viral heamorrhagic syndrome virus (VHSV). Normalized expression for NUC vs ELF-LS and NUC vs VHSV are presented.

Stage/date	NUC	ELF-LS	VHSV	NE ELF-LS	NE VHSV	N-Fold ELF-LS	N-Fold VHSV
PA2M 101111-1	26,5	13,0	24,0	0,0000690	0,2155238	15,0	1182,2
PA2M 101111-2	25,8	11,9	23,2	0,0000553	0,2036155	12,0	1116,9
PA2M 101111-3	13,9	12,8	24,3	0,2988634	1 352,6909608	64970,3	7420136,9
PA2M 101111-4	14,3	12,2	23,3	0,1635211	527,8154573	35548,1	2895312,4
PA2M 101111-5	10,7	13,3	23,6	3,7927912	7 169,5018581	824519,8	39328040,9
PA2M 101111-6	30,5	24,0	32,9	0,0055097	6,4051962	1197,8	35135,5
PA2M 101111-7	10,5	11,8	23,4	1,5604515	7 291,0234958	339228,6	39994643,4
PA2M 101111-8	11,7	11,9	23,2	0,7509380	2 816,4796398	163247,4	15449696,3
PA2M 101111-9	19,3	12,4	23,8	0,0062673	25,2792861	1362,5	138668,6
PA2M 101111-10	21,2	12,1	23,4	0,0014421	5,2418525	313,5	28754,0
PA2M 101111-11	7,6	11,9	23,4	12,3755353	52 414,3505108	2690333,8	287517007,7
PA2M 101111-12	10,6	12,2	23,4	1,9824647	6 996,9068120	430970,6	38381277,1
PA2M 101111-13	24,1	12,8	23,0	0,0003278	0,5765660	71,3	3162,7
PA2M 101111-14	20,3	12,7	24,1	0,0038795	16,1183638	843,4	88416,7
PA2M 101111-15	22,5	11,9	23,4	0,0005086	2,1655352	110,6	11879,0
PA2M 020911-1	28,3	16,2	25,6	0,0001658	0,1966338	36,0	1078,6
PA2M 020911-2	28,2	16,7	25,8	0,0002248	0,2237878	48,9	1227,6
PA2M 020911-3	28,0	16,8	25,6	0,0002917	0,2420568	63,4	1327,8
PA2M 020911-4	28,5	16,7	26,2	0,0002001	0,2649714	43,5	1453,5
PA2M 020911-5	neg	neg	neg	-	-	0,0	0,0
PA2M 020911-6	29,1	19,2	27,0	0,0006309	0,2896979	137,1	1589,1
PA2M 020911-7	24,0	17,7	26,2	0,0076865	5,1367584	1671,0	28177,5
PA2M 020911-8	27,7	16,1	25,8	0,0002255	0,3428750	49,0	1880,8
PA2M 020911-9	27,9	22,6	28,5	0,0124825	1,8208113	2713,6	9988,0
PA2M 020911-10	28,1	26,7	26,9	0,1655208	0,5431482	35982,8	2979,4
PA2M 020911-11	25,7	13,5	24,0	0,0001705	0,3725561	37,1	2043,6
PA2M 020911-12	9,2	13,6	23,9	13,3162719	26 776,8864020	2894841,7	146883633,6
PA2M 020911-13	25,9	14,3	23,8	0,0002400	0,2914993	52,2	1599,0
PA2M 020911-14	25,1	14,1	24,1	0,0003584	0,5906810	77,9	3240,2
PA2M 020911-15	28,3	16,3	24,1	0,0001727	0,0701503	37,5	384,8

Table 8 Preadult 2 female data. Ct- values for *P. theridion* (NUC), lice elongation factor (ELF-LS) and viral heamorrhagic syndrome virus (VHSV). Normalized expression for NUC vs ELF-LS and NUC vs VHSV are presented.

Stage/date	NUC	ELF-LS	VHSV	NE ELF-LS	NE VHSV	N-Fold ELF-LS	N-Fold VHSV
PA2F 101111-1	24,5	11,7	23,9	0,0001085	0,7596963	23,6	4167,3
PA2F 101111-2	24,9	11,5	24,2	0,0000791	0,7609353	17,2	4174,1
PA2F 101111-3	25,1	12,4	24,1	0,0001169	0,5837049	25,4	3201,9
PA2F 101111-4	28,6	18,6	30,5	0,0006166	4,7168881	134,0	25874,3
PA2F 101111-5	24,9	11,0	24,6	0,0000576	0,9817944	12,5	5385,6
PA2F 101111-6	16,9	12,5	24,2	0,0336090	164,7448565	7306,3	903701,9
PA2F 101111-7	13,5	12,0	23,1	0,2422538	783,4287127	52663,9	4297469,6
PA2F 101111-8	23,9	10,9	23,3	0,0001084	0,8062970	23,6	4422,9
PA2F 101111-9	25,2	11,7	24,2	0,0000718	0,5878187	15,6	3224,5
PA2F 101111-10	26,4	11,1	23,8	0,0000215	0,2057130	4,7	1128,4
PA2F 101111-11	24,3	10,9	24,2	0,0000828	1,1026819	18,0	6048,7
PA2F 101111-12	22,3	10,7	neg	0,0002640	-	57,4	0,0
PA2F 101111-13	21,9	10,6	23,0	0,0003301	2,4069368	71,8	13203,2
PA2F 101111-14	24,5	12,1	24,1	0,0001457	0,8838034	31,7	4848,1
PA2F 101111-15	25,2	10,6	23,9	0,0000354	0,4890359	7,7	2682,6
PA2F 020911-1	24,1	16,6	25,7	0,0035758	3,7394907	777,3	20512,8
PA2F 020911-2	24,3	33,0	29,3	115,0557119	35,4380168	25012111,3	194393,9
PA2F 020911-3	30,3	15,1	27,7	0,0000202	0,2057432	4,4	1128,6
PA2F 020911-4	30,8	neg	26,8	0,00	0,0827678	0,0	454,0
PA2F 020911-5	neg	15,3	28,5	0,00	0,00	0,0	0,0
PA2F 020911-6	26,0	20,4	27,9	0,0111359	4,4486555	2420,8	24402,9
PA2F 020911-7	26,8	15,4	26,9	0,0002603	1,3486052	56,6	7397,7
PA2F 020911-8	26,2	15,1	25,6	0,0003312	0,8315005	72,0	4561,2
PA2F 020911-9	28,0	24,6	28,2	0,0436545	1,3516843	9490,1	7414,6
PA2F 020911-10	24,3	18,1	26,1	0,0081395	3,9733128	1769,5	21795,5
PA2F 020911-11	25,3	13,6	24,6	0,0002392	0,7620774	52,0	4180,3
PA2F 020911-12	25,3	14,4	24,6	0,0003812	0,7602253	82,9	4170,2
PA2F 020911-13	30,0	25,4	26,4	0,0183042	0,1023027	3979,2	561,2
PA2F 020911-14	29,4	24,4	25,8	0,0154080	0,1048193	3349,6	575,0
PA2F 020911-15	30,6	25,4	27,3	0,0128206	0,1272492	2787,1	698,0

Table 9 Adult male data. Ct- values for *P. theridion* (NUC), lice elongation factor (ELF-LS) and viral heamorrhagic syndrome virus (VHSV). Normalized expression for NUC vs ELF-LS and NUC vs VHSV are presented.

Stage/date	NUC	ELF-LS	VHSV	NE ELF-LS	NE VHSV	N-Fold ELF-LS	N-Fold VHSV
AM 101111-1	28,5	16,8	31,4	0,0002064	8,9595278	44,9	49147,2
AM 101111-2	25,5	13,3	26,3	0,0001694	2,1180971	36,8	11618,7
AM 101111-3	25,6	13,0	27,8	0,0001296	5,6260592	28,2	30861,5
AM 101111-4	22,6	13,0	27,5	0,0009919	33,8601973	215,6	185738,9
AM 101111-5	25,5	14,3	28,4	0,0003040	8,4738171	66,1	46482,8
AM 101111-6	22,7	12,3	28,4	0,0005526	55,5418259	120,1	304672,7
AM 101111-7	27,1	13,8	28,6	0,0000729	3,2605377	15,8	17885,6
AM 101111-8	26,8	13,9	27,5	0,0000988	1,8778411	21,5	10300,8
AM 101111-9	26,4	13,5	28,7	0,0000989	5,8262979	21,5	31959,9
AM 101111-10	24,7	13,3	27,7	0,0002872	9,1615836	62,4	50255,5
AM 101111-11	25,7	13,9	28,3	0,0002096	7,0197778	45,6	38506,7
AM 101111-12	25,5	13,9	27,6	0,0002331	4,8740973	50,7	26736,7
AM 101111-13	26,5	13,8	27,9	0,0001182	3,1437645	25,7	17245,0
AM 101111-14	25,8	12,9	27,7	0,0001037	4,5525747	22,5	24973,0
AM 101111-15	16,6	13,3	27,5	0,0677953	2 030,3627885	14738,1	11137481,0
AM 020911-1	23,1	15,4	26,3	0,0033626	10,5137592	731,0	57672,8
AM 020911-2	22,4	15,7	26,2	0,0065332	15,4219395	1420,3	84596,5
AM 020911-3	neg	neg	neg	-	-	0,0	0,0
AM 020911-4	26,9	15,7	25,4	0,0003130	0,4587671	68,1	2516,6
AM 020911-5	31,2	24,1	27,4	0,0036434	0,0938895	792,0	515,0
AM 020911-6	27,8	17,1	27,8	0,0003822	1,1624980	83,1	6376,8
AM 020911-7	26,7	20,6	31,5	0,0084938	33,7465517	1846,5	185115,5
AM 020911-8	24,0	15,0	25,6	0,0013417	3,4967685	291,7	19181,4
AM 020911-9	23,4	15,0	25,7	0,0020037	5,6535076	435,6	31012,1
AM 020911-10	11,2	17,8	27,9	46,8554904	96 276,9620363	10185976,2	528123763,2
AM 020911-11	24,4	19,5	29,3	0,0180284	34,1560595	3919,2	187361,8
AM 020911-12	25,8	16,5	27,7	0,0010605	4,3561869	230,5	23895,7
AM 020911-13	23,2	16,1	28,7	0,0046394	48,3871477	1008,6	265425,9
AM 020911-14	27,0	19,3	30,7	0,0028615	15,4330898	622,1	84657,7
AM 020911-15	25,7	15,8	28,3	0,0006982	6,9698695	151,8	38233,0

Table 10 Adult female data. Ct- values for *P. theridion* (NUC), lice elongation factor (ELF-LS) and viral heamorrhagic syndrome virus (VHSV). Normalized expression for NUC vs ELF-LS and NUC vs VHSV are presented.

Stage/date	NUC	ELF-LS	VHSV	NE ELF-LS	NE VHSV	N-Fold ELF-LS	N-Fold VHSV
AF 101111-1	25,1	11,2	26,8	0,0000548	3,7628161	11,9	20640,8
AF 101111-2	24,1	11,9	26,8	0,0001627	7,3744646	35,4	40452,4
AF 101111-3	23,2	11,2	25,9	0,0002001	7,5610942	43,5	41476,1
AF 101111-4	25,4	11,2	26,6	0,0000437	2,6967813	9,5	14793,1
AF 101111-5	23,7	12,3	26,9	0,0002793	10,0764562	60,7	55274,0
AF 101111-6	7,3	11,6	27,5	12,5913184	1 081 426,5864092	2737243,1	5932126091,1
AF 101111-7	23,9	10,5	26,4	0,0000784	6,2167894	17,0	34102,0
AF 101111-8	24,6	11,3	26,6	0,0000860	4,7996329	18,7	26328,2
AF 101111-9	25,0	11,1	26,5	0,0000580	3,4403687	12,6	18872,0
AF 101111-10	24,7	10,3	26,0	0,0000401	2,7445509	8,7	15055,1
AF 101111-11	23,6	11,2	27,0	0,0001544	11,6444312	33,6	63875,1
AF 101111-12	13,6	11,0	27,2	0,1212065	12 245,7903506	26349,2	67173836,3
AF 101111-13	15,3	10,6	26,7	0,0293982	2 825,0731272	6390,9	15496835,6
AF 101111-14	23,2	10,7	26,3	0,0001521	9,8995187	33,1	54303,4
AF 101111-15	23,7	11,6	27,4	0,0001809	15,3419483	39,3	84157,7
AF 020911-1	23,3	11,9	31,6	0,0003079	346,6108120	66,9	1901321,0
AF 020911-2	24,6	11,3	28,2	0,0000827	13,4595078	18,0	73831,6
AF 020911-3	24,9	12,3	28,8	0,0001236	17,0658661	26,9	93614,2
AF 020911-4	23,2	12,6	29,5	0,0004912	86,1012567	106,8	472305,3
AF 020911-5	24,4	11,9	27,7	0,0001425	11,8606516	31,0	65061,2
AF 020911-6	12,2	10,7	27,6	0,2452497	42 258,1780682	53315,1	231805694,3
AF 020911-7	14,1	11,9	27,7	0,1495716	12 096,3318186	32515,6	66353986,9
AF 020911-8	20,9	11,9	28,5	0,0015787	213,7611060	343,2	1172578,7
AF 020911-9	9,0	12,0	29,1	5,2859604	1 017 810,1240085	1149121,8	5583160307,2
AF 020911-10	24,1	11,8	31,0	0,0001589	138,6270985	34,5	760433,9
AF020911-11	18,0	10,5	30,8	0,0042363	7 342,4947341	920,9	40276987,0
AF020911-12	18,9	9,9	26,9	0,0016798	270,2548206	365,2	1482473,0
AF020911-13	18,9	10,1	26,3	0,0018819	187,5009783	409,1	1028529,8
AF020911-14	20,7	10,9	26,5	0,0008700	60,3258648	189,1	330915,3
AF020911-15	19,6	10,8	25,4	0,0018805	62,5224424	408,8	342964,6

Table 11 Data from photographed adult lice. The Ct values for *P. theridion* (NUC), lice elongation factor (ELF-LS) and viral hemorrhagic syndrome virus (VHSV) are presented.

Code	NUC	ELF-LS	VHSV
LS 150312-1	6,3	9,9	25,8
LS 150312-2	8,3	10,7	26,9
LS 150312-3	6,4	10,2	25,8
LS 150312-4	5,3	10,3	26,8
LS 150312-5	6,3	9,0	26,4
LS 150312-6	6,1	9,9	26,5
LS 150312-7	7,0	10,0	25,0
LS 150312-8	5,9	9,8	26,1
LS 150312-9	24,3	10,7	25,2
LS 150312-10	4,9	10,6	25,6
LS 150312-11	5,9	10,6	26,2
LS 150312-12	21,8	10,8	26,0
LS 150312-13	25,8	10,3	26,1
LS 150312-14	6,2	12,3	23,6

Table 12 Data from *C.centrodonti*. Ct-values for *P.theridion* (NUC) and viral hemorrhagic syndrome virus (VHSV) are presented.

Code	NUC	VHSV
CCAM 1	neg	24,8
CCAM 2	34,6	24,9
CCAM 3	34,0	24,9
CCAM 4	neg	25,5
CCAM 5	36,8	25,4
CCAM 6	neg	26,4
CCAM 7	neg	26,0
CCAM 8	neg	25,3
CCAM 9	neg	25,4
CCAM 10	neg	24,4
CCAF 1	neg	25,7
CCAF 2	neg	24,0
CCAF 3	neg	24,4
CCAF 4	neg	24,1
CCAF 5	neg	24,4
CCAF 6	neg	24,4
CCAF 7	neg	25,5
CCAF 8	neg	24,6
CCAF 9	neg	25,1
CCAF 10	neg	24,5

Table 13 Data from lice with inclusions near the second antennae. The Ct values for *P. theridion* (NUC), lice elongation factor (ELF-LS) and viral hemorrhagic syndrome virus (VHSV) are presented.

Code	NUC	ELF-LS	VHSV
LA160112	neg	18,1	22,6
LB160112	39,0	14,8	21,5
LC160112	29,9	13,5	21,6

Table 14 Data from salmon lice obtained from rainbow trout. The Ct values for *P. theridion* (NUC), lice elongation factor (ELF-LS) and viral hemorrhagic syndrome virus (VHSV) are presented.

Code	NUC	ELF-LS	VHSV
AF 110112-1	34,0	12,1	26,5
AF 110112-2	35,9	13,1	26,8
AF 110112-3	35,5	11,4	26,5
AF 110112-4	neg	12,1	26,5
AF 110112-5	37,2	12,4	26,8
AF 110112-6	39,7	13,1	26,4
AF 110112-7	33,5	12,6	26,6
AF 110112-8	34,6	13,0	28,2
AF 110112-9	37,2	11,6	26,4
AF 110112-10	neg	13,2	26,6
AF 110112-11	neg	11,6	29,3
AF 110112-12	neg	10,6	28,5
AF 110112-13	neg	12,5	29,1
AF 110112-14	neg	11,9	28,9
AF 110112-15	39,8	11,3	28,1
AF 110112-16	41,7	11,6	28,9
AF 110112-17	44,0	11,9	28,8
AF 110112-18	neg	11,3	27,0
AF 110112-19	36,3	11,1	27,6
AF 110112-20	neg	12,5	28,4
AF 110112-21	37,1	11,4	29,1
AF 110112-22	37,8	11,2	27,5
AF 110112-23	neg	12,6	29,1
AF 110112-24	34,6	12	28,0
AF 110112-25	37,0	12,9	29,1
AF 110112-26	35,4	11,4	28,0
AF 110112-27	neg	11,4	27,9
AF 110112-28	36,8	11,8	27,8
AF 110112-29	neg	12,3	28,4
AF 110112-30	35,9	11,5	27,5